

UNITED STATES DEPARTMENT OF THE INTERIOR
GEOLOGICAL SURVEY

ESTIMATION OF GROUND MOTION PARAMETERS

By

David M. Boore, Adolph A. Oliver III, Robert A. Page,
and William B. Joyner

OPEN-FILE REPORT

78-509

Prepared on behalf of the Nuclear Regulatory Commission

This report is preliminary and has not been
edited or reviewed for conformity with
Geological Survey standards.

This page intentionally left blank

ABSTRACT

Strong motion data from western North America for earthquakes of magnitude greater than 5 are examined to provide the basis for estimating peak acceleration, velocity, displacement, and duration as a function of distance for three magnitude classes. Data from the San Fernando earthquake are examined to assess the effects of associated structures and of geologic site conditions on peak recorded motions. Small but statistically significant differences are observed in peak values of horizontal acceleration, velocity, and displacement recorded on soil at the base of small structures compared with values recorded at the base of large structures. Values of peak horizontal acceleration recorded at soil sites in the San Fernando earthquake are not significantly different from the values recorded at rock sites, but values of peak horizontal velocity and displacement are significantly greater at soil sites than at rock sites. Three recently published relationships for predicting peak horizontal acceleration are compared and discussed. Considerations are reviewed relevant to ground motion predictions at close distances where there are insufficient recorded data points.

INTRODUCTION

Peak horizontal acceleration is commonly used to scale response spectra or ground motion time histories for use in earthquake-resistant design, particularly in the case of nuclear power plant facilities (Newmark, Blume, and Kapur, 1973). Methods have also been proposed (Newmark and Hall, 1969) for constructing design spectra using three peak parameters, horizontal acceleration, velocity, and displacement, the advantage of using all three parameters being that together they convey some information concerning the shape of the spectrum as well as the amplitude level. In this report we present the analysis of a large number of earthquake data to provide the basis for estimating the peak acceleration, velocity, and displacement and duration of shaking for a hypothetical earthquake of a prescribed magnitude at a prescribed distance from the causative fault. This work is a continuation of that reported by Page and others (1972) and by Page and others (1975).

It is not our purpose to advocate the use of peak parameters in scaling design motions. We look forward ultimately to the development of new methods for prescribing design motions, methods more firmly based in the physics that governs faulting and wave propagation. Pending the development of such methods, we recognize widespread current practice and attempt to present the available strong motion data in a compact and useful form for estimating peak parameters.

DATA CHARACTERISTICS AND METHODS OF PRESENTATION

Sources of data. The data set includes 204 recordings from 19 earthquakes and is listed in Appendix B. The primary source of acceleration data is volume I of the series "Strong Motion Earthquake Accelerograms" published under the

direction of D. E. Hudson by the Earthquake Engineering Research Laboratory of the California Institute of Technology; values of velocity, displacement, and duration came from volume II of the same series. We used volume I for acceleration because volume II gives data at equal time intervals of 0.02 sec. and that tends to bias the peak acceleration toward lower values. A few of the acceleration data came from other sources listed in Appendix B, principally U.S. Earthquakes, an annual publication of the U.S. Department of Commerce.

Distances. In all cases the distance used is the shortest distance between the surface of fault slippage and the recording point. This would clearly be the preferred measure of distance if radiation were uniform over the surface and if the surface were known. The second condition is sometimes not met; the first is probably never met. Other measures of distance have been used in strong motion data analysis, particularly, epicentral distance, hypocentral distance, and distance from the center of energy release. The use of epicentral distance or hypocentral distance has the advantage that they are more commonly known and special studies are not required to determine them. In some cases, however, these measures are clearly inappropriate, as in the case of a long fault rupture with epicenter at one end and recording stations at the other. The Parkfield, California, earthquake of 1966 provides an example of such a situation. The use of distance to the center of energy release is a way of avoiding the assumption of uniform radiation over the rupture surface, but in the case of long ruptures this measure, too, may be inappropriate. In our opinion the best choice for general purposes is the closest distance to the rupture surface, but the uncertainties resulting from nonuniform radiation over the surface should be kept in mind. An illustration

of those uncertainties is provided by the Pacoima Dam recording of the San Fernando earthquake of 1971. On that record the source for the peak velocity and for the peak acceleration are different points on the fault, separated by perhaps 20 km, neither one of which is the closest point to the instrument (Hanks, 1974; Bouchen and Aki, 1977).

With a few exceptions the location of the rupture surface has been inferred from the aftershock distribution. In the case of the Imperial Valley, California, earthquake of 1940 the distance used is chosen in accordance with the interpretations of Richter (1958) and Trifunac and Brune (1970). In the case of the Hebgen Lake, Montana, earthquake of 1959, the distance used is the epicentral distance of the main shock, and in the case of the Puget Sound earthquake of 1949, the distance used is the hypocentral distance of the main shock assuming a minimum focal depth of 45 km. Sources of data used in estimating station distances are included in Table I.

In order to avoid obscuring the attenuation relationships we generally exclude data where the uncertainty in distance is large. Following Page and others (1972), we classify the distances as A, B, or C, according to the uncertainty (less than 2 km, 2 to 5 km, and 5 to 25 km, respectively). C quality data are only used in the case of the magnitude 7.1 Puget Sound earthquake and the magnitude 7.1 Hebgen Lake earthquake. In the plots to follow, the class A, B, or C is indicated by the size of the symbol, the largest for class A and the smallest for class C.

The assignment of distances in the case of the Parkfield earthquake deserves special mention. Originally it was believed that the rupture associated with the Parkfield earthquake extended along the San Andreas fault far enough to the southeast so that it passed within 80 meters of station

number 2 of the Cholame-Shandon array (Cloud and Perez, 1967). Lindh and Boore (1973), however, presented evidence that, at the time of the earthquake, no significant displacement occurred beyond a point 7 km northwest of station number 2. Modeling studies by Trifunac and Udwadia (1975) tend to confirm the Lindh and Boore interpretation and we follow it in this report.

Classification of data. We have divided the data into classes in accordance with magnitude, site geology, and size of associated structure. The data is divided into three magnitude classes (5.0-5.9, 6.0-6.9, and 7.0-7.9) on the basis of the Richter local magnitude (Richter, 1958), if available, otherwise surface wave magnitude is used. Sources of data for assigning magnitudes are included in Table I. The Imperial Valley earthquake is assigned a magnitude of 6.4 in accordance with a determination by Trifunac and Brune (1970) and in contrast with the value 7.1 that is commonly given.

Kanamori and Jennings (written communication) have recently developed a method of determining Richter local magnitude from strong motion records. Their magnitude assignments are in general agreement with ours. The largest difference is for the Puget Sound earthquake of 1949 for which their value is 6.5 in contrast with our value of 7.1.

We assign recording sites to one of two categories, "rock" or "soil" by applying our best judgment to the available site descriptions. We assign stations to the rock category if they are underlain by material described by such terms as "granite", "diorite", "gneiss", "chert", "graywacke", "limestone", "sandstone", "siltstone", or "shale". Stations are assigned to the soil category if they are underlain by sufficient thickness of material described by such terms as "alluvium", "sand", "gravel", "clay", "silt", "mud", "fill", or "glacial outwash". If we judge from the site description

that soil material overlying rock is less than 4 to 5 meters thick we ignore it. Sources for site descriptions are given in Appendix B. The reader should be warned that considerable uncertainty and ambiguity attends the geological classification of recording sites. We do not, however, even suggest conclusions that rely on the validity of the classification of a single station. We are concerned only with trends revealed by comparing whole classes of data.

Much of the data comes from the basements or ground floors of buildings or from the abutments of dams. In the analysis of strong motion data it is commonly assumed that the influence of the structure on the motion of the base can be ignored and that the data as recorded represent free-field ground motion. We have attempted a limited test of this assumption by classifying recording sites in accordance with the size of the associated structure; class 1 for sites at the base of one- or two-story buildings and class 2 for sites at the base of taller buildings or on dam abutments. Comparison of the two classes using data from the San Fernando earthquake is described in a subsequent section. Briefly, there are small but statistically significant differences.

In the case of velocity and displacement one would expect the data from small structures to be more representative of free-field motion. The transfer functions relating motion at the base of structures to free-field motion tend toward unity for frequencies small compared to the fixed-base natural frequencies of the structure. (For examples of theoretical and empirical transfer functions see Duke and others, 1970, and Crouse and Jennings, 1975). The small structures have natural frequencies mostly in the range of 2 to 10 Hertz, which is significantly above the range of frequencies dominant in the

velocity and displacement time histories. The case of acceleration is more complicated. The natural frequencies of the small structures are in the same range as the frequencies dominant in the acceleration time histories, and the effect of the structure may be to raise or lower the acceleration depending on the spectrum of the earthquake and the details of the transfer function. We still believe, however, that the smaller structures provide the better basis for estimating free-field motion, even for acceleration. The reason is that the transfer functions tend to fall below unity for frequencies substantially greater than the natural frequencies of the structures. In some cases, such as the observed transfer function for the Hollywood Storage Building, the attenuation at high frequencies is large. So, we would expect the acceleration values for the large structures to be systematically biased downward. In fact, the comparison of San Fernando data shows smaller accelerations on the average for the large structures. Our main emphasis, therefore, is placed on the data from the small structures, but for the horizontal component data we also provide plots and regression parameters for the whole data set.

Geographical distribution. In an attempt to keep the data sample reasonably homogeneous, only records obtained in the western part of North America were included. In order to avoid bias from the extremely dense cluster of instruments in downtown Los Angeles a special selection procedure was used in the area between 34.00° and 34.11° North Latitude and 118.24° and 118.45° West Longitude. Within each of the two geological site categories only one recording per earthquake was allowed for each structure category, making a maximum of four possible recordings from the designated area for one earthquake. Selection was made by choosing the station with the smallest

identification number of all the eligible stations. In Appendix B stations so chosen are denoted by an asterisk.

Presentation of data. Peak horizontal acceleration, velocity, and displacement data are plotted against distance on log-log grids for each magnitude class. The peak values for horizontal motion are taken from the component with the larger peak. Duration values are plotted against distance on a linear grid. The measure of duration used is the time interval between the first and last horizontal acceleration peaks equal to or greater than 0.05 g. The value is taken from the horizontal component that gives the larger value. This is the definition used by Page and others (1972). It is a relatively crude measure, but it is simple to determine and is of some value in characterizing ground motion. Peak vertical acceleration, velocity, and displacement are plotted on log-log grids in the same way as the horizontal data.

Statistics. The nature of the strong motion data set is not such as to bear the weight of elaborate or subtle statistical inferences. For that reason we emphasize plots showing the individual data points. We do, however, indulge in statistical analysis to the extent of determining least-squares straight lines relating the logarithm of the peak parameters to the logarithm of distance and determining the confidence limits for the prediction of a single value of the dependant variable (Dixon and Massey, 1957).

We have attempted to avoid bias in the regression analysis by not including points that are either too close or too far from the fault. In the first case the data are too sparse to indicate the proper functional form for the regression and in the second the data set is incomplete because not all instruments were triggered by the motion. For small structures the data used

in our regression calculations are contained within the ranges 5-30, 15-55, and 40-150 km for magnitude classes 5.0-5.9, 6.0-6.9, and 7.0-7.9, respectively. For the San Fernando earthquake the range is 15-100 km. For the whole data set including both large and small structures the ranges are the same as for the small structures except for magnitude class 6.0-6.9 for which the range is 10-55 km.

The straight lines obviously fit the data as well as would any simple relationship. Curvature that might be caused by anelastic attenuation is completely obscured by the scatter in the data.

The scatter is approximately constant independent of distance. This suggests that the decision was correct to fit a straight line relationship to the logarithms of variables rather than fit a power law relationship to the variables themselves.

ALL EARTHQUAKES

General comments. Data for all the earthquakes is presented in this section, with emphasis on the data from small structures because, for reasons given previously, we consider those data a better guide to free-field motion. In the succeeding section data from the San Fernando earthquake are examined to assess the effect of structure and the effect of local site geology.

Horizontal acceleration. Peak horizontal acceleration data from the small structures for the three magnitude classes are shown in Figures 1, 2, and 3. The relations among the magnitude classes are summarized in Figure 4, which shows the overlap of the 70 percent prediction intervals. The accelerations clearly increase with magnitude in those distance ranges for which there is overlap between the classes. The scatter for the magnitude 5.0-5.7 data is

significantly greater than that for either of the other two classes. This may in part be due to the fact that a number of different earthquakes contribute substantially to the data set for the 5.0-5.7 class, whereas the 6.0-6.4 class is dominated by data from the 1971 San Fernando earthquake and the 7.1-7.7 class is dominated by data from the 1952 Kern County earthquake.

The rate of attenuation of acceleration with distance for the magnitude 5.0-5.7 class appears to be greater than indicated by the slope of -0.9 for the mean regression line in Figure 1. This is suggested by the systematic tendency for the data points at distances beyond 30 km to lie below an extension of the mean regression line. Data beyond 30 km are excluded to avoid bias toward larger values because ground motions in this distance range are not always sufficient to trigger the existing accelerographs. In this case, however, the data points beyond 30 km lie below not above the mean regression line. The distance range for which a reasonably complete data set is currently available is not adequate for a good determination of slope; the standard error of the slope for the magnitude 5.0-5.7 class is 0.5. Judging from the data at greater distances, the slope of -1.2 ± 0.3 for the mean line for the magnitude 6.0-6.4 class appears to be a better estimate of the rate of attenuation to distances of at least 100 km for that data set. The slope of -2.0 ± 0.4 for the magnitude 7.1-7.7 class may overestimate the rate of attenuation, but the data are scanty.

Horizontal velocity. The peak horizontal velocity data from the small structures for the three magnitude classes are presented in Figures 5, 6, and 7. There are fewer velocity than acceleration points because integrations were not available for all the accelerograms. There are so few points for the magnitude 7.1-7.7 class that regression lines are not included on Figure 7.

As with acceleration, the peak velocity at a given distance tends to increase with magnitude. This is illustrated in Figure 8, which gives the 70 percent prediction intervals for the three magnitude classes. The interval for the 7.1-7.7 class is shown by dashed lines to emphasize the uncertainty in slope.

The slope of -0.6 ± 0.4 for the mean regression lines for the magnitude 6.4 data appears to be an underestimate of the rate of attenuation if one considers the San Fernando data described in the next section, which give better determinations because the distance range extends to 100 km. We were confident that all the instruments out to 100 km triggered in the San Fernando earthquake, but that was not the case for the whole magnitude class.

Horizontal displacement. The peak horizontal displacements for the three magnitude classes are given in Figures 9, 10, and 11. The scatter of the data is larger than for acceleration or velocity in each magnitude class, and the standard errors of the slopes of the mean regression lines exceed 0.5. The displacements are derived from double integration of high-pass filtered accelerograms and therefore represent high-pass filtered versions of the true ground displacement. The longer periods, which are contaminated by processing noise, are removed.

Hanks (1975) has studied the errors in displacement records derived by double integration of filtered accelerograms. He finds that the errors are typically less than 1 cm in the period range 5-8 seconds, 1-2 cm at periods near 10 seconds, and 2-4 cm in the period range 10-15 seconds. This raises the possibility that some of the low-amplitude data points in Figures 9 and 10 may be influenced by noise and may represent upper bounds to the actual ground displacement. Examination of the displacement records reveals that some of the low amplitude records have a character that is suggestive of noise rather

than signal. In spite of this, we have proceeded in the analysis with the understanding that the results may be compromised to some extent by the effect of noise on the weaker motions.

The overlap of the 70 percent prediction intervals for the three magnitude classes is shown in Figure 12. The amplitude increases with magnitude.

Duration. All the horizontal duration data are plotted in Figure 13 with different symbols for the different magnitude classes. The "X" symbol in Figure 13 denotes a zero duration; in such a case the peak acceleration on the record is less than 0.05 g. The upper and lower rows of X's represent zero durations for magnitude classes 6.4 and 5.3-5.7, respectively.

Two obvious and expected features stand out in Figure 13: the durations increase with increasing magnitude, and they decrease with increasing distance. The influence of magnitude is a reflection of the larger fault size and consequent increased time of rupture as magnitude is increased. The effect of distance is the result of the general decrease in amplitude with distance, given that we have used a fixed amplitude in the definition of duration. Had we defined duration in terms of some fraction of the peak amplitude, it is likely that the spreading apart of the seismic phases would have led to an increase of duration with distance.

Vertical data. The vertical data are presented in the same manner as the horizontal data. Peak vertical accelerations for the three magnitude classes are shown in Figures 14, 15, and 16; peak vertical velocities are shown in Figures 17, 18, and 19; and peak vertical displacements are shown in Figures 20, 21, and 22.

The whole data set. For the horizontal components, data from both large and

small structures taken together are presented in Figures 23 through 31.

THE SAN FERNANDO EARTHQUAKE

General comments. The San Fernando earthquake supplied more than one quarter of the total data points in our sample. The large number of data points from a single event provides the best basis for examining the effect of structure and local site conditions. The San Fernando earthquake also gives more accurate values than the whole $M = 6.0-6.9$ data set for the slopes of the regression lines for peak parameters against distance. This is the case because, as previously mentioned, the statistical analysis can be carried out over a greater range of distance for the San Fernando earthquake. The reader is reminded that, to avoid bias, not all the records from downtown Los Angeles are included in the data set.

In comparing peak parameters for different structural types and site conditions we use an analysis of variance technique (Acton, 1959, p. 80-83) to test the statistical significance of the observed differences between one data set and another. To state the matter more precisely, we consider the variance of the residuals and examine the statistical significance of the reduction in variance that occurs when different regression lines are fit to the two different data sets. The technique allows us to break down the reduction of variance into a component attributable to separate slopes and a component attributable to separate means. In what follows when we say a difference is significant we mean that it corresponds to a significant reduction in the variance of the residuals. A word of caution is appropriate concerning the analysis of variance tests. Essentially, they enable us to see how the differences between data sets compare with those that might be caused by

random sampling error. We should not be confident, however, that the strong motion data sets represent random samples, and in any case the statistical tests say nothing about the real physical meaning of the differences between data sets.

The effect of structure. In Figure 32 comparison is made between peak horizontal acceleration values recorded on soil at the base of small structures (S1) and large structures (S2). Figure 33 shows the mean regression lines and the 70 percent prediction intervals determined for the S1 and S2 data separately. The mean regression line for the S1 data lies above that for the S2 data and the analysis of variance tests indicate that the difference is significant at the 90 percent level. The difference in slope is not significant. The same comparisons are made for horizontal velocity in Figures 34 and 35. In the case of velocity the mean regression line for the S1 data lies generally below that for the S2 data, though they cross, and the difference is statistically significant at the 98 percent level, though unimpressive to the eye. The S1 line is steeper, and the difference in slope is significant at the 90 percent level. The horizontal displacement data is given in Figures 36 and 37. For displacement the mean regression line for the S1 data lies below that for the S2 data, and the difference is significant at the 99 percent level. The difference in slope is not significant.

In summary we can say that for most of the distance range covered by the regression analysis peak horizontal acceleration is less and peak horizontal velocity and displacement are greater on the average at the base of large structures than at the base of small structures. The attenuation with distance is greater for the small structures for all three parameters, but the difference is statistically significant only in the case of peak velocity.

The result that acceleration values from the large structures are lower on the average is what would be expected if soil-structure interaction biases those data downward. This encourages us in our preference for the small-structure data as a basis for estimating free-field ground motion. In general, however, the differences between the data from the large structures and the small structures are relatively small compared with the range of either data set, and we do not believe that firm conclusions are warranted solely on the basis of formal statistical tests. The differences may be due to soil-structure interaction, but more study would be required to demonstrate this.

The effect of site geology. Figure 38 gives a comparison of peak horizontal acceleration recorded at the base of small structures on rock and soil.

Figure 39 shows the mean regression line and 70 percent confidence intervals determined for the two data sets separately. The analysis of variance tests indicate that the differences are not significant in either slope or level. Peak horizontal velocity data for small structures on both rock and soil sites are compared in Figures 40 and 41. The mean regression line is higher for soil and that difference is significant at the 98 percent level. The difference in slope is not significant. Peak horizontal displacement data are compared in Figures 42 and 43. The mean regression line for soil is higher and the difference is significant at the 98 percent level. The difference in slope is not significant even at the 75 percent level.

Apparently, peak horizontal acceleration is essentially the same on the average on rock and soil sites, whereas peak horizontal velocity and displacement are both larger on soil sites. This relationship is not the result of any obvious bias in the data. Examination of Figures 38, 40, and 42 does not show any gross effect from bias in the distribution of stations with

distance. To test for bias due to the non-uniform azimuthal distribution of the data (Hanks, 1975) we determined the azimuth of each station with respect to a point in the center of the zone of fault rupture (34.37° N. Lat., 118.42° W. Long.). A mean regression line against distance was determined for all the peak horizontal acceleration data for small structures in the distance range 15-100 km (with distance measured to the closest point on the rupture surface as before). Residuals to that regression line are plotted against azimuth in a polar diagram in Figure 44 with rock sites shown as "X"s and soil sites as diamonds. The circle represents zero residual. No strong systematic difference is apparent between rock and soil. Figure 45 gives the corresponding plot for the velocity data. Although the azimuthal coverage is far from complete, we can say that in any range of azimuth for which both rock and soil points are present, the soil residuals are more positive. Similar results are obtained for the displacement data (Figure 46).

We tentatively conclude that amplification of velocity and displacement is a real effect associated with soil sites. We presume that for the soil sites some sort of amplification mechanisms are operating on the longer periods that are dominant on velocity and displacement records. In the case of the shorter periods that are dominant on acceleration records these mechanisms are counterbalanced by anelastic attenuation. We will not speculate here on the nature of the amplification mechanisms. Similar conclusions on the effect of site conditions on strong motion in the San Fernando earthquake were reported by Duke and others (1972), Trifunac (1976), and Arnold and others (1976).

PREVIOUSLY PUBLISHED CURVES FOR
PEAK ACCELERATION

There are a large number of published correlations between ground motion parameters and distance, magnitude and site conditions. They have been described by Trifunac and Brady (1976) and discussed by Seed and others (1976). We consider here only three recently published, widely known relationships proposed for peak acceleration.

All studies of strong motion data are handicapped by the limited number of data points at small distances from the source. Attempts to predict strong motion parameters at short distance are forced to rely upon rather tenuous assumptions.

Curves for mean peak acceleration are shown in Figure 47 for a magnitude 6.6 earthquake. Also shown (solid lines) is the 70 percent prediction interval for the small-structure, magnitude 6.0-6.4 data set of this report. Most of the points in that data set came from the magnitude 6.4 San Fernando earthquake, so the comparison is appropriate from the standpoint of magnitude. Data from large structures, however, were not excluded in the development of the other curves.

The curve labeled "S" was developed by Schnabel and Seed (1973) for rock sites and is based on strong motion data extended to near distances with the help of theoretical attenuation curves. Because the theoretical curves are based on the conservation of radiated energy, however, they apply strictly only to quantities related to the energy represented by the whole duration of the seismic record. Application of the curves to peak parameters is an approximation of uncertain accuracy. The measure of distance used by Schnabel and Seed is the shortest distance to the rupture surface, the same measure as

used in this report.

The curves labeled "T0" and "T2" are the mean curves given by Trifunac (1976) for soft and hard sites, respectively. These curves are based on a data set very similar to the one used in this report, including data from both large and small structures. The distance measure used by Trifunac is epicentral distance. The curves were fitted to the data on the assumption that the distance dependence is that of the function given by Richter (1958) for calculating local magnitudes in Southern California. The accuracy of that assumption is difficult to evaluate. Furthermore, the distance function given by Richter is not very well defined for distances between 0 and 20 km, which is the range most important for strong motion predictions.

The curve labeled "D" was developed by Donovan (1973) for soil sites. It was obtained by fitting 678 data points by a function of the form

$$y = b_1 e^{b_2 m} (R + 25)^{-b_3}$$

where y is peak acceleration, m is magnitude, R is hypocentral distance in kilometers and b_1 , b_2 , and b_3 are adjustable constants. The arbitrary constant 25 that is added to the distance is for the purpose of reducing the predicted values at small distances. The size of the constant has a very large influence on the near values, but sufficient near data points are not available for a meaningful determination of the appropriate size. Donovan states that the function fits the data better when the arbitrary constant is 25 than when it is zero, but it is unclear why it should be 25 rather than 15, 10, or 5.

The corresponding curves are compared in Figure 48 for a magnitude 7.6

earthquake. The solid lines show the 70 percent prediction interval for the magnitude 7.1-7.7 data set of this report. Most of the points in that data set came from the magnitude 7.7 Kern County earthquake.

The amount of disagreement shown in Figures 47 and 48 is not surprising in view of the different assumptions, different measures of distance, and different data sets used in arriving at the different curves. The disagreement is, as might be expected, the greatest at short distances.

ESTIMATION OF PEAK PARAMETERS AT SHORT DISTANCES

General comments. The regression lines given in a previous section of this report provide the means for estimating peak ground motion parameters at distances greater than 5 km for magnitude 5.0-5.9 earthquakes, at distances greater than 15 km for magnitude 6.0-6.9 earthquakes and at distances greater than 40 km for magnitude 7.0-7.9 earthquakes. Unfortunately, most of the damage from earthquakes can be expected to occur at shorter distances. Attempts have been made, as described in the preceding section, to provide curves for estimating at shorter distances. For reasons given in the preceding section we do not have complete confidence in those curves. We will not venture our own set of curves, but will discuss briefly some of the considerations bearing on ground motion estimates near the source. Further discussion of these questions in greater depth is given by Boore (1974).

There have been a number of studies using simplified models of the faulting process to set limits on the ground motion at the fault surface (Housner, 1965; Ambraseys, 1969; Brune, 1970; Ida, 1973). Brune's (1970) near source model assumes that rupture occurs instantaneously over the fault

plane. The peak particle velocity is proportional to the stress drop and equals 100 cm/sec for a stress drop of 100 bars. The peak acceleration is infinite if all frequencies are included, but if frequencies above 10 Hz are filtered out of the acceleration pulse the peak value is 2 g. This is a useful model for relating ground motion to the physics of the rupture process, but it does not give firm upper limits. An argument can be made for larger motions if one takes rupture propagation into account (Ida, 1973; Andrews, 1976). Furthermore, the peak values of ground motion may represent localized high stress drops as Hanks and Johnson (1976) have suggested for peak acceleration. Such localized stress drops might easily exceed one kilobar.

The peak acceleration at the surface is limited by the strength of near surface materials as has been pointed out by Ambrasey (1974). For sites near the source underlain by soil material of low strength, this factor may control the value of peak acceleration. This consideration may also apply to rock sites if the rock is sufficiently weathered. Determination of the limiting acceleration, however, would require reliable measurement of the dynamic, in situ strength of the soil at a particular site. In the absence of adequate measurements one must presume that the acceleration could be at least as large as 0.5g, which was recorded on a thickness of more than 60 meters of water-saturated alluvium at station number 2 in the Parkfield earthquake (Shannon and Wilson, Inc. and Agbabian Associates, 1976).

In the case of peak displacement, as pointed out by Trifunac (1976), if one assumes no overshoot, the peak is limited to less than one half the static dislocation amplitude. The latter is known for many historical earthquakes and may be estimated as a function of magnitude (Bonilla and Buchanan, 1970).

The accelerogram recorded at Pacoima Dam during the San Fernando

earthquake has major significance for near source ground motion estimates. The instrument is located only 3 km from the rupture surface at a rock site where the topographic relief is severe. The peak recorded horizontal acceleration is 1.25g, velocity 113 cm/sec, and displacement 38 cm. This is the only accelerogram ever recorded within 5 km for an earthquake of magnitude as large as 6.4, and as such ought to have strong influence on estimates of near-source ground motion. The possibility of topographic amplification needs consideration. A two-dimensional finite-difference study by Boore (1973) suggests that the acceleration may have been amplified by as much as 50 percent but that the velocity and displacement were relatively unaffected. Given these considerations, it would be difficult for us to accept estimates less than about 0.8g, 110 cm/sec, and 40 cm, respectively, for the mean values of peak acceleration, velocity and displacement at rock sites within 5 km of fault rupture in a magnitude 6.5 earthquake. We recognize that these numbers represent one earthquake with a particular focal mechanism and that estimates are bound to change when more data becomes available. We presume that the statistical scatter about the mean will be at least as great for the near-in sites as at the greater distances where data is available.

The accelerograph at Pacoima dam was only 3 km from the nearest point on the rupture surface, but the nearest point was not the source of the peak motions. As noted previously the source for the peak velocity and for the peak acceleration are different points on the rupture surface separated by perhaps as much as 20 km (Hanks, 1974; Bouchon and Aki, 1977).

Above magnitude 6.5 there are essentially no data for estimating the effect of magnitude on near-fault peak acceleration, velocity and displacement, other than the static fault offset divided by 2 as a bound on

the peak displacement. Conservatism requires the presumption of some increase with magnitude. Hanks and Johnson (1976) presented a set of peak acceleration data at source distance of approximately 10 km for earthquakes in the magnitude range 3.2-7.1. The only data point above magnitude 6.5 was for the Imperial Valley earthquake of 1940 which they assign a magnitude of 7.1 in contrast to our value 6.4, so the data set can be applied to magnitudes greater than 6.5 only as an extrapolation. The data set shows some dependence of peak accelerations on magnitude, but Hanks and Johnson argue that the data are consistent with the idea of magnitude-independent source properties. The data plotted as the logarithm of peak acceleration against magnitude can be fit by a straight line with a slope equivalent to an increase by a factor of 1.4 per magnitude unit. This should not be used for extrapolation beyond magnitude 6.5, however, because the data set was deliberately chosen to represent relatively high values, and thus the slope of the line fitting the data may not be the same as the slope of the line representing mean values or, for that matter, of the line representing values for any fixed probability.

At sites other than rock sites accelerations might be less because of the limited strength of near-surface materials, but, as previously noted, determining how much less would require dynamic, in-situ measurements of soil properties. The amplification of peak velocity at soil sites compared to rock sites may not be so great close to the fault because of the energy lost in nonlinear soil deformation, but numerical modeling (Joyner and Chen, 1975) demonstrates the possibility of amplification of velocity by as much as 30 percent even under conditions of intense deformation. The possibility of greater amplification cannot be excluded. Amplification of displacement at soil sites should be expected close to the fault, as at greater distances, if

the soil column is sufficiently thick.

ACKNOWLEDGMENTS

We are grateful to R. P. Maley for assistance in obtaining information on strong motion recording site conditions and to A. G. Brady for unpublished strong motion data. R. B. Matthieson, T. C. Hanks, and A. G. Brady reviewed the manuscript and suggested improvements.

TABLE I
Sources of Data Used in Assigning Magnitudes
and Station Distances

<u>Earthquake</u>	<u>Date (GMT)</u>			<u>Sources</u>
	<u>Month</u>	<u>Day</u>	<u>Year</u>	
Bear Valley, California	2	24	72	Ellsworth(1975)
Bear Valley, California	11	28	74	Person(1975);W.H.K. Lee (written communication, 1976)
Ferndale, California	6	7	75	Nason and others(1975) Stewart Smith (written communication, 1976)
Daly City, California	3	22	57	Tocher(1959);Cloud(1959)
Lytle Creek, California	9	12	70	T.C. Hanks (written communication, 1971)
Parkfield, California	6	28	66	McEvilly and others(1967) Lindh and Boore(1973) Trifunac and Udawadia(1974) Lindh (oral communication, 1976)
Fairbanks, Alaska	6	21	67	Gedney and Berg(1969)
Santa Rosa, California	10	2	69	Steinbrugge and others(1970) Unger and Eaton(1970) Unger and Eaton (written communication, 1976)
Oroville, California	1	8	75	Bufe and others(1976) Lahr and others(1976)
Point Mugu, California	2	21	73	Ellsworth and others(1973) Boore and Stierman(1976) Stierman and Ellsworth(1976)
Managua, Nicaragua	12	23	72	Dewey and others(1973) Ward and others(1973) Knudson and Hansen A.(1973)
Imperial Valley, California	5	19	40	Trifunac and Brune(1970) Trifunac(1972);Richter(1958)

CONTINUED

TABLE 1 (CONTINUED)

<u>Earthquake</u>	<u>Date (GMT)</u>			<u>Sources</u>
	<u>Month</u>	<u>Day</u>	<u>Year</u>	
Borrego Mountain, California	4	9	68	Allen and Nordquist(1972) Hamilton(1972)
San Fernando, California	2	9	71	Allen and others(1973) Allen and others(1971) R.L. Wesson (written communication, 1974)
Puget Sound, Washington	4	13	49	Nuttli(1952);Page and others (1972)
Hebgen Lake, Montana	8	18	59	Tocher(1962);Page and others (1972)
Sitka, Alaska	7	30	72	Page and Gawthrop(1973) Gawthrop and Page (unpub- lished data)
Kern County, California	7	21	52	Gutenberg(1955) Richter(1955);Richter(1958) Page and others(1972)

A P P E N D I X A

STATISTICAL PARAMETERS

Linear regression analysis (Dixon and Massey, 1957) was employed to describe the distance dependence of the peak parameters. Using the symbol y for the peak parameter and the symbol x for distance we fit the data by a straight line

$$v = A + B u$$

where $v = \log_{10} y$

and $u = \log_{10} x$.

Values for A and B are given by the following equations

$$A = \frac{\sum v - B \sum u}{n}$$

$$B = \frac{n \sum uv - \sum u \sum v}{n \sum u^2 - (\sum u)^2}$$

where the summations are taken over all the points in the data set and n is the number of points. The scatter in the data is measured by $s_{v|u}$, the standard error of estimate of y for a given u. That quantity is obtained from the following equations:

$$s_{v|u} = \frac{n-1}{n-2} (s_v^2 - B s_u^2)$$

$$s_u^2 = \frac{1}{n(n-1)} [n \sum u^2 - (\sum u)^2]$$

$$s_v^2 = \frac{1}{n(n-1)} [n \sum v^2 - (\sum v)^2].$$

For a given confidence level, the prediction interval for a single prediction of v given u is

$$(A + Bu) \pm t_{\alpha/2, n-2} s_{v|u} \sqrt{1 + \frac{1}{n} + \frac{(u - \bar{u})^2}{(n-1)s_u^2}}$$

where \bar{u} is the mean of u values, the confidence level is $(1 - \alpha)$, and $t_{\alpha/2, n-2}$ is the abscissa of the Student's t distribution for a cumulative probability of $(1 - \alpha/2)$ and $(n - 2)$ degrees of freedom. The lines describing the prediction intervals are curved because of statistical uncertainty in the regression coefficient B . A measure of that uncertainty is the standard error of B , which is given by

$$s_B = \frac{s_{v|u}}{s_u \sqrt{n-1}}$$

Table A1 lists the statistical parameters A , B , $s_{v|u}$, s_B and n for the data sets discussed in the text. The number of the Figure displaying the data set is also given.

Table A1

<u>Data Set</u>	<u>Figure No.</u>	<u>A</u>	<u>B</u>	<u>$s_{v/u}$</u>	<u>s_{B}</u>	<u>n</u>
HORIZONTAL ACCELERATION:						
M = 5.0-5.7 class 1	1	0.17	-0.93	0.37	0.46	19
M = 6.0-6.4 class 1	2	0.96	-1.23	0.20	0.32	16
M = 7.1-7.7 class 1	3	2.65	-2.01	0.26	0.43	9
M = 5.0-5.7 all	23	0.05	-0.86	0.35	0.40	24
M = 6.0-6.4 all	24	0.81	-1.20	0.20	0.15	44
M = 7.1-7.7 all	25	2.65	-2.00	0.21	0.31	14
San Fernando R1	39	1.45	-1.56	0.18	0.23	10
San Fernando S1	39	1.09	-1.34	0.18	0.25	12
San Fernando S2	33	0.90	-1.29	0.15	0.15	18
HORIZONTAL VELOCITY:						
M = 5.3-5.7 class 1	5	2.35	-1.22	0.38	0.61	11
M = 6.4 class 1	6	1.93	-0.58	0.25	0.45	14
M = 7.1-7.7 class 1	7	2.45	-0.72	0.16	0.42	6
M = 5.3-5.7 all	26	2.31	-1.26	0.35	0.48	16
M = 6.4 all	27	2.35	-0.85	0.20	0.19	35
San Fernando R1	41	3.12	-1.51	0.26	0.39	9
San Fernando S1	41	3.06	-1.31	0.16	0.23	11
San Fernando S2	35	2.60	-0.96	0.08	0.08	18
HORIZONTAL DISPLACEMENT:						
M = 5.3-5.7 class 1	9	1.81	-1.15	0.36	0.59	11
M = 6.4 class 1	10	1.48	-0.55	0.30	0.53	14
M = 7.1-7.7 class 1	11	2.34	-0.86	0.22	0.56	6
M = 5.3-5.7 all	29	1.60	-1.03	0.34	0.46	16
M = 6.4 all	30	1.91	-0.77	0.28	0.27	35
San Fernando R1	43	2.72	-1.52	0.25	0.38	9
San Fernando S1	43	2.07	-0.90	0.25	0.37	11
San Fernando S2	37	2.09	-0.76	0.19	0.18	18
VERTICAL ACCELERATION:						
M = 5.0-5.7 class 1	14	-0.27	-0.77	0.29	0.36	19
M = 6.0-6.4 class 1	15	1.36	-1.70	0.20	0.32	16
M = 7.1-7.7 class 1	16	1.55	-1.58	0.21	0.39	8
VERTICAL VELOCITY:						
M = 5.3-5.7 class 1	17	1.62	-0.96	0.30	0.48	11
M = 6.4 class 1	18	1.86	-0.80	0.18	0.32	14
VERTICAL DISPLACEMENT:						
M = 5.3-5.7 class 1	20	1.22	-0.93	0.29	0.47	11
M = 6.4 class 1	21	1.15	-0.53	0.14	0.25	14

A P P E N D I X B

STRONG MOTION DATA

Key for listing of strong motion data

Associated with each earthquake there is a six-digit number followed by a four-digit number. The first two digits of the six-digit number denote the year, the second two the month and the third two the day. The first two digits of the four-digit number represent the hour (Universal Time) and the second two the minute.

Abbreviations are explained below:

- MAG - Earthquake Magnitude. Richter (1958) local magnitude if available, otherwise surface wave magnitude.
- STA # - Station number as given by the U.S. Geological Survey (1976b).
- STRUC - Code for associated structure. One if data were recorded at the base of a one- or two-story building, two if data were recorded at the base of a larger building or on a dam abutment.
- DIST - Shortest distance to the surface of fault slippage.
- AC - Accuracy code for distance. A if the uncertainty is less than 2 km, B if it is between 2 and 5 km, and C if it is between 5 and 25 km.
- ACCEL - Peak acceleration as a fraction of the acceleration of gravity.
- VEL - Peak velocity in cm/sec.
- DISP - Peak displacement in cm.
- DUR - Duration in seconds, defined as the time interval between the first and last horizontal acceleration peaks equal to or greater than 0.05 g.
- SRC - Code denoting source of strong motion data. List is given following the data.
- GEO - Code for geologic conditions at recording site. S

for soil (greater than 4 to 5 meters in thickness) and R for rock.

REF - Code for source of information on stations. List of references follows station list.

* - Denotes station selected from the special area in downtown Los Angeles as described in the text.

LISTING OF STRONG MOTION DATA

720224 1556 BEAR VALLEY, CALIFORNIA										MAG = 5.0						
SOIL STATIONS:										***** HORIZONTAL *****			***** VERTICAL *****			STATION LOCATION
STA#	STRUC	DIST	AC	ACCEL	VEL	DISP	DUR	SRC	ACCEL	VEL	DISP	SRC				
1028	1	31.0	A	0.030					B	0.010			B	HOLLISTER - CITY HALL		
741128 2301 BEAR VALLEY, CALIFORNIA										MAG = 5.2						
ROCK STATIONS:										***** HORIZONTAL *****			***** VERTICAL *****			STATION LOCATION
STA#	STRUC	DIST	AC	ACCEL	VEL	DISP	DUR	SRC	ACCEL	VEL	DISP	SRC				
1032	1	18.0	A	0.011					E	0.013			E	SAGO CENTRAL - HARRIS RANCH		
SOIL STATIONS:										***** HORIZONTAL *****			***** VERTICAL *****			STATION LOCATION
STA#	STRUC	DIST	AC	ACCEL	VEL	DISP	DUR	SRC	ACCEL	VEL	DISP	SRC				
1377	1	8.9	A	0.120					G	0.050			G	SAN JUAN BAUTISTA (C126) - 24 POLK		
1028	1	10.8	A	0.170					G	0.070			G	HOLLISTER - CITY HALL		
1250	1	10.8	A	0.140					G	0.030			G	GILROY (C6) - GEOL BLDG, GAL COL		
1202	1	37.0	A	0.030					G	0.050			G	STONE CANYON EAST, CALIF.		
750607 846 FERNDALE, CALIFORNIA										MAG = 5.2						
ROCK STATIONS:										***** HORIZONTAL *****			***** VERTICAL *****			STATION LOCATION
STA#	STRUC	DIST	AC	ACCEL	VEL	DISP	DUR	SRC	ACCEL	VEL	DISP	SRC				
1249	1	32.0	B	0.220					I	0.030			I	CAPE MENDOCINO (C5) - PETROLIA		
1278	1	64.0	B	0.100					I				I	SHELTER COVE, STA 2 (C41) - PWR PLT		
SOIL STATIONS:										***** HORIZONTAL *****			***** VERTICAL *****			STATION LOCATION
STA#	STRUC	DIST	AC	ACCEL	VEL	DISP	DUR	SRC	ACCEL	VEL	DISP	SRC				
1023	1	24.0	B	0.240					I	0.050			I	FERNDALE - OLD CITY HALL, BROWN ST		
1398	1	34.0	B	0.190					I	0.030			I	PETROLIA (C156) - GENERAL STORE		
570322 1944 DALY CITY, CALIFORNIA										MAG = 5.3						
ROCK STATIONS:										***** HORIZONTAL *****			***** VERTICAL *****			STATION LOCATION
STA#	STRUC	DIST	AC	ACCEL	VEL	DISP	DUR	SRC	ACCEL	VEL	DISP	SRC				
1117	1	8.0	B	0.127	4.9	2.3	1.6	A	0.051	1.2	0.7	A	SAN FRANCISCO - GOLDEN GATE PARK			
SOIL STATIONS:										***** HORIZONTAL *****			***** VERTICAL *****			STATION LOCATION
STA#	STRUC	DIST	AC	ACCEL	VEL	DISP	DUR	SRC	ACCEL	VEL	DISP	SRC				
1080	2	12.0	B	0.103	5.0	1.1	1.4	A	0.050	2.3	0.6	A	SAN FRANCISCO - STATE BLDG			
1065	2	14.0	B	0.055	2.9	1.3	0.0	A	0.036	1.3	0.4	A	SAN FRANCISCO - ALEXANDER BLDG			
1078	2	14.0	B	0.048	5.0	1.4	0.0	A	0.034	1.5	0.9	A	SAN FRANCISCO - SOUTHERN PACIFIC BLDG			
1049	2	24.0	B	0.047	1.9	1.5	0.0	A	0.023	0.9	1.3	A	OAKLAND - CITY HALL			
1081	2	58.0	B	0.007					B	0.005			B	SAN JOSE - BANK OF AMERICA BLDG		
700912 1430 LYITLE CREEK, CALIFORNIA										MAG = 5.4						

ROCK STATIONS:
 STA# STRUC DIST AC ACCEL VEL DISP DUR SRC ACCEL VEL DISP SRC STATION LOCATION

290	1	15.0	B	0.205	9.6	2.2	2.8	A	0.076	3.2	1.4	A	WRIGHTWOOD - 6074 PARK DRIVE
111	1	18.0	B	0.086	5.5	2.4	1.1	A	0.093	2.6	1.2	A	CEDAR SPRINGS - ALLEN RANCH
116	1	19.0	B	0.179				A	0.094			A	DEVILS CANYON - FILTER PLANT
278	2	32.0	B	0.022				A	0.018			A	SAN DIMAS - PUDDINGSTONE RESERVOIR
104	2	46.0	B	0.054				A	0.016			A	ARCADIA - SANTA ANITA RESERVOIR
266	1	58.0	B	0.015				B	0.010			B	PASADENA - CIT SEISMOLOGY LAB
137	2	70.0	B	0.015				A	0.006			A	*LOS ANGELES - WATER & POWER
110	1	110.0	B	0.025				A	0.011			A	CASTAIC - OLD RIDGE ROUTE

SOIL STATIONS:
 STA# STRUC DIST AC ACCEL VEL DISP DUR SRC ACCEL VEL DISP SRC STATION LOCATION

112	1	18.0	B	0.073	4.0	1.2	0.4	A	0.044	1.3	0.4	A	CEDAR SPRINGS - PUMP PLANT
274	2	28.0	B	0.119	4.8	1.8	1.0	A	0.055	1.8	1.5	A	SAN BERNARDINO - HALL OF RECORDS
113	1	29.0	B	0.045	2.5	0.9	0.0	A	0.042	1.3	0.7	A	COLTON - S. CAL. EDISON CO.
129	2	34.0	B	0.019				B	0.009			B	LOMA LINDA - UNIV. MED. CENTER
264	2	57.0	B	0.023	1.5	1.8	0.0	A	0.015	0.7	0.5	A	PASADENA - CIT MILLIKAN LIBRARY
267	2	60.0	B	0.025	2.0	2.4	0.0	A	0.017	1.9	1.4	A	PASADENA - CIT JPL LAB
181	2	66.0	B	0.026				A	0.012			A	LOS ANGELES - 1640 SOUTH MARENGO
133	2	77.0	B	0.015				A	0.006			A	*HOLLYWOOD STORAGE - BASEMENT
135	1	77.0	B	0.021				A	0.007			A	*HOLLYWOOD STORAGE - P.E. LOT
125	1	95.0	B	0.010				A	0.006			A	LAKE HUGHES ARRAY 1 - FIRE STATION
103	1	113.0	B	0.020				B	0.005			B	ANZA - ANZA POST OFFICE

660628 426 PARKFIELD, CALIFORNIA MAG = 5.5

ROCK STATIONS:
 STA# STRUC DIST AC ACCEL VEL DISP DUR SRC ACCEL VEL DISP SRC STATION LOCATION

1438	1	16.1	A	0.411	22.5	5.5	3.7	A	0.165	4.4	1.4	A	CHOLAME-SHANDON: TEMBLOR
1083	1	63.6	A	0.018	1.1	1.2	0.0	A	0.007	1.3	0.9	A	SAN LUIS OBISPO - CITY REC. BLDG
110	1	204.0	A	0.004				B					CASTAIC - OLD RIDGE ROUTE

SOIL STATIONS:
 STA# STRUC DIST AC ACCEL VEL DISP DUR SRC ACCEL VEL DISP SRC STATION LOCATION

1013	1	6.6	A	0.509	78.1	26.4	12.1	A	0.349	14.1	4.3	A	CHOLAME-SHANDON ARRAY NO. 2
1014	1	9.3	A	0.467	25.4	7.1	7.9	A	0.181	7.3	3.4	A	CHOLAME-SHANDON ARRAY NO. 5
1015	1	13.0	A	0.279	11.8	4.4	7.8	A	0.138	4.5	2.1	A	CHOLAME-SHANDON ARRAY NO. 8
1016	1	17.3	A	0.072	8.0	5.7	0.6	A	0.061	5.0	2.6	A	CHOLAME-SHANDON ARRAY NO. 12
1095	1	105.0	A	0.012	2.2	2.5	0.0	A	0.007	1.1	1.5	A	TAFT - LINCOLN HS TUNNEL
1011	1	112.0	A	0.006				B					BUENA VISTA - GROUND STATION
1028	1	123.0	A	0.003				B					HOLLISTER - CITY HALL
283	1	162.0	A	0.004				B	0.002			B	SANTA BARBARA - COURTHOUSE
272	1	208.0	A	0.005				B	0.001			B	PORT HUENEME - NAVY LABORATORY
133	2	261.0	A	0.001				B					*HOLLYWOOD STORAGE - BASEMENT
135	1	261.0	A	0.001				B					*HOLLYWOOD STORAGE - P.E. LOT
475	1	272.0	A	0.001				B					PASADENA - CIT ATHENAEUM

670621 1804 FAIRBANKS, ALASKA MAG = 5.6

ROCK STATIONS:
 STA# STRUC DIST AC ACCEL VEL DISP DUR SRC ACCEL VEL DISP SRC STATION LOCATION

2707	1	15.0	B	0.060				C	0.060			C	FAIRBANKS, ALASKA - UNIV OF ALASKA
------	---	------	---	-------	--	--	--	---	-------	--	--	---	------------------------------------

691002 456 SANTA ROSA, CALIFORNIA

MAG = 5.6

ROCK STATIONS:			***** HORIZONTAL *****				***** VERTICAL *****				STATION LOCATION		
STA#	STRUC	DIST	AC	ACCEL	VEL	DISP	DUR	SRC	ACCEL	VEL	DISP	SRC	STATION LOCATION
1057	1	77.0	B	0.007				B	0.002			B	PLEASANT HILL - DIABLO VALLEY COL.
1074	2	79.0	B	0.011				B	0.004			B	SAN FRANCISCO - 390 MAIN
SOIL STATIONS:			***** HORIZONTAL *****				***** VERTICAL *****				STATION LOCATION		
1093	1	62.0	B	0.005				B	0.001			B	SAN PABLO - CONTRA COSTA COLLEGE
1065	2	79.0	B	0.008				B	0.003			B	SAN FRANCISCO - ALEXANDER BLDG
1071	2	79.0	B	0.015				B	0.007			B	SAN FRANCISCO - BETHLEHEM PAC BLDG
1078	2	79.0	B	0.016				B	0.007			B	SAN FRANCISCO - SOUTHERN PACIFIC BG
1049	2	82.0	B	0.006				B	0.002			B	OAKLAND - CITY HALL
1001	1	109.0	B	0.018				B	0.002			B	APEEL ARRAY - STATION 1
1002	1	110.0	B	0.017				B	0.002			B	APEEL ARRAY - STATION 2

691002 619 SANTA ROSA, CALIFORNIA

MAG = 5.7

ROCK STATIONS:			***** HORIZONTAL *****				***** VERTICAL *****				STATION LOCATION		
STA#	STRUC	DIST	AC	ACCEL	VEL	DISP	DUR	SRC	ACCEL	VEL	DISP	SRC	STATION LOCATION
1057	1	77.0	B	0.009				B	0.002			B	PLEASANT HILL - DIABLO VALLEY COL.
1074	2	79.0	B	0.012				B	0.004			B	SAN FRANCISCO - 390 MAIN
SOIL STATIONS:			***** HORIZONTAL *****				***** VERTICAL *****				STATION LOCATION		
1093	1	62.0	B	0.003				B	0.003			B	SAN PABLO - CONTRA COSTA COLLEGE
1065	2	79.0	B	0.012				B	0.003			B	SAN FRANCISCO - ALEXANDER BLDG
1071	2	79.0	B	0.027				B	0.007			B	SAN FRANCISCO - BETHLEHEM PAC BLDG
1078	2	79.0	B	0.020				B	0.008			B	SAN FRANCISCO - SOUTHERN PACIFIC BG
1049	2	82.0	B	0.013				B	0.004			B	OAKLAND - CITY HALL
1001	1	109.0	B	0.029				B	0.002			B	APEEL ARRAY - STATION 1
1002	1	110.0	B	0.021				B	0.009			B	APEEL ARRAY - STATION 2

750801 2020 OROVILLE, CALIFORNIA

MAG = 5.7

ROCK STATIONS:			***** HORIZONTAL *****				***** VERTICAL *****				STATION LOCATION		
STA#	STRUC	DIST	AC	ACCEL	VEL	DISP	DUR	SRC	ACCEL	VEL	DISP	SRC	STATION LOCATION
1051	1	8.0	A	0.110	5.0	1.6	0.0	H	0.120	5.3	2.7	H	OROVILLE SEISMOGRAPH STATION
1293	1	32.0	A	0.040				H	0.030			H	PARADISE (C58) - KEWG TRNSMTR BLDG
SOIL STATIONS:			***** HORIZONTAL *****				***** VERTICAL *****				STATION LOCATION		
1291	1	30.0	A	0.070				H	0.040			H	MARYSVILLE (C56) - CDOT MAINT BLDG
1292	1	31.0	A	0.080				H	0.030			H	CHICO (C57) - 2334 FAIR STREET

730221 1445 POINT MUGU, CALIFORNIA

MAG = 6.0

ROCK STATIONS:			***** HORIZONTAL *****				***** VERTICAL *****				STATION LOCATION		
STA#	STRUC	DIST	AC	ACCEL	VEL	DISP	DUR	SRC	ACCEL	VEL	DISP	SRC	STATION LOCATION

655 1 53.0 B 0.031 E 0.014 E JENSEN FILTER PLT - 13100 BALBOA, LA

SOIL STATIONS:
 STA# STRUC DIST AC ACCEL VEL DISP DUR SRC ACCEL VEL DISP SRC STATION LOCATION

272	1	24.0	B	0.130			D	0.040		D	PORT HUENEME - NAVY LABORATORY
610	2	51.0	B	0.043			E	0.016		E	LOS ANGELES - 18321 VENTURA
657	2	51.0	B	0.036			E	0.012		E	SANTA MONICA - 201 OCEAN
118	2	53.0	B	0.042			E	0.016		E	LOS ANGELES - 16661 VENTURA
497	2	53.0	B	0.060			D	0.010		D	LOS ANGELES - 16633 VENTURA
512	2	54.0	B	0.036			E	0.016		E	LOS ANGELES - 16255 VENTURA
259	2	55.0	B	0.032			E	0.013		E	LOS ANGELES - 16055 VENTURA
461	2	55.0	B	0.040			E	0.023		E	LOS ANGELES - 15910 VENTURA

721223 629 MANAGUA, NICARAGUA MAG = 6.2

SOIL STATIONS:
 STA# STRUC DIST AC ACCEL VEL DISP DUR SRC ACCEL VEL DISP SRC STATION LOCATION

3501	1	5.0	A	0.390			D	0.330		D	MANAGUA, NIC. - ESSO REFINERY
------	---	-----	---	-------	--	--	---	-------	--	---	-------------------------------

400519 436 IMPERIAL VALLEY, CALIFORNIA MAG = 6.4

SOIL STATIONS:
 STA# STRUC DIST AC ACCEL VEL DISP DUR SRC ACCEL VEL DISP SRC STATION LOCATION

117	1	12.0	B	0.359	36.9	19.8	29.3	A	0.278	10.8	5.6	A	EL CENTRO - IRRIGATION SUBSTA.
-----	---	------	---	-------	------	------	------	---	-------	------	-----	---	--------------------------------

680409 228 BORREGO MTN., CALIFORNIA MAG = 6.4

ROCK STATIONS:
 STA# STRUC DIST AC ACCEL VEL DISP DUR SRC ACCEL VEL DISP SRC STATION LOCATION

270	1	105.0	A	0.018			F	0.006		F	PERRIS - RESERVOIR		
280	1	122.0	A	0.048	4.2	2.9	0.0	A	0.064	3.7	1.7	A	SAN ONOFRE - SCE NUCLEAR PLANT
116	1	141.0	A	0.011			F	0.009		F	DEVILS CANYON - FILTER PLANT		
278	2	168.0	A	0.017			F	0.004		F	SAN DIMAS - PUDDINGSTONE RESERVOIR		
104	2	190.0	A	0.004			F	0.001		F	ARCADIA - SANTA ANITA RESERVOIR		
266	1	200.0	A	0.007			F	0.002		F	PASADENA - CIT SEISMOLOGY LAB		
136	2	203.0	A	0.012	3.1	2.3	0.0	A	0.005	1.2	1.0	A	*LOS ANGELES - SUBWAY TERMINAL
190	2	207.0	A	0.007			F	0.009		F	LOS ANGELES - 2011 ZONAL		
279	2	229.0	A	0.009			F	0.006		F	SAN FERNANDO - PACOIMA DAM		
121	2	249.0	A	0.003			F	0.001		F	FAIRMONT STATION - RESERVOIR		
110	1	256.0	A	0.008			F	0.003		F	CASTAIC - OLD RIDGE ROUTE		

SOIL STATIONS:
 STA# STRUC DIST AC ACCEL VEL DISP DUR SRC ACCEL VEL DISP SRC STATION LOCATION

117	1	45.0	A	0.142	25.8	12.2	3.1	A	0.036	3.4	3.9	A	EL CENTRO - IRRIGATION SUBSTA.
277	2	105.0	A	0.032	6.1	4.4	0.0	A	0.014	1.9	1.3	A	SAN DIEGO - LIGHT & POWER
113	1	130.0	A	0.031	3.5	4.3	0.0	A	0.022	1.8	1.1	A	COLTON - S. CAL. EDISON CO.
274	2	132.0	A	0.018			F	0.003		F	SAN BERNARDINO - HALL OF RECORDS		
112	1	147.0	A	0.006			F	0.003		F	CEDAR SPRINGS - PUMP PLANT		
281	2	157.0	A	0.013	4.4	3.5	0.0	A	0.006	2.2	1.9	A	SANTA ANA - ORANGE CO. ENG. BLDG
130	1	187.0	A	0.010	3.2	5.0	0.0	A	0.006	1.8	1.8	A	LONG BEACH - TERMINAL ISLAND
131	2	187.0	A	0.005			F	0.003		F	LONG BEACH - UTILITIES BLDG.		
288	2	196.0	A	0.019	4.7	2.7	0.0	A	0.008	2.4	1.5	A	VERNON - CENTRAL MFG. TERMINAL

264	2	197.0	A	0.011	2.3	1.8	0.0	A	0.007	1.1	0.8	A	PASADENA - CIT MILLIKAN LIBRARY
475	1	197.0	A	0.010	2.5	2.0	0.0	A	0.004	1.0	1.1	A	PASADENA - CIT ATHENAEUM
181	2	199.0	A	0.013				F	0.003			F	LOS ANGELES - 1640 SOUTH MARENGO
269	1	203.0	A	0.006				F	0.006			F	PEARBLOSSOM - PUMPING PLANT
267	2	204.0	A	0.008	1.3	0.8	0.0	A	0.005	1.0	0.7	A	PASADENA - CIT JPL LAB
122	2	208.0	A	0.023				F	0.017			F	GLENDALE - 633 E. BROADWAY
133	2	211.0	A	0.011				F	0.004			F	*HOLLYWOOD STORAGE - BASEMENT
135	1	211.0	A	0.013	3.2	2.1	0.0	A	0.005	1.1	1.1	A	*HOLLYWOOD STORAGE - P.E. LOT
118	2	227.0	A	0.008				F	0.001			F	LOS ANGELES - 16661 VENTURA
241	2	228.0	A	0.011				F	0.006			F	LOS ANGELES - 8244 ORION
125	1	253.0	A	0.009				F					LAKE HUGHES ARRAY 1 - FIRE STATION
2005	2	259.0	A	0.003				F	0.001			F	MOJAVE GENERATING PLANT
1052	1	281.0	A	0.013				F	0.013			F	OSO PUMPING PLANT
272	1	288.0	A	0.003				F					PORT HUENEME - NAVY LABORATORY
283	1	341.0	A	0.002				F					SANTA BARBARA - COURTHOUSE
1004	1	342.0	A	0.003				F	0.001			F	BAKERSFIELD - HARVEY AUDITORIUM
1095	1	359.0	A	0.002				F					TAFT - LINCOLN HS TUNNEL

710209 1400 SAN FERNANDO, CALIFORNIA

MAG = 6.4

ROCK STATIONS:			***** HORIZONTAL *****						***** VERTICAL *****							
STA#	STRUC	DIST	AC	ACCEL	VEL	DISP	DUR	SRC	ACCEL	VEL	DISP	SRC	STATION LOCATION			
279	2	3.2	A	1.251	113.2	37.7	13.3	A	0.718	58.3	19.3	A	SAN FERNANDO - PACOIMA DAM			
220	2	16.9	A	0.181	15.0	5.4	6.7	A	0.085	5.0	2.4	A	LOS ANGELES - 3838 LANKERSHIM			
266	1	18.4	A	0.204	11.6	5.0	6.7	A	0.093	5.9	2.3	A	PASADENA - CIT SEISMOLOGY LAB			
141	1	19.4	A	0.188	20.5	7.3	9.6	A	0.138	7.4	3.4	A	LOS ANGELES - GRIFFITH OBSERVATORY			
128	1	21.0	A	0.374	14.6	8.9	14.5	A	0.164	4.1	3.3	A	LAKE HUGHES ARRAY 12 - CWR SITE			
126	1	24.0	A	0.200	8.6	1.7	5.7	A	0.170	7.1	1.6	A	LAKE HUGHES ARRAY 4 - CWR SITE			
127	1	24.0	A	0.147	4.8	2.4	4.6	A	0.089	3.0	2.2	A	LAKE HUGHES ARRAY 9 - CWR SITE			
110	1	26.0	A	0.335	27.8	9.5	19.6	A	0.180	6.4	3.5	A	CASTAIC - OLD RIDGE ROUTE			
104	2	26.0	A	0.223	6.7	5.9	10.0	A	0.070	4.5	2.5	A	ARCADIA - SANTA ANITA RESERVOIR			
190	2	26.6	A	0.083	13.8	10.3	4.2	A	0.060	7.1	3.8	A	LOS ANGELES - 2011 ZONAL			
137	2	27.1	A	0.188	23.4	13.7	6.4	A	0.078	10.3	6.5	A	*LOS ANGELES - WATER & POWER			
121	2	30.0	A	0.103	8.4	1.7	1.8	A	0.043	3.4	1.7	A	FAIRMONT STATION - RESERVOIR			
278	2	47.0	A	0.078	4.6	2.1	1.7	A	0.039	2.3	1.8	A	SAN DIMAS - PUDDINGSTONE RESERVOIR			
290	1	59.0	A	0.057	3.8	1.2	0.1	A	0.037	2.0	1.2	A	WRIGHTWOOD - 6074 PARK DRIVE			
1096	1	64.0	A	0.028	1.4	0.8	0.0	A	0.018	1.0	0.5	A	FORT TEJON - CWR SITE			
1027	1	66.0	A	0.057	2.8	0.9	0.0	A	0.047	2.1	1.2	A	EDMONSTON - GROUND STATION			
111	1	87.0	A	0.021				A	0.010			A	CEDAR SPRINGS - ALLEN RANCH			
282	1	120.0	A	0.019	3.7	2.3	0.0	A	0.011	1.7	1.4	A	GOLETA - UC FLUID MECHANICS LAB			
280	1	121.0	A	0.016	2.8	2.1	0.0	A	0.012	1.5	2.0	A	SAN ONOFRE - SCE NUCLEAR PLANT			

SOIL STATIONS:			***** HORIZONTAL *****						***** VERTICAL *****							
STA#	STRUC	DIST	AC	ACCEL	VEL	DISP	DUR	SRC	ACCEL	VEL	DISP	SRC	STATION LOCATION			
241	2	7.7	A	0.258	30.0	14.9	18.7	A	0.178	31.9	14.6	A	LOS ANGELES - 8244 ORION			
458	2	10.7	A	0.118	31.6	17.6	22.7	A	0.111	18.1	7.0	A	LOS ANGELES - 15107 VAN OWEN			
267	2	13.6	A	0.215	13.9	4.9	7.9	A	0.146	5.9	2.6	A	PASADENA - CIT JPL LAB			
461	2	14.8	A	0.148	22.3	8.4	19.5	A	0.120	8.0	2.6	A	LOS ANGELES - 15910 VENTURA			
466	2	15.0	A	0.225	28.3	13.5	18.2	A	0.108	9.4	4.3	A	LOS ANGELES - 15250 VENTURA			
253	2	15.4	A	0.263	31.6	18.3	23.1	A	0.101	9.6	3.8	A	LOS ANGELES - 14724 VENTURA			
122	2	16.5	A	0.273	30.8	11.1	10.2	A	0.142	15.6	5.6	A	GLENDALE - 633 E. BROADWAY			
264	2	21.0	A	0.206	16.4	6.9	10.8	A	0.108	9.0	2.4	A	PASADENA - CIT MILLIKAN LIBRARY			
475	1	22.0	A	0.114	14.3	7.4	8.1	A	0.106	6.6	2.7	A	PASADENA - CIT ATHENAEUM			
482	2	22.6	A	0.121	17.3	8.7	9.1	A	0.084	8.1	3.4	A	ALHAMBRA - 900 SOUTH FREEMONT			
133	2	23.0	A	0.154	19.4	13.1	10.0	A	0.058	6.0	3.8	A	*HOLLYWOOD STORAGE - BASEMENT			
135	1	23.0	A	0.217	21.1	14.7	9.3	A	0.119	5.0	3.0	A	*HOLLYWOOD STORAGE - P.E. LOT			
181	2	26.5	A	0.147	17.6	12.0	10.0	A	0.086	9.0	4.1	A	LOS ANGELES - 1640 SOUTH MARENGO			
125	1	27.0	A	0.152	17.9	3.4	13.1	A	0.102	11.7	2.8	A	LAKE HUGHES ARRAY 1 - FIRE STATION			

262	1	32.0	A	0.150	14.2	3.8	14.5	A	0.105	7.8	2.4	A	PALMDALE - FIRE STATION
288	2	33.0	A	0.111	17.5	14.8	9.1	A	0.047	6.7	4.0	A	VERNON - CENTRAL MFG. TERMINAL
244	2	36.0	A	0.035	11.8	8.8	0.0	A	0.047	6.9	3.9	A	LOS ANGELES - 8639 LINCOLN
247	2	37.0	A	0.045	13.3	10.3	0.0	A	0.025	5.7	3.5	A	LOS ANGELES - 9841 AIRPORT BLVD
229	2	37.0	A	0.069	13.8	9.4	4.6	A	0.028	5.4	3.6	A	LOS ANGELES - 5250 CENTURY BLVD
269	1	41.0	A	0.148	5.4	2.5	10.2	A	0.056	2.3	1.7	A	PEARBLOSSOM - PUMPING PLANT
1052	1	49.0	A	0.112	8.5	2.3	6.0	A	0.041	3.8	1.2	A	OSO PUMPING PLANT
411	1	54.0	A	0.043	5.0	3.4	0.0	A	0.020	2.2	1.3	A	PALOS VERDES - 2516 VIA TEJON
131	2	58.0	A	0.028	9.6	7.3	0.0	A	0.015	6.1	3.6	A	LONG BEACH - UTILITIES BLDG.
132	2	58.0	A	0.038	9.5	8.0	0.0	A	0.027	4.9	3.8	A	LONG BEACH - STATE COLLEGE
476	2	58.0	A	0.040	5.8	2.7	0.0	A	0.017	2.3	1.9	A	FULLERTON - 2600 NUTWOOD AVE.
130	1	59.0	A	0.030	10.4	8.7	0.0	A	0.016	4.2	2.8	A	LONG BEACH - TERMINAL ISLAND
272	1	62.0	A	0.027	7.3	4.9	0.0	A	0.011	3.2	2.2	A	PORT HUENEME - NAVY LABORATORY
472	2	66.0	A	0.033	8.5	6.5	0.0	A	0.020	3.9	2.5	A	ORANGE - 400 W. CHAPMAN
281	2	70.0	A	0.029	8.0	5.7	0.0	A	0.020	2.4	1.7	A	SANTA ANA - ORANGE CO. ENG. BLDG
114	2	78.0	A	0.036	7.0	6.9	0.0	A	0.010	3.5	2.3	A	COSTA MESA - 666 W. NINETEENTH
1102	1	82.0	A	0.034	2.5	2.1	0.0	A	0.015	2.4	3.3	A	WHEELER RIDGE - GROUND STATION
112	1	88.0	A	0.030				A	0.013			A	CEDAR SPRINGS - PUMP PLANT
113	1	91.0	A	0.039	2.6	1.3	0.0	A	0.026	1.5	1.3	A	COLTON - S. CAL. EDISON CO.
274	2	93.0	A	0.047	3.5	1.3	0.0	A	0.019	1.5	0.8	A	SAN BERNARDINO - HALL OF RECORDS
465	1	104.0	A	0.044	4.6	2.4	0.0	A	0.022	3.4	1.6	A	SAN JUAN CAPISTRANO - CITY HALL
123	1	134.0	A	0.044	2.9	1.7	0.0	A	0.027	2.3	1.3	A	HEMET - FIRE STATION
103	1	168.0	A	0.037	2.6	1.2	0.0	A	0.015	1.4	1.1	A	ANZA - ANZA POST OFFICE

490413 1955 PUGET SOUND, WASHINGTON

MAG = 7.1

SOIL STATIONS:

STA#	STRUC	DIST	AC	ACCEL	HORIZONTAL	VEL	DISP	DUR	SRC	ACCEL	VERTICAL	DISP	SRC	STATION LOCATION
2101	1	48.0	C	0.306	21.4	10.4	22.3	A	0.111	7.0	4.0	A	OLYMPIA - HIGHWAY TEST LAB	
2170	1	69.0	C	0.072	8.2	2.7	14.8	A	0.024	2.4	2.3	A	SEATTLE ARMY BASE - 4735 E MARGINAL	

590818 637 HEBGEN LAKE, MONTANA

MAG = 7.1

ROCK STATIONS:

STA#	STRUC	DIST	AC	ACCEL	HORIZONTAL	VEL	DISP	DUR	SRC	ACCEL	VERTICAL	DISP	SRC	STATION LOCATION
2201	1	175.0	C	0.043				B	0.021			B	BUTTE, MONT. - SCHOOL OF MINES	
2202	2	208.0	C	0.013				B	0.008			B	HELENA, MONT. - CARROL COLLEGE	
2204	1	454.0	C	0.001				B	0.001			B	HUNGRY HORSE - DOWNSTREAM STATION	

SOIL STATIONS:

STA#	STRUC	DIST	AC	ACCEL	HORIZONTAL	VEL	DISP	DUR	SRC	ACCEL	VERTICAL	DISP	SRC	STATION LOCATION
2205	2	95.0	C	0.055				B	0.026			B	BOZEMAN, MONT. - STATE COLLEGE	

720730 2145 SITKA, ALASKA

MAG = 7.6

ROCK STATIONS:

STA#	STRUC	DIST	AC	ACCEL	HORIZONTAL	VEL	DISP	DUR	SRC	ACCEL	VERTICAL	DISP	SRC	STATION LOCATION
2714	1	45.0	B	0.110				B	0.050			B	SITKA, ALASKA - MAGNETIC OBS.	
2708	1	145.0	B	0.010				B					JUNEAU, AUKA BAY - BUR OF COMM FISH	

SOIL STATIONS:

STA#	STRUC	DIST	AC	ACCEL	HORIZONTAL	VEL	DISP	DUR	SRC	ACCEL	VERTICAL	DISP	SRC	STATION LOCATION
2715	1	300.0	B	0.010				B					YAKUTAT, ALASKA - AIRPORT PUMP HOUSE	

520721 1152 KERN COUNTY, CALIFORNIA

MAG = 7.7

ROCK STATIONS:				***** HORIZONTAL *****					***** VERTICAL *****					STATION LOCATION
STA#	STRUC	DIST	AC	ACCEL	VEL	DISP	DUR	SRC	ACCEL	VEL	DISP	SRC		
136	2	115.0	B	0.032					B	0.008			B	*LOS ANGELES - SUBWAY TERMINAL
1083	1	148.0	B	0.014					B	0.009			B	SAN LUIS OBISPO - CITY REC. BLDG

SOIL STATIONS:				***** HORIZONTAL *****					***** VERTICAL *****					STATION LOCATION
STA#	STRUC	DIST	AC	ACCEL	VEL	DISP	DUR	SRC	ACCEL	VEL	DISP	SRC		
1095	1	42.0	B	0.196	17.7	9.1	19.6	A	0.123	6.7	5.0	A	TAFT - LINCOLN HS TUNNEL	
283	1	85.0	B	0.135	19.3	5.8	13.8	A	0.051	5.0	2.1	A	SANTA BARBARA - COURTHOUSE	
133	2	107.0	B	0.058	9.4	5.9	0.1	A	0.024	4.2	2.2	A	*HOLLYWOOD STORAGE - BASEMENT	
135	1	107.0	B	0.062	8.9	6.4	0.1	A	0.022	3.1	3.4	A	*HOLLYWOOD STORAGE - P.E. LOT	
475	1	109.0	B	0.054	9.1	2.9	0.1	A	0.033	4.5	3.0	A	PASADENA - CIT ATHENAEUM	
288	2	122.0	B	0.037					B	0.012			B	VERNON - CENTRAL MFG. TERMINAL
131	2	145.0	B	0.016					B	0.006			B	LONG BEACH - UTILITIES BLDG.
113	1	156.0	B	0.014					B	0.012			B	COLTON - S. CAL. EDISON CO.
1008	1	224.0	B	0.018					B	0.006			B	BISHOP - LA WATER DEPT GARAGE
277	2	282.0	B	0.005					B	0.001			B	SAN DIEGO - LIGHT & POWER
1028	1	293.0	B	0.010					B	0.005			B	HOLLISTER - CITY HALL
2001	1	359.0	B	0.004					B				B	HAWTHORNE - US NAVY AMMO. DEPOT
1081	2	366.0	B	0.004					B				B	SAN JOSE - BANK OF AMERICA BLDG
117	1	370.0	B	0.004					B				B	EL CENTRO - IRRIGATION SUBSTA.
1049	2	407.0	B	0.001					B				B	OAKLAND - CITY HALL
1078	2	425.0	B	0.004					B				B	SAN FRANCISCO - SOUTHERN PACIFIC BG

SOURCES OF STRONG MOTION DATA

CODE REFERENCE

- A STRONG-MOTION EARTHQUAKE ACCELERograms, VOL. I, PARTS A-Y, VOL. III, PARTS A-Y, EARTHQUAKE ENGINEERING RESEARCH LABORATORY, CALIFORNIA INSTITUTE OF TECHNOLOGY, PASADENA, 1969-1975.
- B UNITED STATES EARTHQUAKES, ANNUAL PUBLICATION OF THE U.S. DEPT. OF COMMERCE.
- C THE FAIRBANKS, ALASKA, EARTHQUAKE OF JUNE 21, 1967, PRELIMINARY ENGINEERING SEISMOLoGICAL REPORT, BY W.K. CLOUD AND C.F. KNUDSON, PUBLISHED BY THE U.S. DEPT. OF COMMERCE, COAST AND GEODETIC SURVEY.
- D SEISMIC ENGINEERING PROGRAM REPORT, OCTOBER-DECEMBER 1974, U.S. GEOLOGICAL SURVEY CIRCULAR 713, 1974.
- E WRITTEN COMMUNICATION FROM A.G. BRADY, SEISMIC ENGINEERING BRANCH, U.S. GEOLOGICAL SURVEY, 1977.
- F STRONG-MOTION INSTRUMENTAL DATA ON THE BORREGO MOUNTAIN EARTHQUAKE OF 9 APRIL 1968, A JOINT PUBLICATION OF THE COAST AND GEODETIC SURVEY, U.S. DEPT. OF COMMERCE, AND THE EARTHQUAKE ENGINEERING RESEARCH LABORATORY, CALIFORNIA INSTITUTE OF TECHNOLOGY, AUGUST 1968.
- G SEISMIC ENGINEERING PROGRAM REPORT, JANUARY-MARCH 1975, U.S. GEOLOGICAL SURVEY CIRCULAR 717-A, 1975.
- H STRONG-MOTION SEISMograph RESULTS FROM THE OROVILLE EARTHQUAKE OF 1 AUGUST 1975, BY R.P. MALEY, VIRGILIO PEREZ, AND B.J. MORRILL, P. 115-122 IN SPECIAL REPORT 124, CALIFORNIA DIVISION OF MINES AND GEOLOGY, 1975.
- I SEISMIC ENGINEERING PROGRAM REPORT, JULY-SEPTEMBER 1975, U.S. GEOLOGICAL SURVEY CIRCULAR 717-C, 1976.

LISTING OF STATIONS

STA#	STRUC	GEO	LOCATION	STRUCTURE	REF	GEOLOGY	REF
103	1	S	ANZA - ANZA POST OFFICE	1 STORY BLDG	1	ALLUVIUM	2
104	2	R	ARCADIA - SANTA ANITA RESERVOIR	ABUTMENT, C DAM	1	GRANITE/DIORITE	2
110	1	R	CASTAIC - OLD RIDGE ROUTE	INST SHELTER	1	SANDSTONE	1
111	1	R	CEDAR SPRINGS - ALLEN RANCH	1 STORY BLDG	1	GRANITIC	2
112	1	S	CEDAR SPRINGS - PUMP PLANT	1 STORY BLDG	1	SHALLOW ALLUVIUM	2
113	1	S	COLTON - S. CAL. EDISON CO.	1 STORY BLDG	1	DEEP ALLUVIUM	1
114	2	S	COSTA MESA - 666 W. NINETEENTH	18 STORY BLDG	1	ALLUVIUM	1
116	1	R	DEVILS CANYON - FILTER PLANT	1 STORY BLDG	1	LS/GNEISS	2
117	1	S	EL CENTRO - IRRIGATION SUBSTA.	2 STORY BLDG	1	>300 M ALLUVIUM	1
118	2	S	LOS ANGELES - 16661 VENTURA	8 STORY RC BLDG	1	8M ALLUV/SHALE	1
121	2	R	FAIRMONT STATION - RESERVOIR	ABUTMENT, E DAM	1	GRANITE	1
122	2	S	GLENDALE - 633 E. BROADWAY	3 STORY BLDG	1	>8 M ALLUVIUM	1
123	1	S	HEMET - FIRE STATION	1 STORY BLDG	1	ALLUVIUM	1
125	1	S	LAKE HUGHES ARRAY 1 - FIRE STATION	1 STORY BLDG	1	300 M ALLUVIUM	1
126	1	R	LAKE HUGHES ARRAY 4 - CWR SITE	INST SHELTER	1	WEATHERED GRANIT	1
127	1	R	LAKE HUGHES ARRAY 9 - CWR SITE	1 STORY BLDG	1	GNEISS	1
128	1	R	LAKE HUGHES ARRAY 12 - CWR SITE	1 STORY BLDG	1	THIN ALLUVIUM	1
129	2	S	LOMA LINDA - UNIV. MED. CENTER	10 STORY BLDG	3	APP 250 M ALLUV	3
130	1	S	LONG BEACH - TERMINAL ISLAND	1 STORY BLDG	1	DEEP ALLUVIUM	1
131	2	S	LONG BEACH - UTILITIES BLDG.	4 STORY BLDG	1	DEEP ALLUVIUM	1
132	2	S	LONG BEACH - STATE COLLEGE	9 STORY BLDG	1	>15 M ALLUVIUM	1
133	2	S *	HOLLYWOOD STORAGE - BASEMENT	14 STORY RC	1	130 M ALLUVIUM	1
135	1	S *	HOLLYWOOD STORAGE - P.E. LOT	INST SHELTER	1	130 M ALLUVIUM	1
136	2	R *	LOS ANGELES - SUBWAY TERMINAL	12 STORY BLDG	3	120 M SHALE	3
137	2	R *	LOS ANGELES - WATER & POWER	15 STORY STEEL	1	MIocene SILTSTNE	2
141	1	R	LOS ANGELES - GRIFFITH OBSERVATORY	INST SHELTER	1	GRANITE	1
181	2	S	LOS ANGELES - 1640 SOUTH MARENGO	7 STORY RC	1	>16 M ALLUVIUM	1
190	2	R	LOS ANGELES - 2011 ZONAL	9 STORY RC	1	ALLUVIUM 0-10 M	1
220	2	R	LOS ANGELES - 3838 LANKERSHIM	20 STORY RC	1	SH & SS	1
229	2	S	LOS ANGELES - 5250 CENTURY BLVD	7 STORY STEEL	1	>16 M ALLUVIUM	1
241	2	S	LOS ANGELES - 8244 ORION	7 STORY RC	1	>13 M ALLUVIUM	1
244	2	S	LOS ANGELES - 8639 LINCOLN	12 STORY RC	1	>18 M ALLUVIUM	1
247	2	S	LOS ANGELES - 9841 AIRPORT BLVD	14 STORY RC	1	>23 M ALLUVIUM	1
253	2	S	LOS ANGELES - 14724 VENTURA	12 STORY RC	1	>24 M ALLUVIUM	1
259	2	S	LOS ANGELES - 16055 VENTURA	12 STORY BLDG	1	12M ALLUV/SHALE	1
262	1	S	PALMDALE - FIRE STATION	1 STORY BLDG	1	ALLUVIUM	2
264	2	S	PASADENA - CIT MILLIKAN LIBRARY	9 STORY RC	1	APP 300 M ALLUV	2
266	1	R	PASADENA - CIT SEISMOLOGY LAB	2 STORY BLDG	1	GRANITE	1
267	2	S	PASADENA - CIT JPL LAB	9 STORY STEEL	1	SANDY GRAVEL	2
269	1	S	PEARBLOSSOM - PUMPING PLANT	INST SHELTER	1	130 M ALLUVIUM	2
270	1	R	PERRIS - RESERVOIR	INST SHELTER	1	ALLUV VEN/GRANIT	2
272	1	S	PORT HUENEME - NAVY LABORATORY	1 STORY WAREHSE	1	>300 M ALLUVIUM	1
274	2	S	SAN BERNARDINO - HALL OF RECORDS	6 STORY BLDG	1	>35 M ALLUVIUM	1
277	2	S	SAN DIEGO - LIGHT & POWER	4 STORY BLDG	1	DEEP ALLUVIUM	1
278	2	R	SAN DIMAS - PUDDINGSTONE RESERVOIR	ABUTMENT-EARTH	1	VOL CLASTICS-SH	2
279	2	R	SAN FERNANDO - PACOIMA DAM	ABUTMENT-CONCRET	1	JOINED GNEISS	2
280	1	R	SAN ONOFRE - SCE NUCLEAR PLANT	1 STORY WAREHSE	1	SOFT SANDSTONE	1
281	2	S	SANTA ANA - ORANGE CO. ENG. BLDG	3 STORY BLDG	1	ALLUVIUM	1
282	1	R	GOLETA - UC FLUID MECHANICS LAB	1 STORY BLDG	1	4 M ALLUV/SILTST	1
283	1	S	SANTA BARBARA - COURTHOUSE	2 STORY BLDG	1	>10 M ALLUVIUM	1
288	2	S	VERNON - CENTRAL MFG. TERMINAL	6 STORY BLDG	1	DEEP ALLUVIUM	1
290	1	R	WRIGHTWOOD - 6074 PARK DRIVE	2 STORY BLDG	1	ALLUV VEN/IGN	2
319	2	S *	LOS ANGELES - UCLA ENGINEERING BLDG	4 STORY BLDG	3	21 M ALLUVIUM	3
411	1	S	PALOS VERDES - 2516 VIA TEJON	2 STORY BLDG	1	SHALLOW SANDS/SH	2
458	2	S	LOS ANGELES - 15107 VAN OWEN	7 STORY RC	1	>23 M ALLUVIUM	1
461	2	S	LOS ANGELES - 15910 VENTURA	18 STORY STEEL	1	>12 M ALLUVIUM	1

465	1	S	SAN JUAN CAPISTRANO - CITY HALL	1 STORY BLDG	1	ALLUVIUM	2
466	2	S	LOS ANGELES - 15250 VENTURA	12 STORY RC	1	>12 M ALLUVIUM	1
472	2	S	ORANGE - 400 W. CHAPMAN	19 STORY BLDG	1	>100 M ALL/SHALE	2
475	1	S	PASADENA - CIT ATHENAEUM	2 STORY RC	3	APPROX 200 M ALL	3
476	2	S	FULLERTON - 2600 NUTWOOD AVE.	10 STORY RC	1	>20 M ALLUVIUM	1
482	2	S	ALHAMBRA - 900 SOUTH FREMONT	12 STORY STEEL	1	APPROX 100 M ALL	2
497	2	S	LOS ANGELES - 16633 VENTURA	14 STORY BLDG	1	ALLUVIUM	1
512	2	S	LOS ANGELES - 16255 VENTURA	12 STORY BLDG	1	20M ALLUV/SHALE	1
610	2	S	LOS ANGELES - 18321 VENTURA	10 STORY BLDG	1	>5M ALLUVIUM	1
655	1	R	JENSEN FILTER PLT - 13100 BALBOA, LA	2 STORY BLDG	1	ROCK	7
657	2	S	SANTA MONICA - 201 OCEAN	18 STORY BLDG	1	SOIL	7
1001	1	S	APEEL ARRAY - STATION 1	INST SHELTER	1	210M ALLUVIUM	1
1002	1	S	APEEL ARRAY - STATION 2	INST SHELTER	1	8M MUD/85M ALLUV	1
1004	1	S	BAKERSFIELD - HARVEY AUDITORIUM	AUDITORIUM	1	>250 M ALLUVIUM	1
1008	1	S	BISHOP - LA WATER DEPT GARAGE	1 STORY BLDG	3	200 M ALLUVIUM	3
1011	1	S	BUENA VISTA - GROUND STATION	INST SHELTER	1	ALLUVIUM	2
1013	1	S	CHOLAME-SHANDON ARRAY NO. 2	INST SHELTER	1	45 M ALLUV/SS	1
1014	1	S	CHOLAME-SHANDON ARRAY NO. 5	INST SHELTER	1	ALLUVIUM	1
1015	1	S	CHOLAME-SHANDON ARRAY NO. 8	1 STORY BLDG	1	THIN ALLUVIUM/SS	1
1016	1	S	CHOLAME-SHANDON ARRAY NO. 12	INST SHELTER	1	30 M TERRACE/SS	1
1023	1	S	FERNDALE - OLD CITY HALL, BROWN ST	2 STORY BLDG	1	ALLUVIUM	1
1027	1	R	EDMONSTON - GROUND STATION	INST SHELTER	1	5 M ALLUV/GNEISS	2
1028	1	S	HOLLISTER - CITY HALL	1 STORY BLDG	3	13 M ALLUVIUM	3
1032	1	R	SAGO CENTRAL - HARRIS RANCH	INST SHELTER	1	ROCK	6
1049	2	S	OAKLAND - CITY HALL	15 STORY BLDG	3	76 M MUD-ALLUVI	3
1051	1	R	OROVILLE SEISMOGRAPH STATION	1 STORY BLDG	1	METAVOLCANICS	1
1052	1	S	OSO PUMPING PLANT	INST SHELTER	1	ALLUVIUM	2
1057	1	R	PLEASANT HILL - DIABLO VALLEY COL.	2 STORY BLDG	3	2 M ALUV/SS	3
1065	2	S	SAN FRANCISCO - ALEXANDER BLDG	15 STORY BLDG	3	46 M ALLUVIUM	3
1071	2	S	SAN FRANCISCO - BETHLEHEM PAC BLDG	14 STORY BLDG	1	70M ALLUVIUM	1
1074	2	R	SAN FRANCISCO - 390 MAIN	7 STORY BLDG	1	SHALE/SS	1
1078	2	S	SAN FRANCISCO - SOUTHERN PACIFIC BG	12 STORY BLDG	3	90 M FILL-ALLUV	3
1080	2	S	SAN FRANCISCO - STATE BLDG	7 STORY BLDG	3	61 M ALLUVIUM	3
1081	2	S	SAN JOSE - BANK OF AMERICA BLDG	13 STORY BLDG	3	APPROX 750 M ALL	3
1083	1	R	SAN LUIS OBISPO - CITY REC. BLDG	2 STORY BLDG	1	2 M LOAM/FRAZ SH	2
1093	1	S	SAN PABLO - CONTRA COSTA COLLEGE	2 STORY BLDG	3	6 M FILL-ALLUV	3
1095	1	S	TAFT - LINCOLN HS TUNNEL	1 STORY SCH BLDG	1	ALLUVIUM	1
1096	1	R	FORT TEJON - CWR SITE	1 STORY BLDG	1	GRANITE	1
1102	1	S	WHEELER RIDGE - GROUND STATION	INST SHELTER	1	APPROX 100 M ALL	2
1117	1	R	SAN FRANCISCO - GOLDEN GATE PARK	INST SHELTER	3	FRAN CHERT-SHALE	3
1202	1	S	STONE CANYON EAST, CALIF.	1 STORY BLDG	1	SOIL	8
1249	1	R	CAPE MENDOCINO (C5) - PETROLIA	INST SHELTER	1	CRETACEOUS ROCK	1
1250	1	S	GILROY (C6) - GEOL BLDG, GAL COL	1 STORY BLDG	1	TERRACE DEPOSITS	1
1278	1	R	SHELTER COVE, STA 2 (C41) - PWR PLT	INST SHELTER	1	FRANCISCAN ROCK	1
1291	1	S	MARYSVILLE (C56) - CDOT MAINT BLDG	1 STORY BLDG	1	100M ALLUVIUM	1
1292	1	S	CHICO (C57) - 2334 FAIR STREET	1 STORY BLDG	1	90M ALLUVIUM	1
1293	1	R	PARADISE (C58) - KEWG TRNSMTR BLDG	1 STORY BLDG	1	VOLCANIC ROCK	1
1377	1	S	SAN JUAN BAUTISTA (C126) - 24 POLK	1 STORY BLDG	1	SOIL	6
1398	1	S	PETROLIA (C156) - GENERAL STORE	INST SHELTER	1	ALLUVIUM	1
1438	1	R	CHOLAME-SHANDON; TEMLOR	INST SHELTER	1	ROCK	9
2001	1	S	HAWTHORNE - US NAVY AMMO. DEPOT	1 STORY BLDG	1	ALLUVIUM	1
2005	2	S	MOJAVE GENERATING PLANT	LRG POWER PLANT	3	APPROX 70 M ALLU	3
2101	1	S	OLYMPIA - HIGHWAY TEST LAB	INST SHELTER	1	ALLUVIUM	5
2170	1	S	SEATTLE ARMY BASE - 4735 E MARGINAL	1 STORY BLDG	1	ALLUVIUM	5
2201	1	R	BUTTE, MONT. - SCHOOL OF MINES	2 STORY BLDG	3	GRANITIC INTRUS	3
2202	2	R	HELENA, MONT. - CARROL COLLEGE	5 STORY BLDG	3	GRANITICS	3
2204	1	R	HUNGRY HORSE - DOWNSTREAM STATION	INST SHELTER	3	LIMESTONE	3
2205	2	S	BOZEMAN, MONT. - STATE COLLEGE	3 STORY BLDG	3	APPROX 170 M ALL	3
2707	1	R	FAIRBANKS, ALASKA - UNIV OF ALASKA	INST SHELTER	3	SCHIST	3
2708	1	R	JUNEAU, AUKE BAY - BUR OF COMM FISH	1 STORY BLDG	1	SLATE	1
2714	1	R	SITKA, ALASKA - MAGNETIC OBS.	INST SHELTER	1	GRAYWACKE	1

2715	1	S	YAKUTAT, ALASKA - AIRPORT PUMP HOUSE	1 STORY BLDG	1	GLACIAL OUTWASH	1
3501	1	S	MANAGUA, NIC. - ESSO REFINERY	1 STORY BLDG	4	ALLUVIUM	4

REFERENCE LISTING

CODE REFERENCE

- 1 U.S. GEOLOGICAL SURVEY, 1976, STRONG-MOTION ACCELEROGRAPH STATION LIST - 1975 U.S. GEOLOGICAL SURVEY OPEN-FILE REPORT NO. 76-79.
- 2 MALEY, R.P., AND CLOUD, W.K., 1973, STRONG-MOTION ACCELEROGRAPH RECORDS, 'IN' SAN FERNANDO, CALIFORNIA, EARTHQUAKE OF FEBRUARY 9, 1971, O. 3: U.S. DEPARTMENT OF COMMERCE, NATIONAL OCEANIC AND ATMOSPHERIC ADMINISTRATION, P. 325-348.
- 3 MALEY, R.P., 1975, WRITTEN COMMUNICATION.
- 4 VALERA, J.E., 1973, SOIL CONDITIONS AND LOCAL SOIL EFFECTS DURING THE MANAGUA EARTHQUAKE OF DECEMBER 23, 1972, 'IN' MANAGUA, NICARAGUA EARTHQUAKE OF DECEMBER 23, 1972, VOLUME II EARTHQUAKE ENGINEERING RESEARCH INSTITUTE, P.232-264.
- 5 TRIFUNAC, M.D., AND BRADY, A.G., 1975, ON THE CORRELATION OF SEISMIC INTENSITY SCALES WITH THE PEAKS OF RECORDED STRONG GROUND MOTION: SEISMOL. SOC. AMERICA BULL., V. 65, P. 139-162.
- 6 JENNINGS, C.W., AND STRAND, R.G., 1959, GEOLOGIC MAP OF CALIFORNIA, SANTA CRUZ SHEET, SCALE 1:250,000, CALIFORNIA DIVISION OF MINES AND GEOLOGY.
- 7 JENNINGS, C.W. AND STRAND, R.G., 1969, GEOLOGIC MAP OF CALIFORNIA, LOS ANGELES SHEET, SCALE 1:250,000, CALIFORNIA DIVISION OF MINES AND GEOLOGY.
- 8 MALEY, R.P., 1977, ORAL COMMUNICATION.
- 9 CLOUD, W.K., AND PEREZ, V., 1967, ACCELEROGrams - PARKFIELD EARTHQUAKE: SEISMOL. SOC. AMERICA BULL., V.57, P.1179-1192.

REFERENCES

Acton, F.S., 1959, Analysis of straight-line data: New York, Dover, 267 p.

Allen, C.R., Engen, G.R., Hanks, T.C., Nordquist, J.M., and Thatcher, W.R., 1971, Main shock and larger aftershocks of the San Fernando earthquake, February 9 through March 1, 1971, in The San Fernando, California, earthquake of February 9, 1971: U.S. Geol. Survey Prof. Paper 733, p. 17-20.

Allen, C.R., Hanks, T.C., Whitcomb, J.H., 1973, San Fernando earthquake: seismological studies and their tectonic implications, in San Fernando, California, earthquake of February 9, 1971, v. 3: National Oceanic and Atmospheric Admin., U.S. Dept. Commerce, p. 13-21.

Allen, C.R., and Nordquist, J.M., 1972, Foreshock, main shock, and larger aftershocks of the Borrego Mountain earthquake, in The Borrego Mountain earthquake of April 9, 1968: U.S. Geol. Survey Prof. Paper 787, p. 16-23.

Ambraseys, N.N., 1969, Maximum intensity of ground movements caused by faulting: World Conference on Earthquake Engineering, 4th, Santiago, Chile, Proc., v. 1, p. A2-154-A2-171.

Ambraseys, N.N., 1974, Dynamics and response of foundation materials in epicentral regions of strong earthquakes: World Conference on Earthquake Engineering, 5th, Rome, Italy, 1973, Proc., v. 1, p. CXXVI-CXLVIII.

Andrews, D.J., 1976, Rupture propagation with finite stress in antiplane strain: Jour. Geophys. Research, v. 81, p. 3575-3582.

Arnold, Peter, Vanmarcke, E.H., and Gazetas, George, 1976, Frequency content of ground motions during the 1971 San Fernando earthquake: Massachusetts Inst. Tech., Dept. Civil Engineering, Publication R76-3, 73 p.

Bonilla, M.G., and Buchanan, J.M., 1970, Interim report on worldwide historic

surface faulting: U.S. Geol. Survey Open-file rept., 32 p.

Boore, D.M., 1973, The effect of simple topography on seismic waves: implications for the accelerations recorded at Pacoima Dam, San Fernando valley, California: *Seismol. Soc. America Bull.*, v. 63, p. 1603-1609.

Boore, D.M., 1974, Empirical and theoretical study of near-fault wave propagation: World Conference on Earthquake Engineering, 5th, Rome, Italy, 1973, Proc., v. 2, p. 2397-2408.

Boore, D.M., and Stierman, D.J., 1976, Source parameters of the Pt. Mugu, California, earthquake of February 21, 1973: *Seismol. Soc. America Bull.*, v. 66, p. 385-404.

Bouchon, M., and Aki, K., 1977, Discrete wave-number representation of seismic-source wave fields: *Seismol. Soc. America Bull.*, v. 67, p. 259-277.

Brune, J.N., 1970, Tectonic stress and the spectra of seismic shear waves from earthquakes: *Jour. Geophys. Research*, v. 75, p. 4997-5009.

Bufe, C.G., Lester, F.W., Lahr, K.M., Lahr, J.C., Seekins, L.C., and Hanks, T.C., 1976, Oroville earthquakes: normal faulting in the Sierra Nevada foothills: *Science*, v. 192, p. 72-74.

Cloud, W.K., 1959, Intensity and ground motion of the San Francisco earthquake of March 22, 1957, in San Francisco earthquakes of March 1957: California Div. Mines Spec. Rept. 57, p. 49-57.

Cloud, W.K., and Knudson, C.F., no date, Preliminary engineering seismological report, in The Fairbanks, Alaska, earthquake of June 21, 1967: Coast and Geodetic Survey, U.S. Dept. Commerce, p. 33-60.

Cloud, W.K., and Perez, Virgilio, 1967, Accelerograms - Parkfield earthquake: *Seismol. Soc. America Bull.*, v. 57, p. 1179-1192.

Crouse, C.B., and Jennings, P.C., 1975, Soil-structure interaction during the San Fernando earthquake: *Seismol. Soc. America Bull.*, v. 65, p. 13-36.

Dewey, J.W., Algermissen, S.T., Langer, C., Dillinger, W., and Hopper, M., 1973, The Managua earthquake of 23 December 1972: location, focal mechanism, aftershocks, and relationship to recent seismicity of Nicaragua, in Managua, Nicaragua earthquake of December 23, 1972: *Earthquake Engineering Research Institute Conference, Proc.*, v. 1, p. 66-88.

Dixon, W.J., and Massey, F.J., Jr., 1957, *Introduction to statistical analyses*: New York, McGraw-Hill, 488 p.

Donovan, N. C., 1973, A statistical evaluation of strong motion data including the February 9, 1971 San Fernando earthquake: *World Conference on Earthquake Engineering*, 5th, Rome, Italy, *Proc.*, v. 1, p. 1252-1261.

Duke, C.M., Johnsen, K.E., Larson, L.E., and Engman, D.C., 1972, Effects of site classification and distance on instrumental indices in the San Fernando earthquake: University of California, Los Angeles, School of Engineering and Applied Science, UCLA-ENG-7247, 29 p.

Duke, C.M., Luco, J.E., Carriveau, A.R., Hradilek, P.J., Lastrico, R., and Ostrom, D., 1970, Strong earthquake motion and site conditions: Hollywood: *Seismol. Soc. America Bull.*, v. 60, p. 1271-1289.

Earthquake Engineering Research Laboratory, 1969-1975, Strong-motion earthquake accelerograms, v. 1, Parts A-Y, v. 2, Parts A-Y: California Institute of Technology, Earthquake Engineering Research Laboratory.

Ellsworth, W.L., 1975, Bear Valley, California, earthquake sequence of February-March 1972: *Seismol. Soc. America Bull.*, v. 65, p. 483-506.

Ellsworth, W.L., Campbell, R.H., Hill, D.P., Page, R.A., Alewine, R.W., III, Hanks, T.C., Heaton, T.H., Hileman, J.A., Kanamori, H., Minster, B., and Whitcomb, J.H., 1973, Point Mugu, California, earthquake of 21 February 1973 and its aftershocks: *Science*, v. 182, p. 1127-1129.

Gedney, Larry, and Berg, Edward, 1969, The Fairbanks earthquakes of June 21, 1967; aftershock distribution, focal mechanisms, and crustal parameters: *Seismol. Soc. America Bull.*, v. 59, p. 73-100.

Gutenberg, B., 1955, Magnitude determination for larger Kern County shocks, 1952; effects of station azimuth and calculation methods, in *Earthquakes in Kern County California during 1952*: *California Div. Mines Bull.* 171, p. 171-175.

Hamilton, R.M., 1972, Aftershocks of the Borrego Mountain earthquake from April 12 to June 12, 1968, in *The Borrego Mountain earthquake of April 9, 1968*: U.S. Geol. Survey Prof. Paper 787, p. 31-54.

Hanks, T.C., 1974, The faulting mechanism of the San Fernando earthquake: *Jour. Geophys. Research*, v. 79, p. 1215-1229.

Hanks, T.C., 1975, Strong ground motion of the San Fernando, California earthquake: ground displacements: *Seismol. Soc. America Bull.*, v. 65, p. 193-225.

Hanks, T.C., and Johnson, D.A., 1976, Geophysical assessment of peak accelerations: *Seismol. Soc. America Bull.*, v. 66, p. 959-968.

Housner, G.W., 1965, Intensity of earthquake ground shaking near the causative fault: *World Conference on Earthquake Engineering*, 3rd, Wellington, New Zealand, Proc., v. 1, p. III-94-III-109.

Ida, Yoshiaki, 1973, The maximum acceleration of seismic ground motion: *Seismol. Soc. America Bull.*, v. 63, p. 959-968.

Jennings, C.W., and Strand, R.G., 1959, Geologic map of California, Santa Cruz sheet, scale 1:250,000: California Div. Mines and Geology.

Jennings, C.W., and Strand, R.G., 1969, Geologic map of California, Los Angeles sheet, scale 1:250,000: California Div. Mines and Geology.

Joyner, W.B., and Chen, A.T.F., 1975, Calculation of nonlinear ground response in earthquakes: *Seismol. Soc. America Bull.*, v. 65, p. 1315-1336.

Knudsen, C.F., and Hansen A., Francisco, 1973, Accelerograph and seismoscope records from Managua, Nicaragua, earthquakes, in Managua, Nicaragua earthquake of December 23, 1972: Earthquake Engineering Research Institute Conference, Proc., v. 1, p. 180-205.

Lahr, K.M., Lahr, J.C., Lindh, A.G., Bufe, C.G., and Lester, F.W., 1976, The August 1975 Oroville earthquakes: *Seismol. Soc. America Bull.*, v. 66, p. 1085-1099.

Lindh, A.G., and Boore, D.M., 1973, Another look at the Parkfield earthquake, using strong motion instruments as a seismic array (abs.): *Seismol. Soc. America, Earthquake Notes*, v. 44, p. 24.

Maley, R.P., and Cloud, W.K., 1973, Strong-motion accelerograph records, in San Fernando, California, earthquake of February 9, 1971, v. 3: National Oceanic and Atmospheric Admin., U.S. Dept. Commerce, p. 325-348.

Maley, R.P., Perez, Virgilio, and Morrill, B.J., 1975, Strong-motion seismograph results from the Oroville earthquake of 1 August 1975, in Oroville, California, earthquake 1 August 1975: California Div. Mines and Geology Spec. Rept. 124, p. 115-122.

McEvilly, T.V., Bakun, W.H., and Casaday, K.B., 1967, The Parkfield, California, earthquakes of 1966: *Seismol. Soc. America Bull.*, v. 57, p. 1221-1244.

Nason, Robert, Harp, E.L., La Gesse, Harry, and Maley, R.P., 1975, Investigations of the 7 June 1975 earthquake in Humbolt County, California: U.S. Geol. Survey open-file rept. 75-404, 28 p.

Newmark, N.M., Blume, J.A., and Kapur, K.K., 1973, Seismic design spectra for nuclear power plants: Am. Soc. Civil Engineers Proc., Jour. Power Div., v. 99, p. 287-303.

Newmark, N.M., and Hall, W.J., 1969, Seismic design criteria for nuclear reactor facilities: World Conference Earthquake Engineering, 4th, Santiago, Chile, Proc., v. 2, p. B4-37-B4-50.

Nuttli, O.W., 1952, The Western Washington earthquake of April 13, 1949: Seismol. Soc. America Bull., v. 42, p. 21-28.

Page, R.A., Boore, D.M., Joyner, W.B., and Coulter, H.W., 1972, Ground motion values for use in the seismic design of the trans-Alaska pipeline system: U.S. Geol. Survey Circ. 672, 23 p.

Page, R.A., Boore, D.M., and Dieterick, J.H., 1975, Estimation of bedrock motion at the ground surface, in R.D. Borcherdt, ed., Studies for seismic zonation of the San Francisco Bay region: U.S. Geol. Survey Prof. Paper 941-A, p. A31-A38.

Page, R.A., and Gawthrop, W., 1973, The Sitka, Alaska, earthquake of 30 July 1972 and its aftershocks (abs.): Seismol. Soc. America, Earthquake Notes, v. 44, p. 16-17.

Person, W.J. (ed.), 1975, Seismological notes--November-December 1974: Seismol. Soc. America Bull., v. 65, p. 1035-1038.

Richter, C.F., 1955, Foreshocks and aftershocks, in Earthquakes in Kern County California during 1952: California Div. Mines Bull. 171, p. 171-175.

Richter, C.F., 1958, Elementary seismology: San Francisco, W.H. Freeman, 768 p.

Schnabel, P.B., and Seed, H.B., 1973, Accelerations in rock for earthquakes in the western United States: Seismol. Soc. America Bull., v. 63, p. 501-516.

Seed, H.B., Murarka, R., Lysmer, J., and Idriss, I.M., 1976, Relationships of maximum acceleration, maximum velocity, distance from source, and local site conditions for moderately strong earthquakes: Seismol. Soc. America Bull., v. 66, p. 1323-1342.

Shannon and Wilson, Inc., and Agbabian Associates, 1976, Geotechnical and strong motion earthquake data from U.S. accelerograph stations Ferndale, Chalome, and El Centro, California Volume I: NUREG-0029 Vol. 1 NRC-6, Clearinghouse, Springfield, VA 22151.

Steinbrugge, K.V., Cloud, W.K., and Scott, N.H., 1970, The Santa Rosa, California, earthquakes of October 1, 1969: U.S. Dept. Commerce, 99 p.

Stierman, D.J., and Ellsworth, W.L., 1976, Aftershocks of the February 21, 1973 Point Mugu, California earthquake: Seismol. Soc. America Bull., v. 66, p. 1931-1952.

Tocher, Don, 1959, Seismographic results from the 1957 San Francisco earthquakes, in San Francisco earthquakes of March 1957: California Div. Mines Spec. Rept., p. 59-71.

Tocher, Don, 1962, The Hebgen Lake, Montana, earthquake of August 17, 1959, MST: Seismol. Soc. America Bull., v. 52, p. 153-162.

Trifunac, M.D., 1972, Tectonic stress and the source mechanism of the Imperial Valley, California, earthquake of 1940: Seismol. Soc. America Bull., v. 62, p. 1283-1302.

Trifunac, M.D., 1976, Preliminary analysis of the peaks of strong earthquake ground motion--dependence of peaks on earthquake magnitude, epicentral distance, and recording site conditions: *Seismol. Soc. America Bull.*, v. 66, p. 189-219.

Trifunac, M.D., and Brady, A.G., 1975, On the correlation of seismic intensity scales with the peaks of recorded strong ground motion: *Seismol. Soc. America Bull.*, v. 65, p. 139-162.

Trifunac, M.D., and Brady, A.G., 1976, Correlations of peak acceleration, velocity, and displacement with earthquake magnitude, distance, and site conditions: *Earthquake Engineering and Structural Dynamics*, v. 4, p. 455-471.

Trifunac, M.D., and Brune, J.N., 1970, Complexity of energy release during the Imperial Valley, California earthquake of 1940: *Seismol. Soc. America Bull.*, v. 60, p. 137-160.

Trifunac, M.D., and Udwadia, F.E., 1974, Parkfield, California, earthquake of June 27, 1966: a three-dimensional moving dislocation: *Seismol. Soc. America Bull.*, v. 64, p. 511-533.

Unger, J.D., and Eaton, J.P., 1970, Aftershocks of the October 1, 1969, Santa Rosa, California, earthquakes: *Geol. Soc. America Abs. with Programs*, v. 2, p. 155.

U.S. Coast and Geodetic Survey and Earthquake Engineering Research Laboratory, 1968, Strong-motion instrumental data on the Borrego Mountain earthquake of 9 April 1968: U.S. Coast and Geodetic Survey, Earthquake Engineering Research Laboratory, California Institute of Technology, 119 p.

U.S. Dept. of Commerce, serial publication, U.S. Earthquakes: a serial publication of the U.S. Dept. of Commerce.

U.S. Geol. Survey, 1974, Seismic engineering program report, October-December 1974: U.S. Geol. Survey Circ. 713, 19 p.

U.S. Geol. Survey, 1975, Seismic engineering program report, January-March 1975: U.S. Geol. Survey Circ. 717A, 17 p.

U.S. Geol. Survey, 1976a, Seismic engineering program report, July-September 1975: U.S. Geol. Survey Circ. 717C, 17 p.

U.S. Geol. Survey, 1976b, Strong-motion accelerograph station list--1975: U.S. Geol. Survey open-file rept. 76-79, 81 p.

Valera, J.E., 1973, Soil conditions and local soil effects during the Managua earthquake of December 23, 1972, in Managua, Nicaragua earthquake of December 23, 1972: Earthquake Engineering Research Institute Conference, Proc., v. 1, p. 232-264.

Ward, P. L., Harlow, David, Gibbs, James, and Aburto Q., Arturo, 1973, Location of the main fault that slipped during the Managua earthquake as determined from locations of some aftershocks, in Managua, Nicaragua earthquake of December 23, 1972: Earthquake Engineering Research Institute Conference, Proc., v. 1, p. 89-96.

Figure 1. Peak horizontal acceleration versus distance to the slipped fault for the magnitude range 5.0-5.7 recorded at the base of small structures. The x's represent rock sites and the diamonds soil sites. The center line is the mean regression line. The outer pair of lines represents the 95 percent prediction interval, and the inner pair represents the 70 percent prediction interval. Length of lines represents the distance interval considered in the regression analysis.

MAGNITUDE 5.0-5.7 SMALL STRUCTURES

X = ROCK

◇ = SOIL

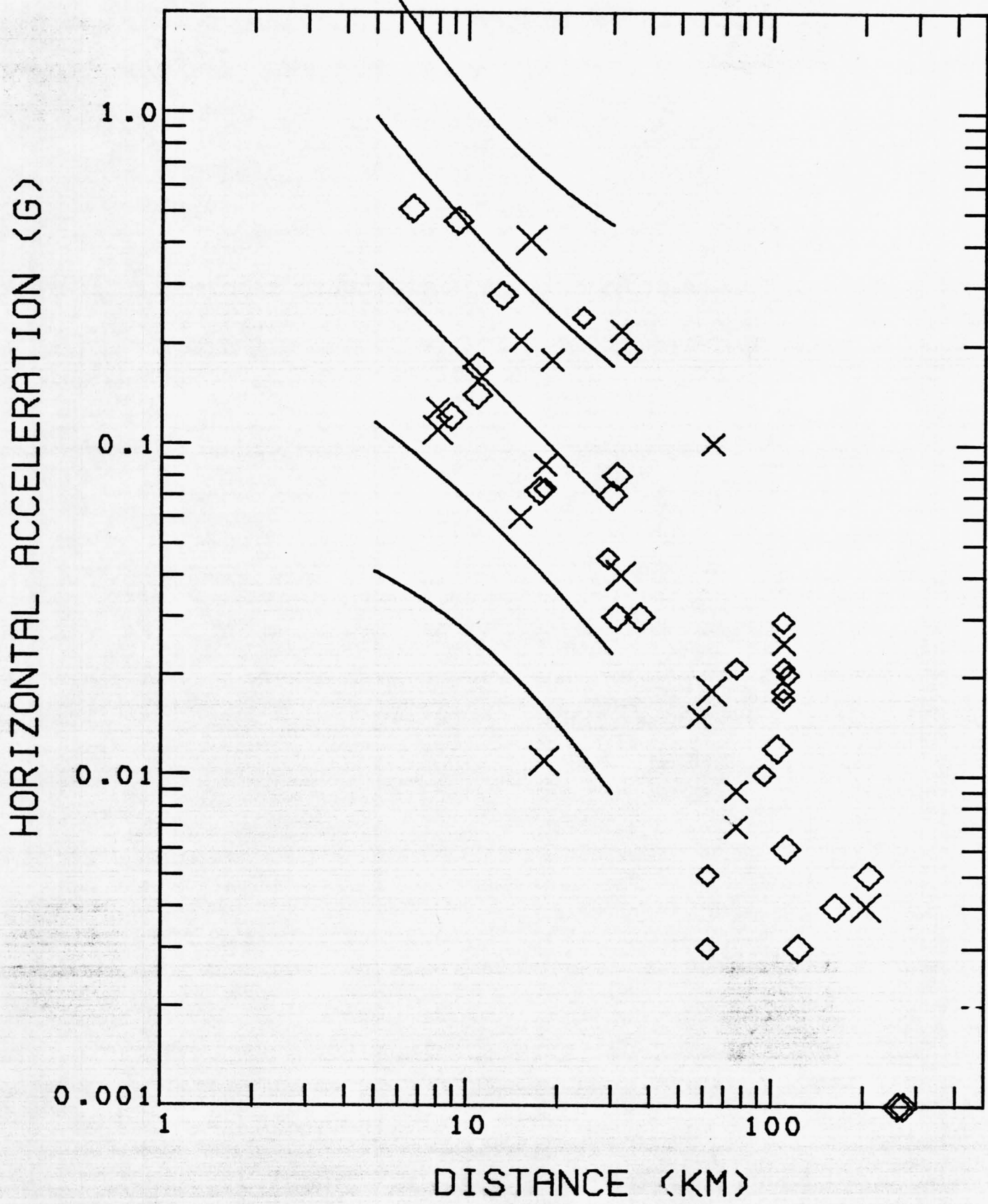


Figure 2. Peak horizontal acceleration versus distance to the slipped fault for the magnitude range 6.0-6.4 recorded at the base of small structures. Symbols and curves same as in Figure 1.

MAGNITUDE 6.0-6.4 SMALL STRUCTURES

X = ROCK

◇ = SOIL

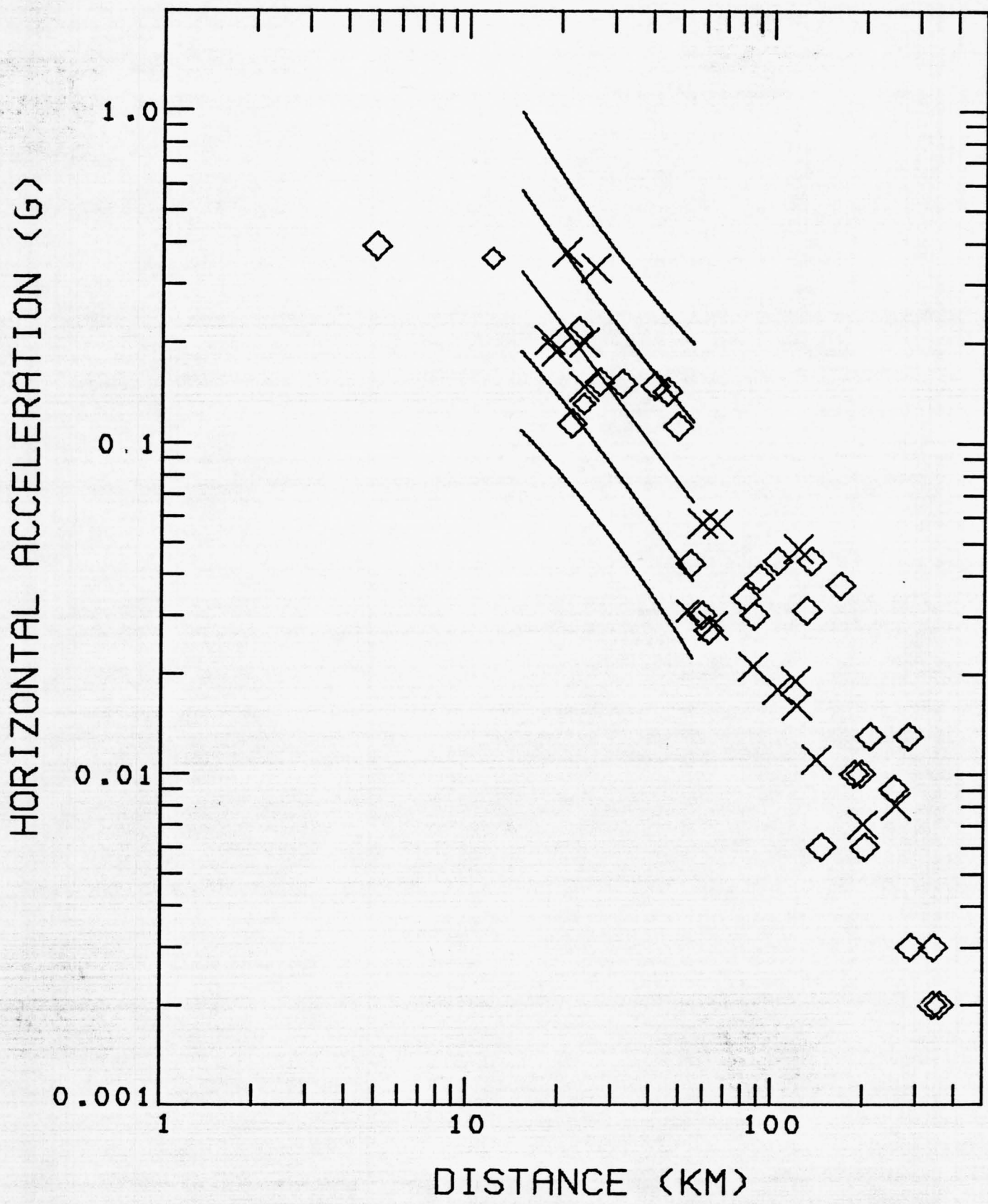


Figure 3. Peak horizontal acceleration versus distance to the slipped fault for the magnitude range 7.1-7.7 recorded at the base of small structures. Symbols and curves same as in Figure 1.

MAGNITUDE 7.1-7.7 SMALL STRUCTURES

\times = ROCK

\diamond = SOIL

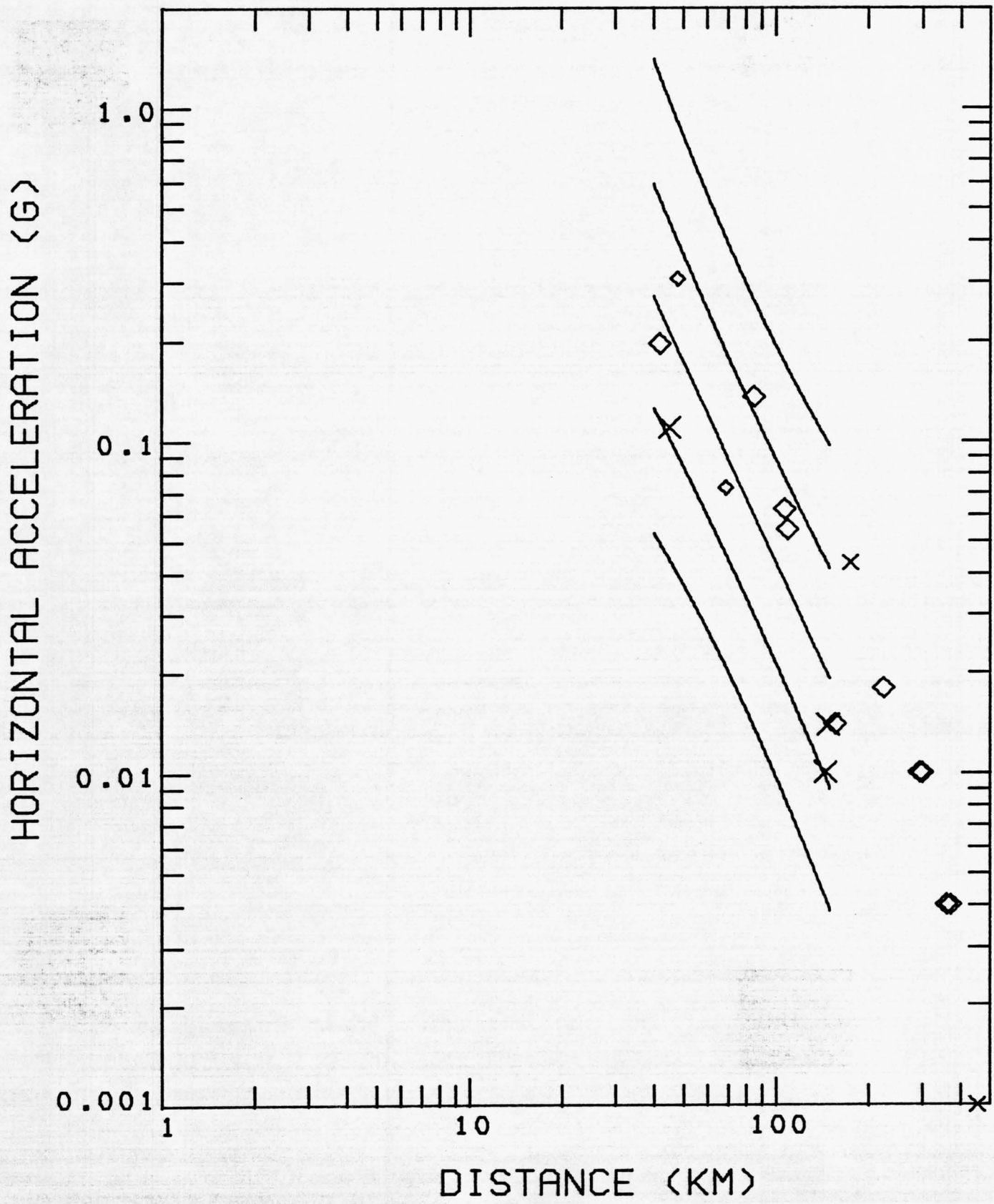


Figure 4. Comparison of the 70 percent prediction intervals for peak horizontal acceleration recorded at the base of small structures for the magnitude classes 5.0-5.7, 6.0-6.4, 7.1-7.7. Curves taken from Figures 1-3.

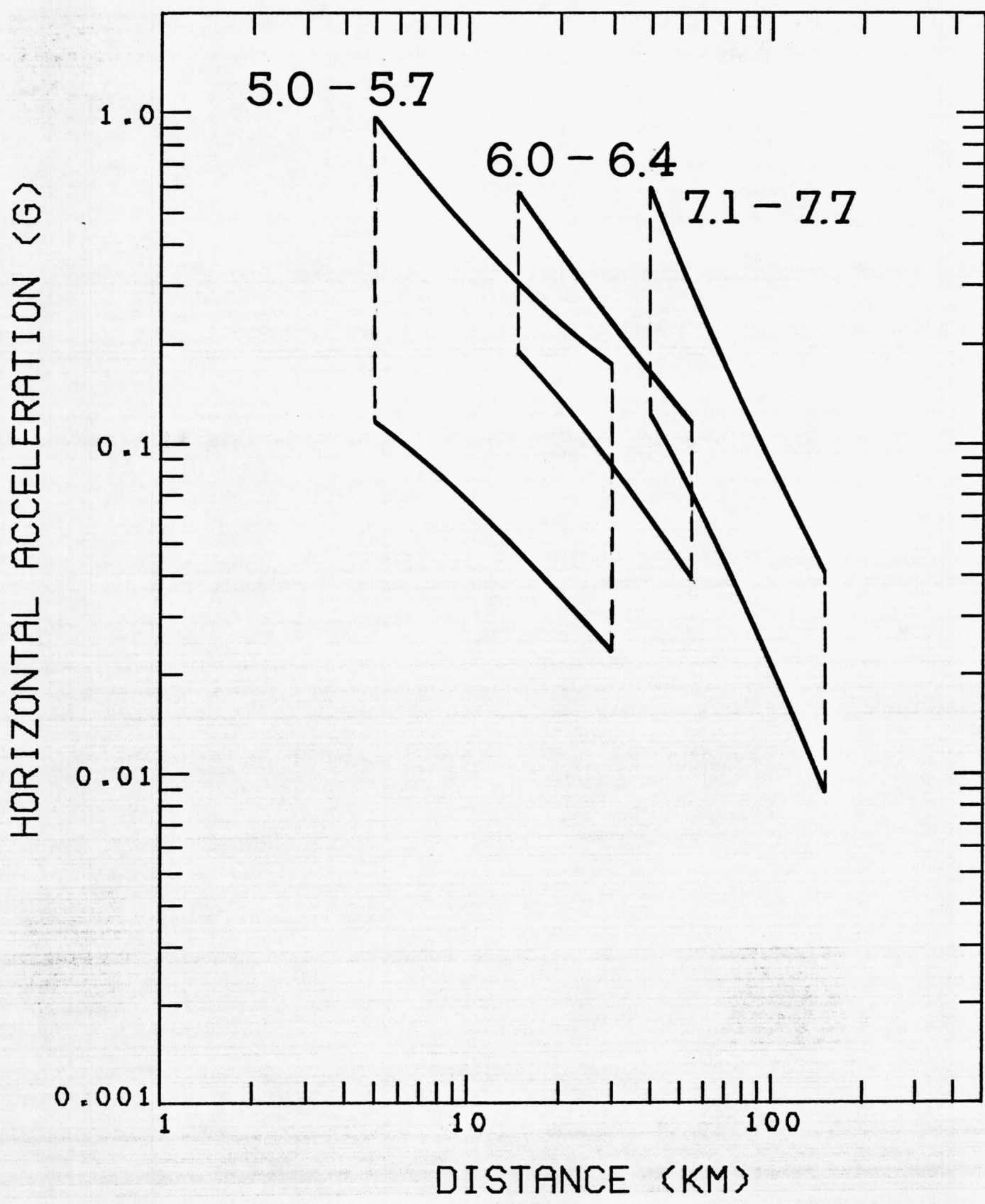


Figure 5. Peak horizontal velocity versus distance from the slipped fault for the magnitude range 5.3-5.7 recorded at the base of small structures. Symbols and curves same as in Figure 1.

MAGNITUDE 5.3-5.7 SMALL STRUCTURES

X = ROCK

◇ = SOIL

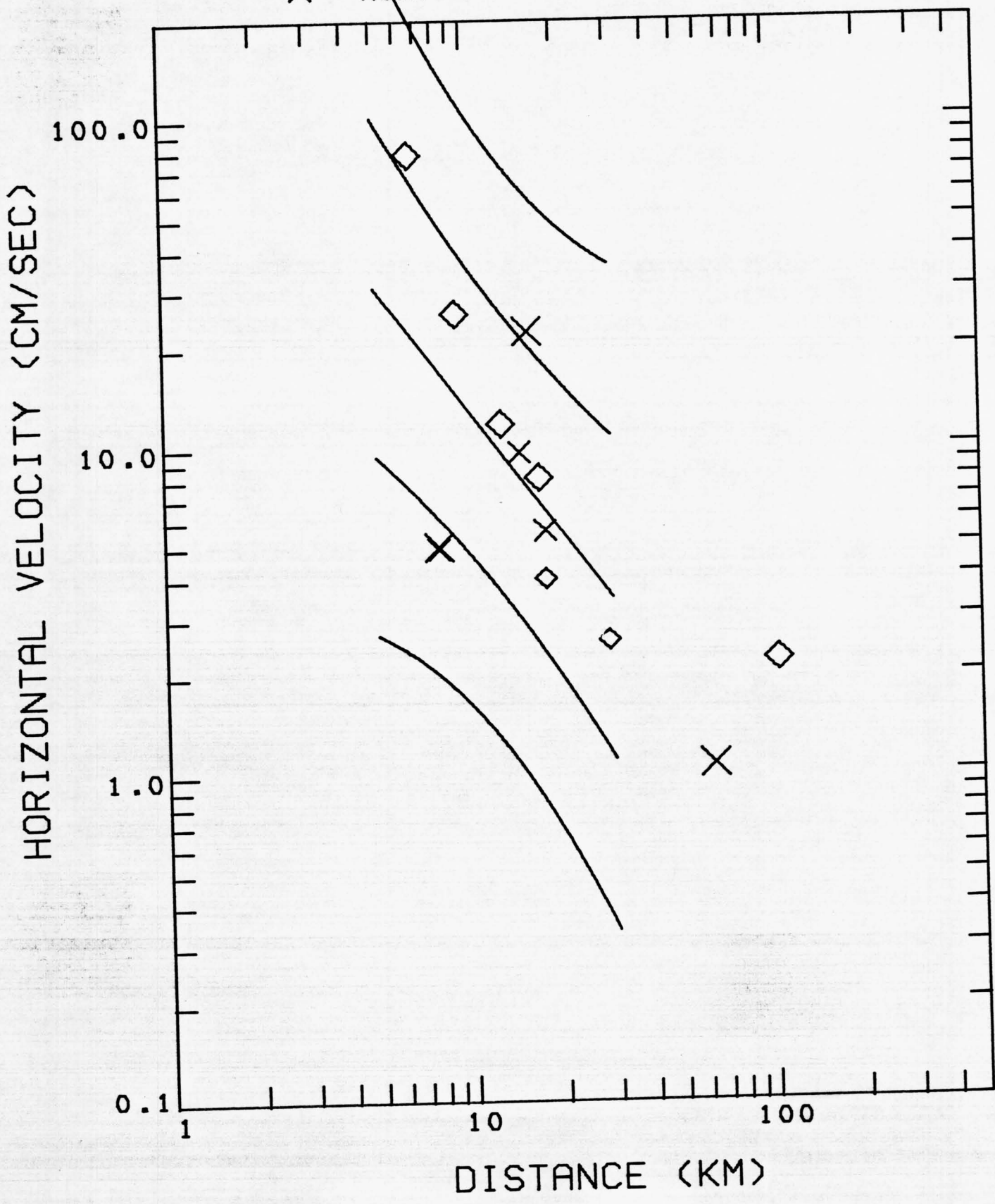


Figure 6. Peak horizontal velocity versus distance to the slipped fault for magnitude 6.4 recorded at the base of small structures. Symbols and curves same as in Figure 1.

MAGNITUDE 6.4 SMALL STRUCTURES

X = ROCK

◇ = SOIL

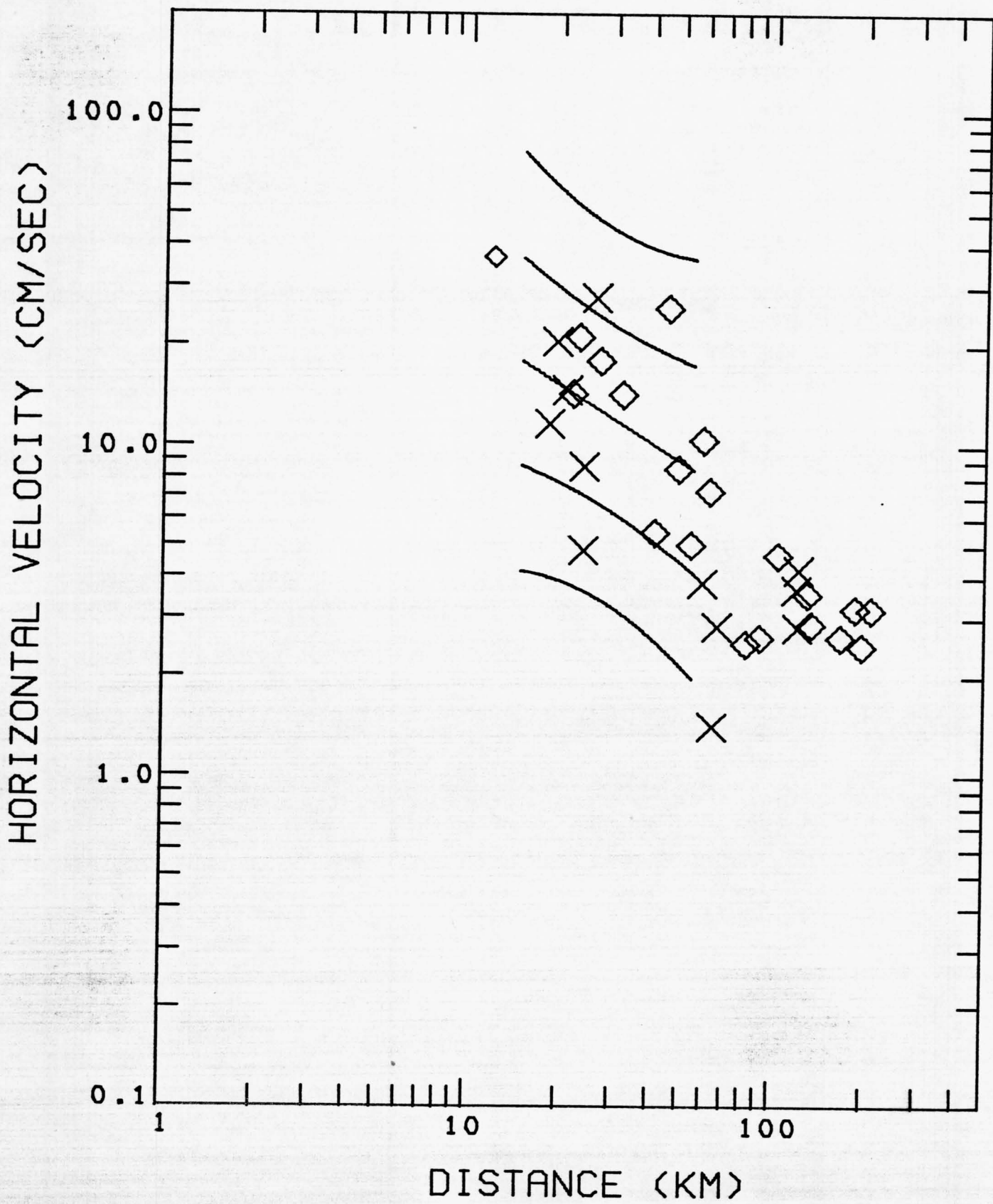


Figure 7. Peak horizontal velocity versus distance to the slipped fault for the magnitude range 7.1-7.7 recorded at the base of small structures. Symbols as in Figure 1.

MAGNITUDE 7.1-7.7 SMALL STRUCTURES

X = ROCK

◇ = SOIL

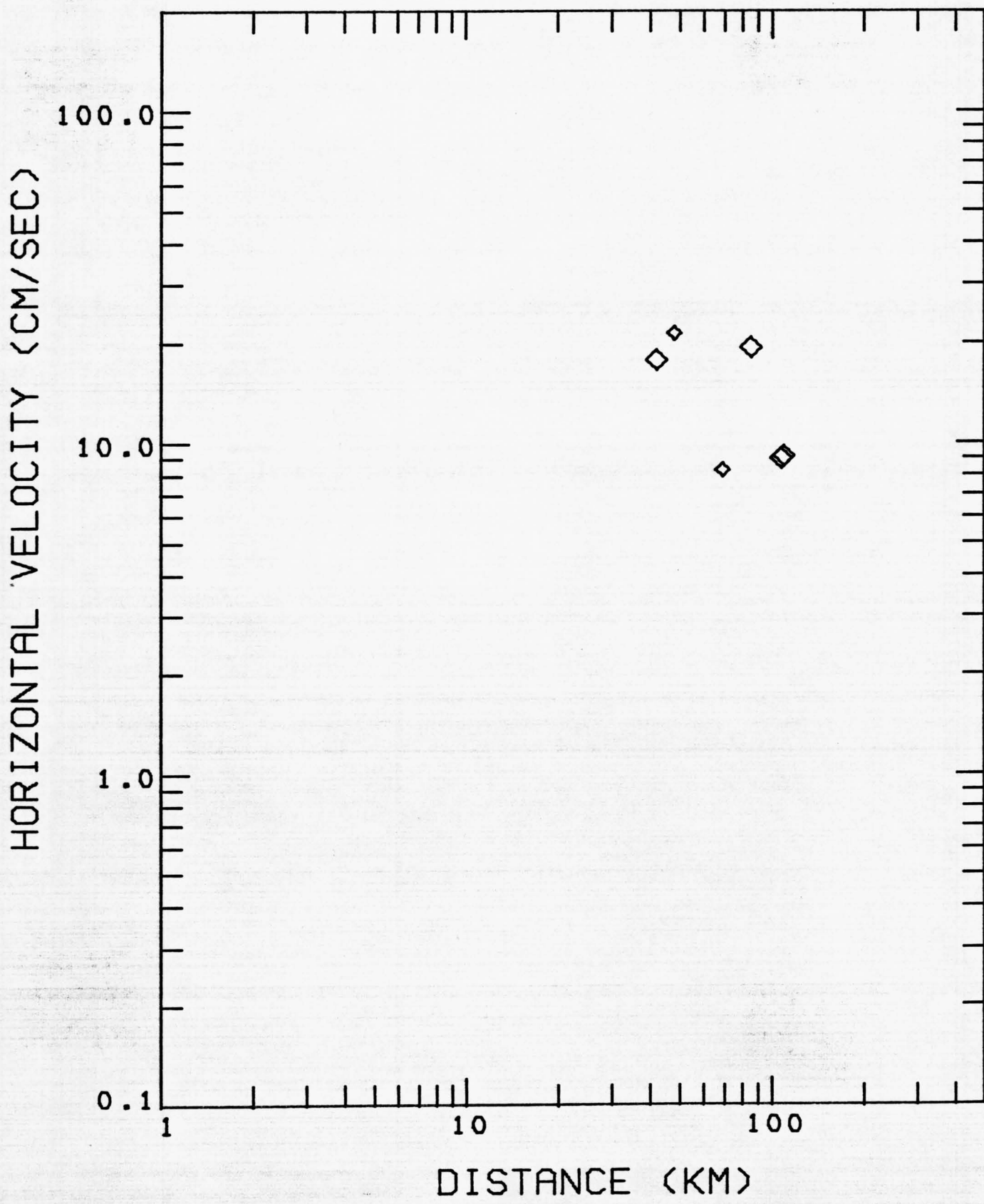


Figure 8. Comparison of the 70 percent prediction intervals for peak horizontal velocity recorded at the base of small structures for the three magnitude classes 5.3-5.7, 6.4, and 7.1-7.7. Curves for magnitude classes 5.3-5.7 and 6.4 taken from Figures 6 and 7.

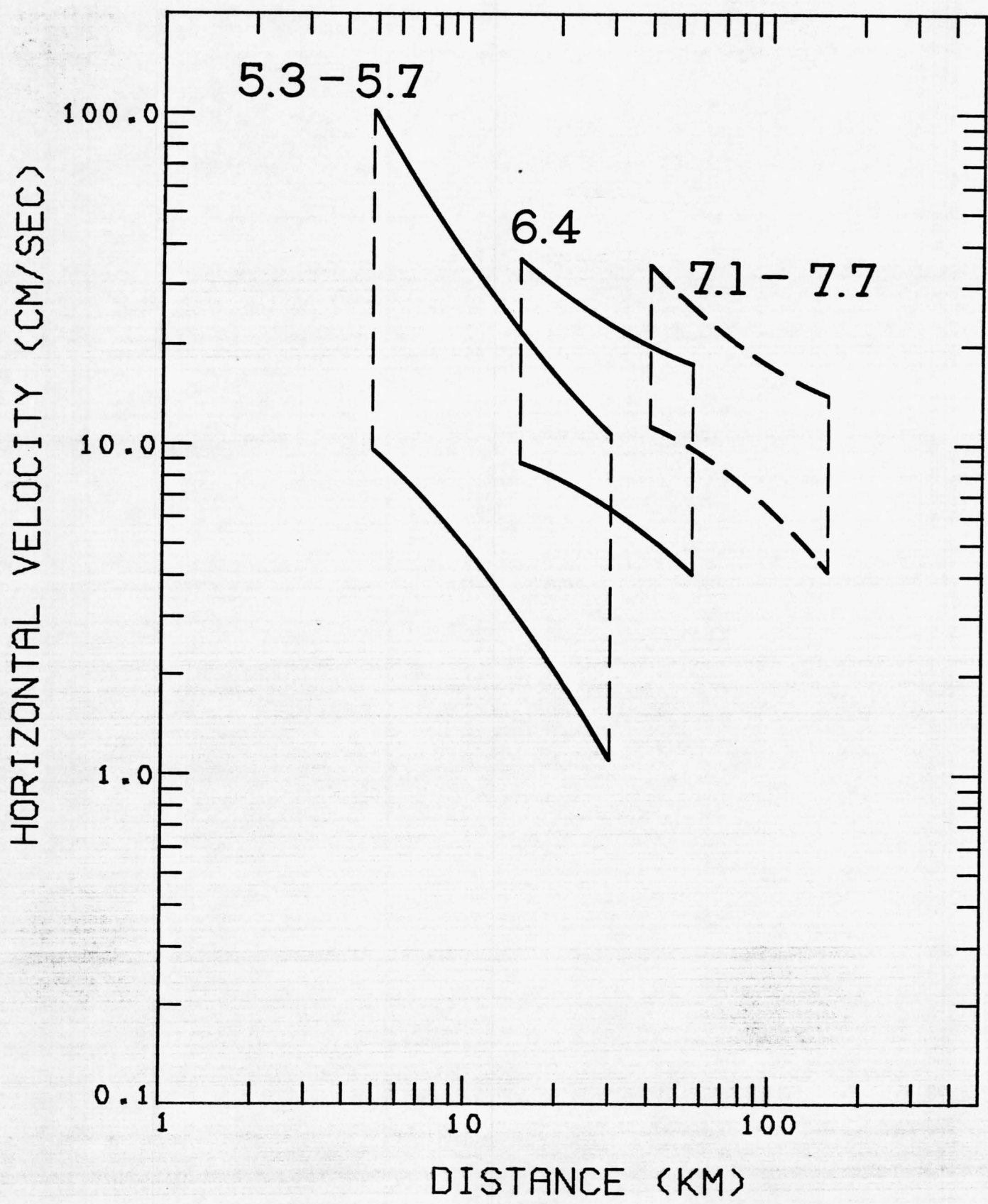


Figure 9. Peak horizontal displacement versus distance to the slipped fault for the magnitude range 5.3-5.7 recorded at the base of small structures. Symbols and curves same as in Figure 1.

MAGNITUDE 5.3-5.7 SMALL STRUCTURES

X = ROCK

◊ = SOIL

HORIZONTAL DISPLACEMENT (CM)

10.0

1.0

0.1

DISTANCE (KM)

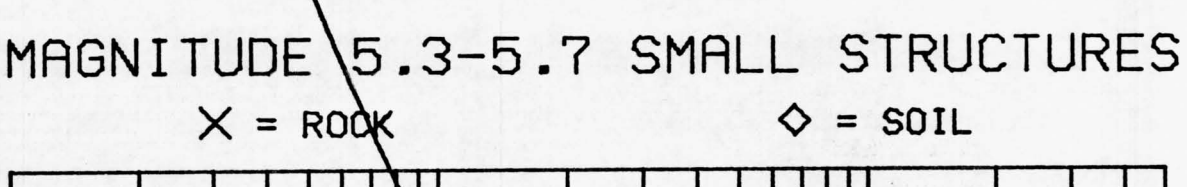
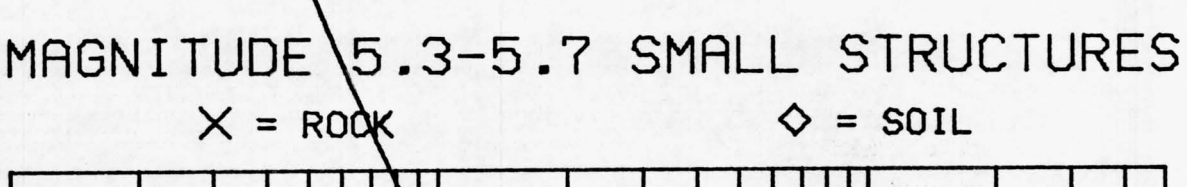


Figure 10. Peak horizontal displacement versus distance to the slipped fault for magnitude 6.4 recorded at the base of small structures. Symbols and curves same as in Figure 1.

MAGNITUDE 6.4 SMALL STRUCTURES

X = ROCK

◇ = SOIL

HORIZONTAL DISPLACEMENT (CM)

10.0

1.0

0.1

DISTANCE (KM)

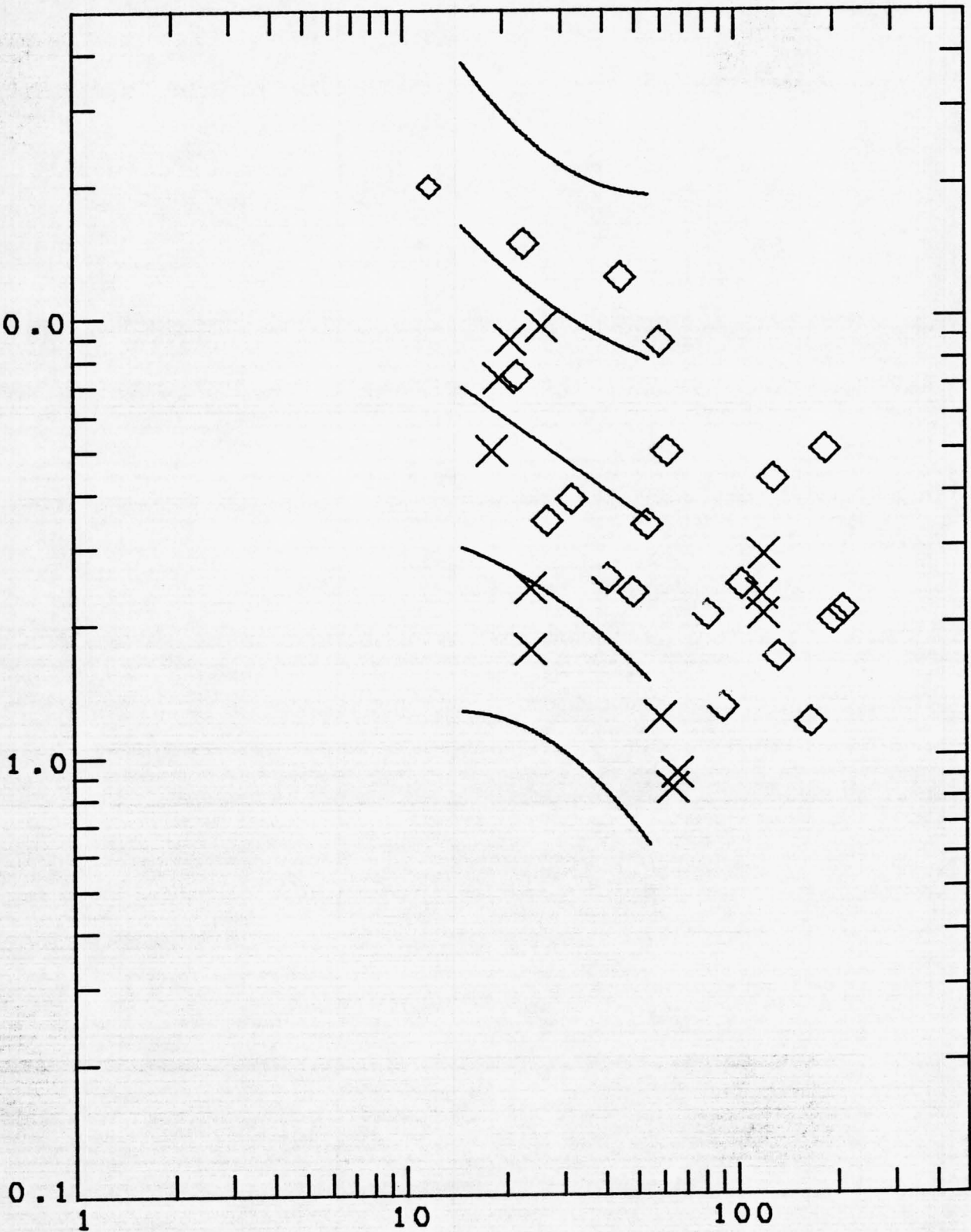


Figure 11. Peak horizontal displacement versus distance to the slipped fault for the magnitude range 7.1-7.7 recorded at the base of small structures. Symbols same as in Figure 1.

MAGNITUDE 7.1-7.7 SMALL STRUCTURES

X = ROCK

◇ = SOIL

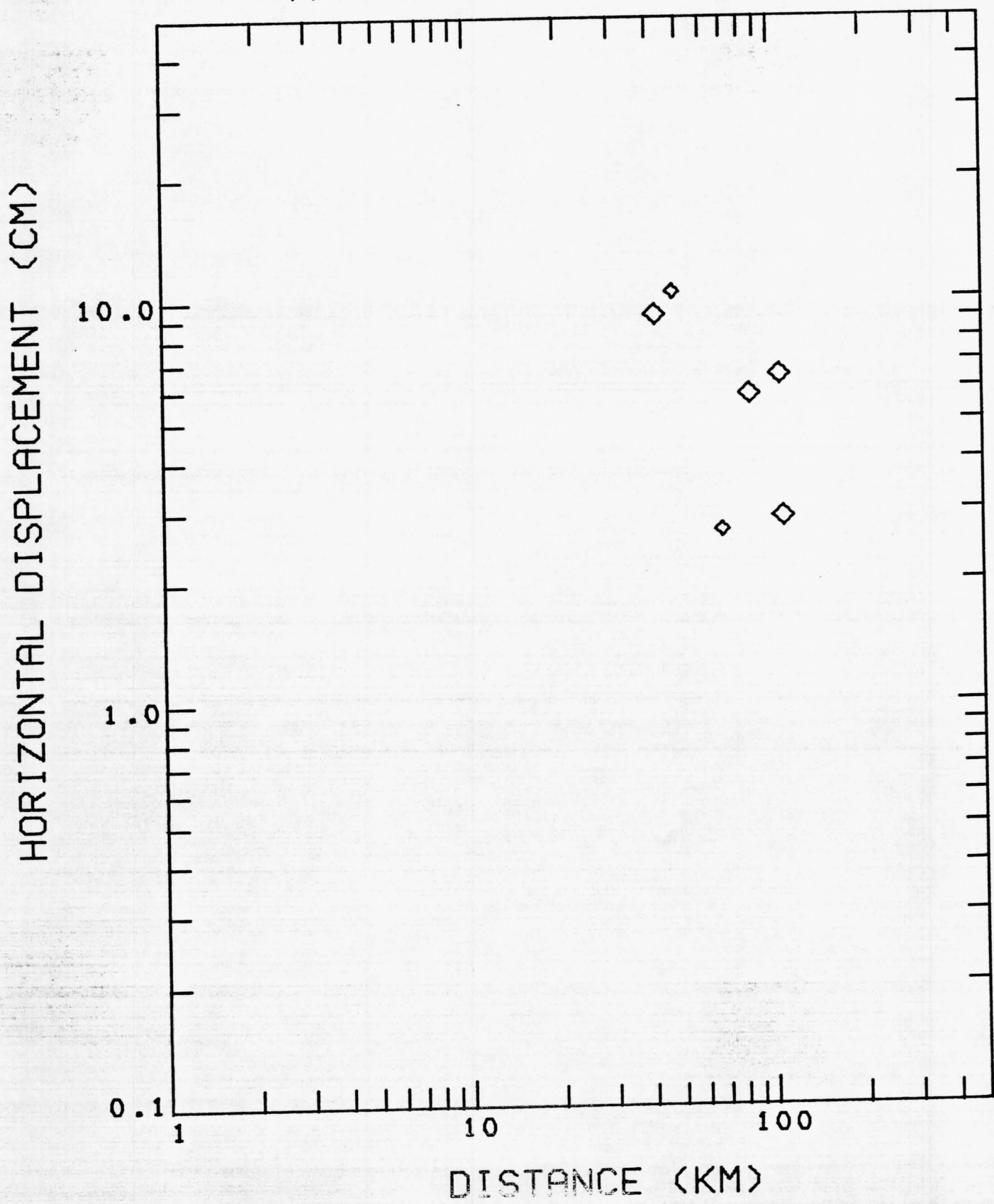


Figure 12. Comparison of the 70 percent prediction intervals for peak horizontal displacement recorded at the base of small structures for the three magnitude classes 5.3-5.7, 6.4, and 7.1-7.7. Curves for magnitude classes 5.3-5.7 and 6.4 taken from Figures 11 and 12.

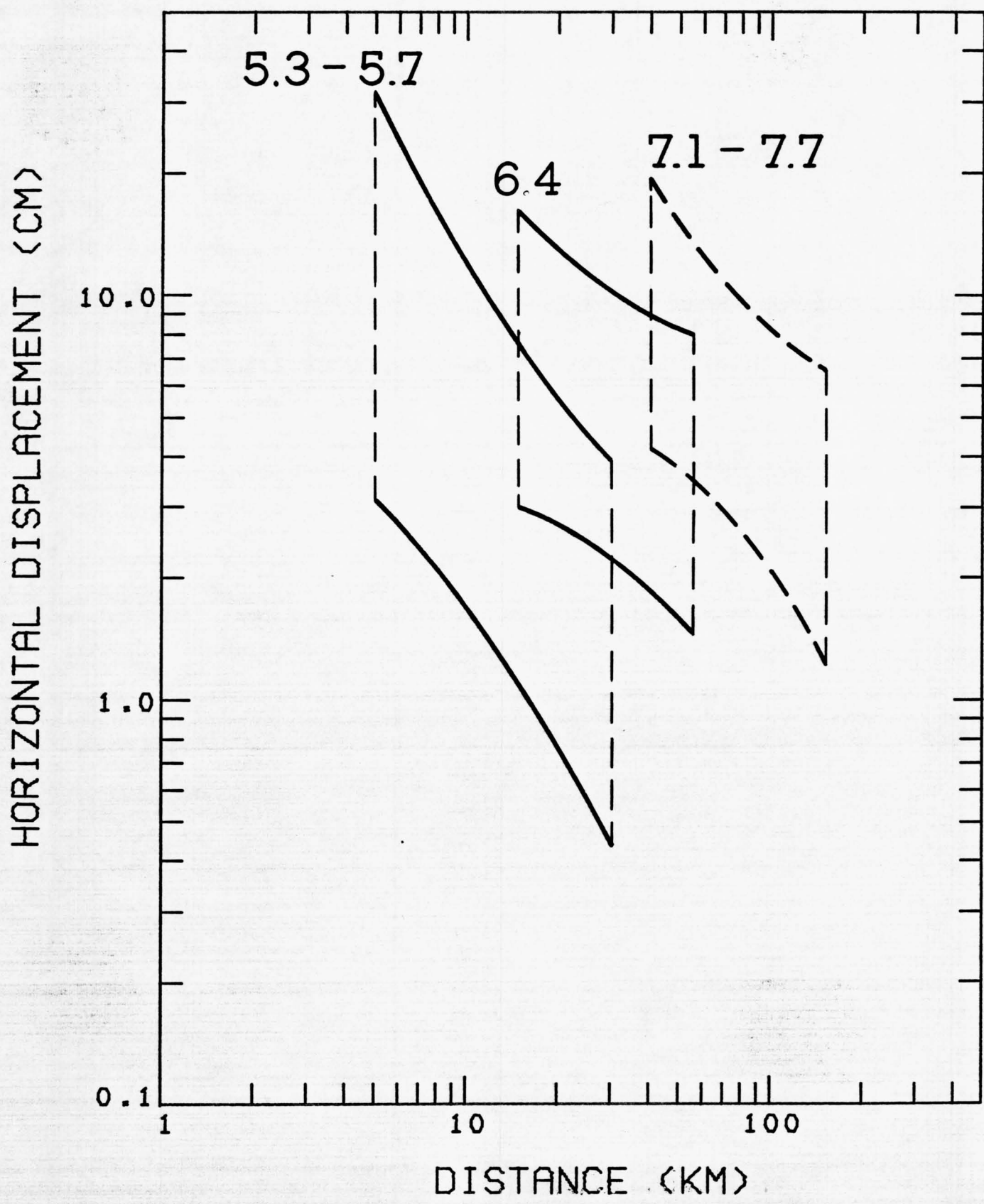


Figure 13. Duration versus distance from the slipped fault for recordings from small structures. Triangles represent the magnitude class 5.0-5.7, hexagons represent the magnitude class 6.0-6.4, and inverted triangles represent the magnitude class 7.1-7.9. X's represent "zero durations" as explained in the text.

SMALL STRUCTURES

Δ = MAG 5

\diamond = MAG 6

∇ = MAG 7

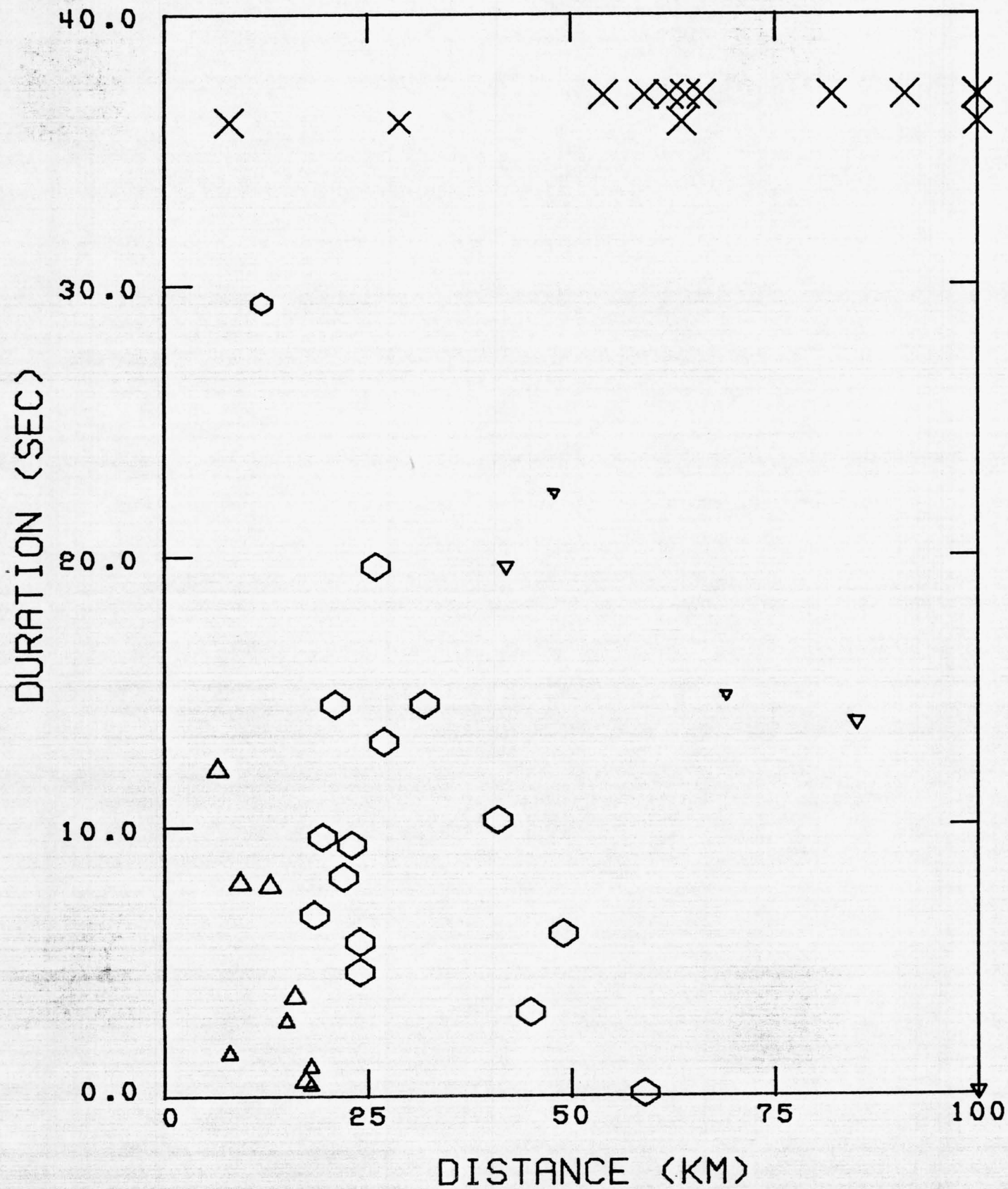


Figure 14. Peak vertical acceleration versus distance to the slipped fault for the magnitude range 5.0-5.7 recorded at the base of small structures. Symbols and curves same as in Figure 1.

MAGNITUDE 5.0-5.7 SMALL STRUCTURES

\times = ROCK

\diamond = SOIL

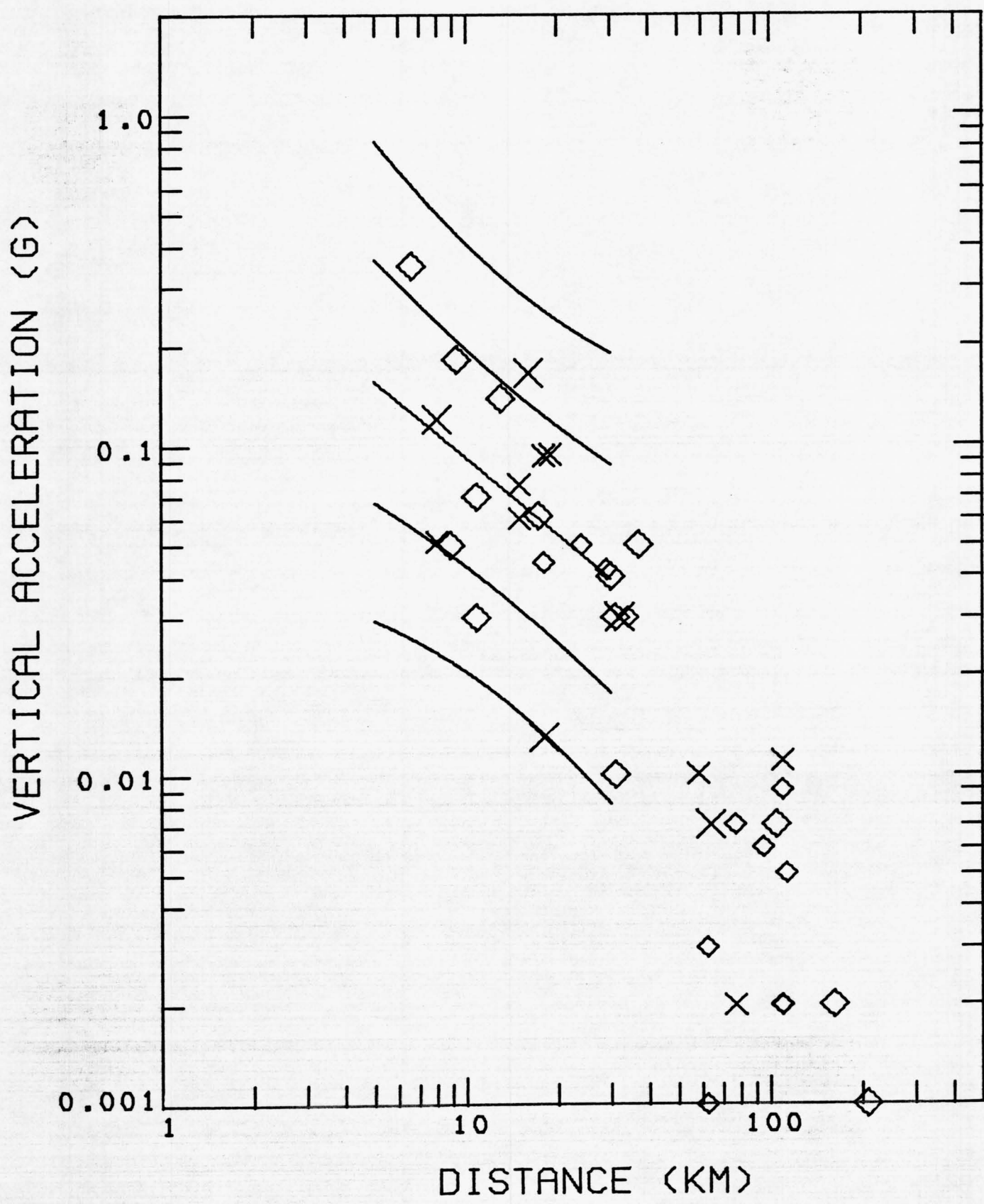


Figure 15. Peak vertical acceleration versus distance to the slipped fault
for the magnitude range 6.0-6.4 recorded at the base of small
structures. Symbols and curves same as in Figure 1.

MAGNITUDE 6.0-6.4 SMALL STRUCTURES

X = ROCK

◇ = SOIL

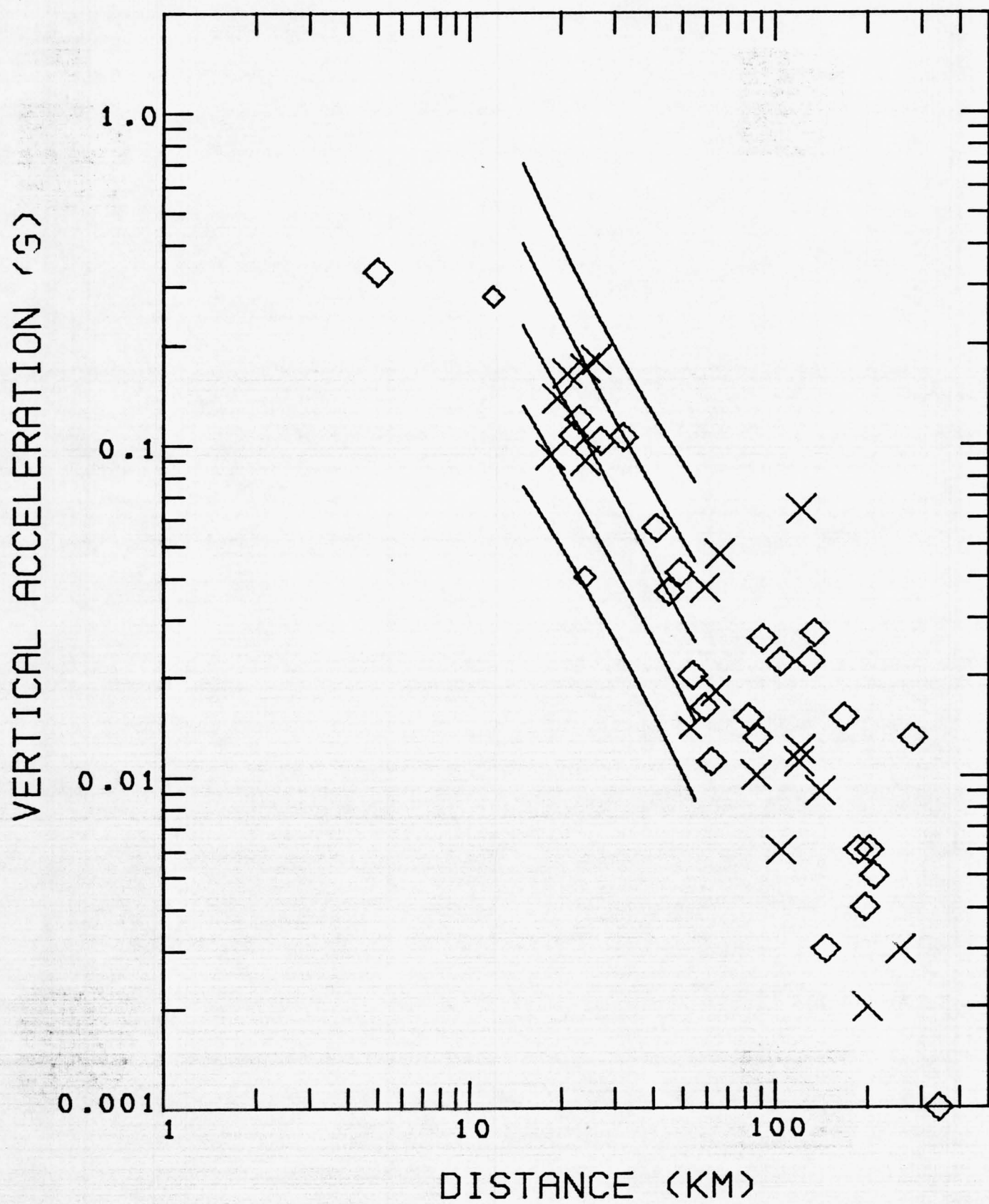


Figure 16. Peak vertical acceleration versus distance to the slipped fault
for the magnitude range 7.1-7.7 recorded at the base of
small structures. Symbols and curves same as in Figure 1.

MAGNITUDE 7.1-7.7 SMALL STRUCTURES

X = ROCK

◇ = SOIL

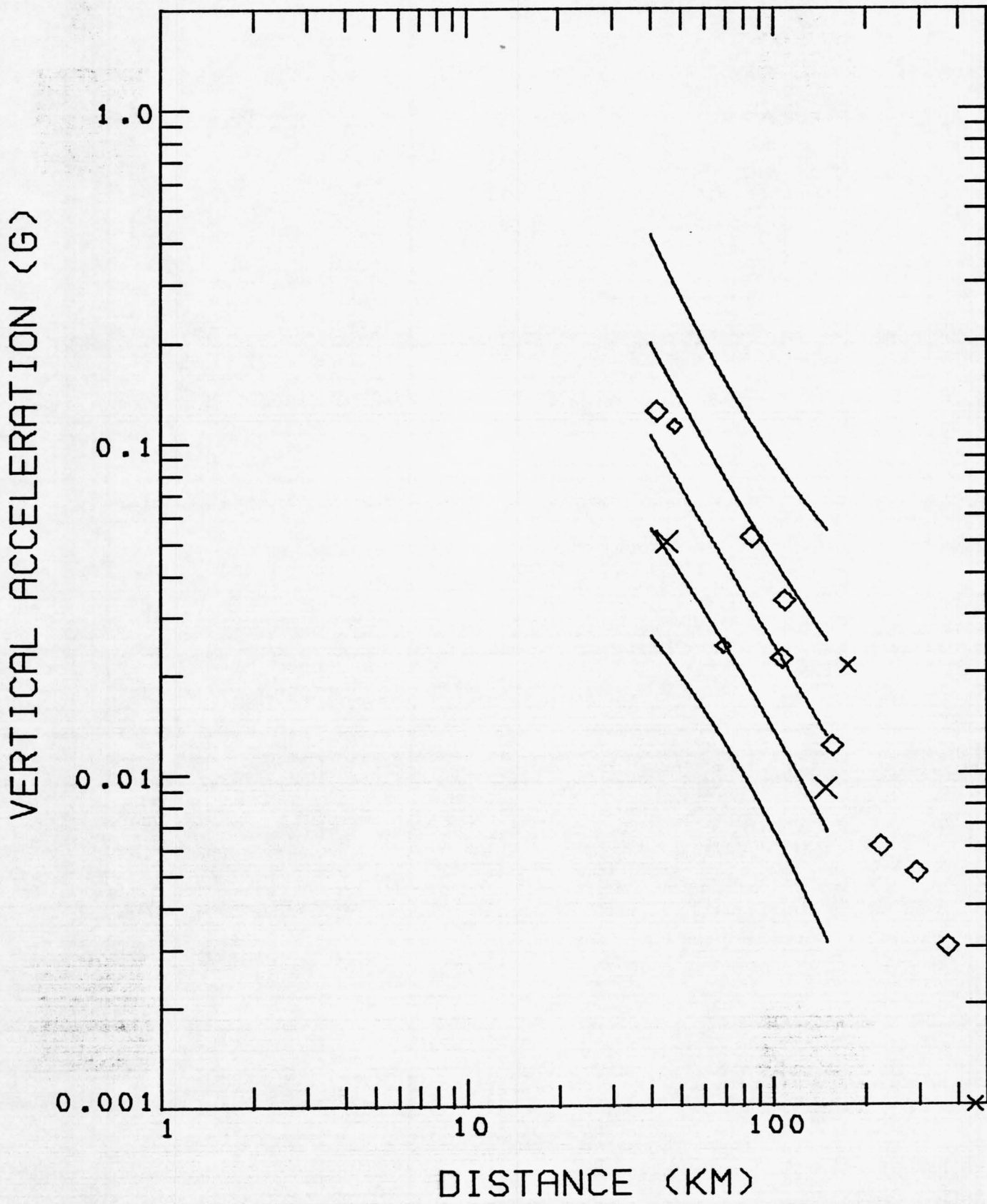


Figure 17. Peak vertical velocity versus distance to the slipped fault for the magnitude range 5.3-5.7 recorded at the base of small structures. Symbols and curves same as in Figure 1.

MAGNITUDE 5.3-5.7 SMALL STRUCTURES

X = ROCK

◇ = SOIL

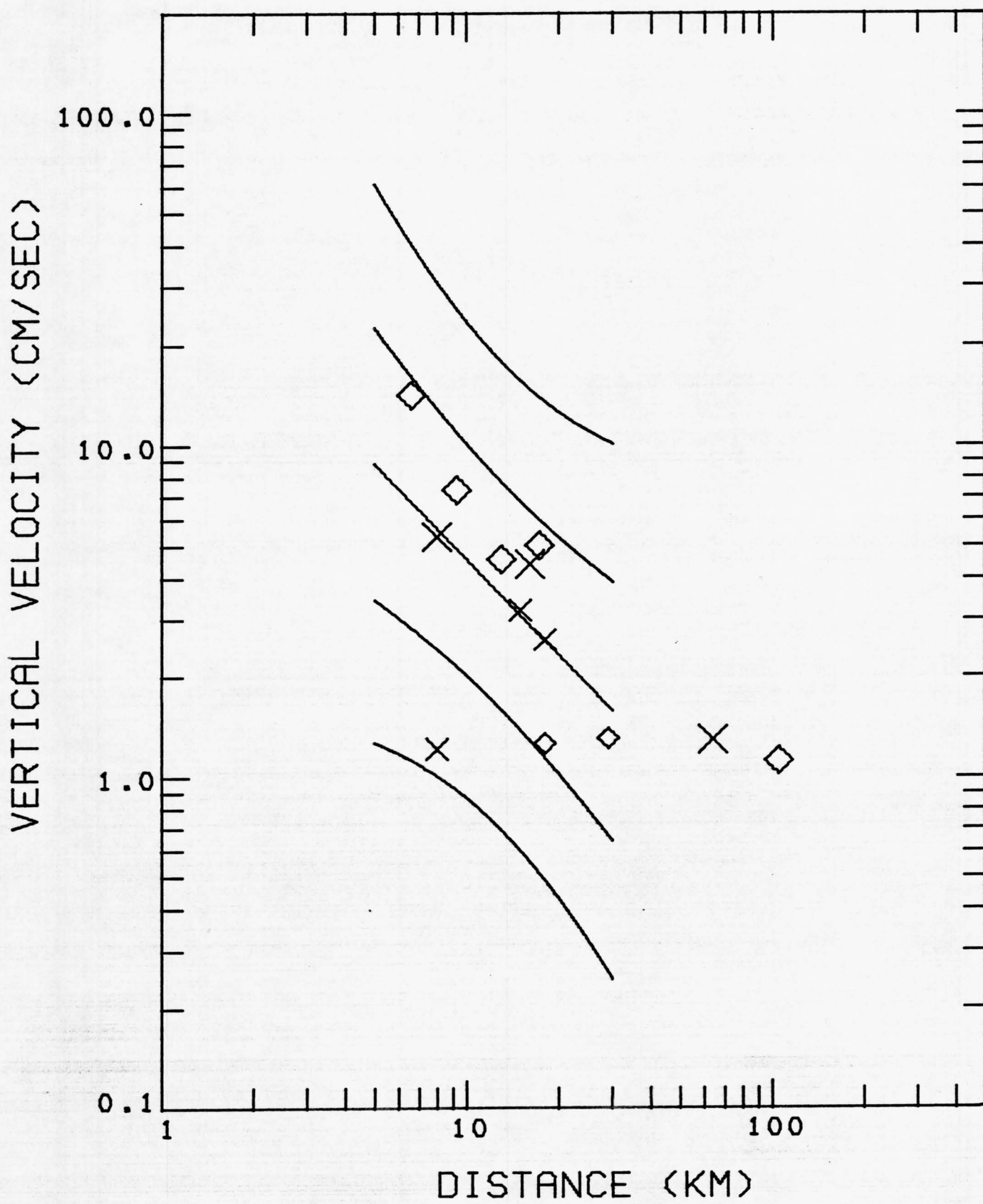


Figure 18. Peak vertical velocity versus distance to the slipped fault for magnitude 6.4 recorded at the base of small structures. Symbols and curves same as in Figure 1.

MAGNITUDE 6.4 SMALL STRUCTURES

X = ROCK

◇ = SOIL

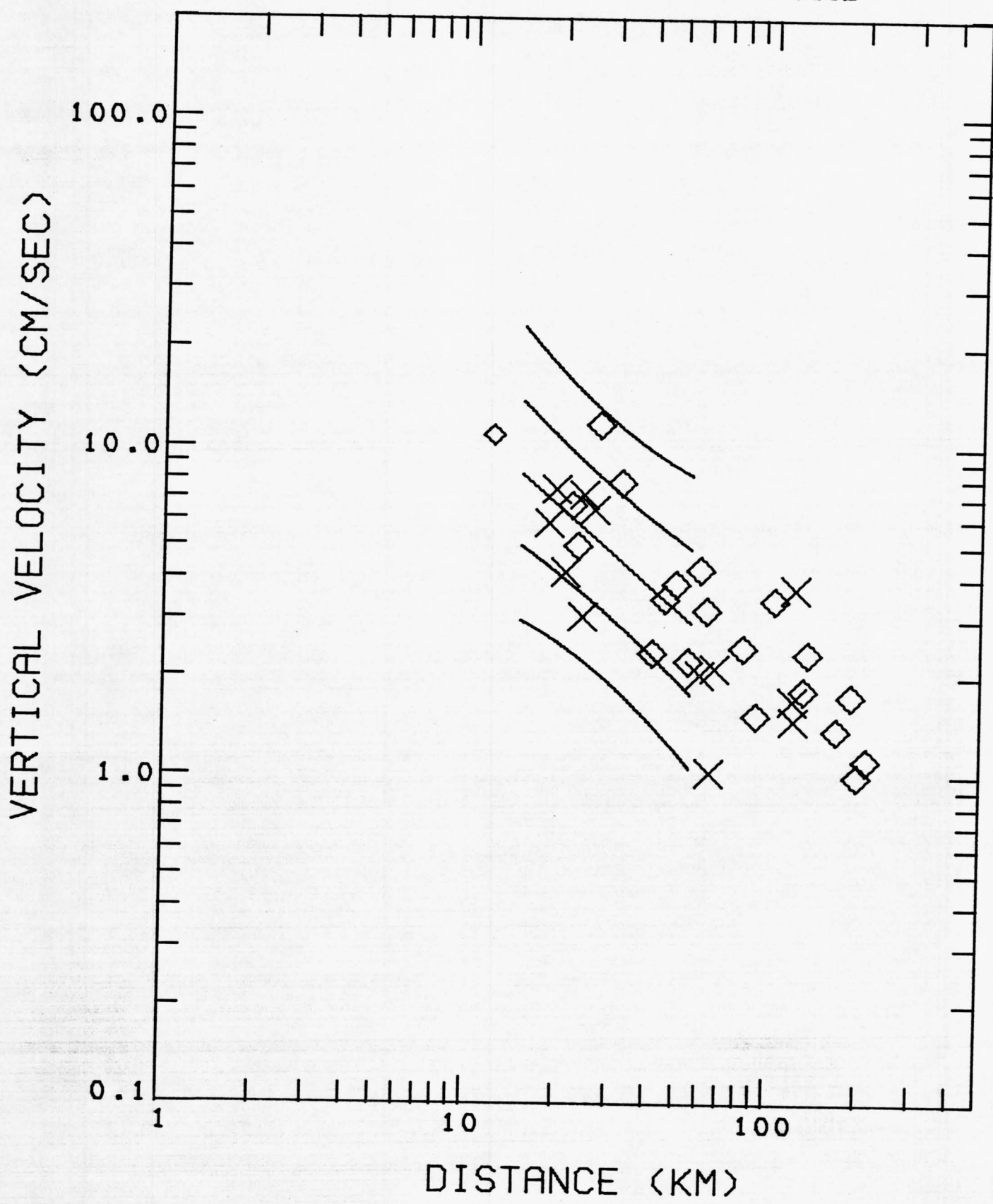


Figure 19. Peak vertical velocity versus distance to the slipped fault for the magnitude range 7.1-7.7 recorded at the base of small structures. Symbols same as in Figure 1.

MAGNITUDE 7.1-7.7 SMALL STRUCTURES

X = ROCK

◇ = SOIL

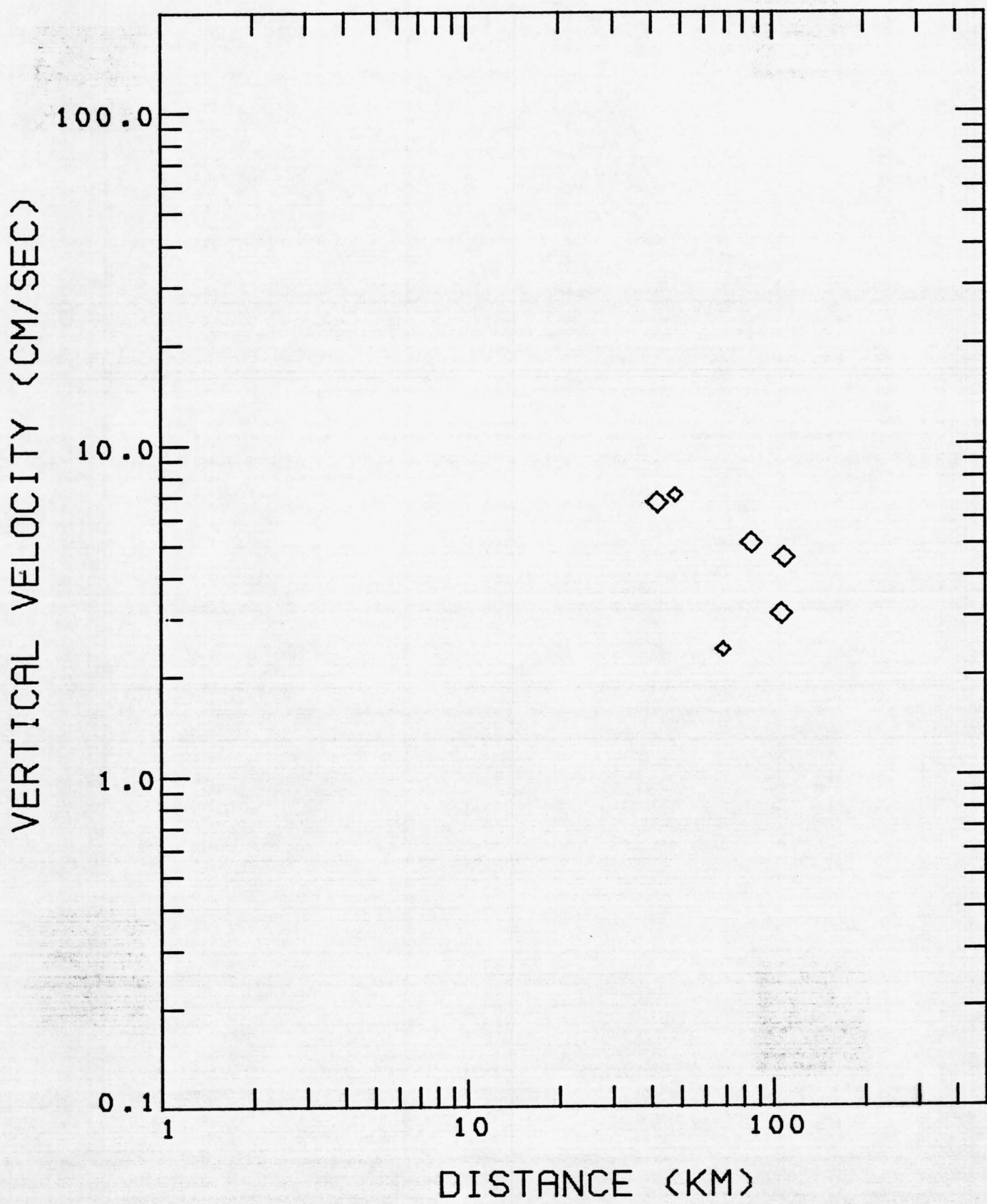


Figure 20. Peak vertical displacement versus distance to the slipped fault for the magnitude range 5.3-5.7 recorded at the base of small structures. Symbols and curves same as in Figure 1.

MAGNITUDE 5.3-5.7 SMALL STRUCTURES
X = ROCK \diamond = SOIL

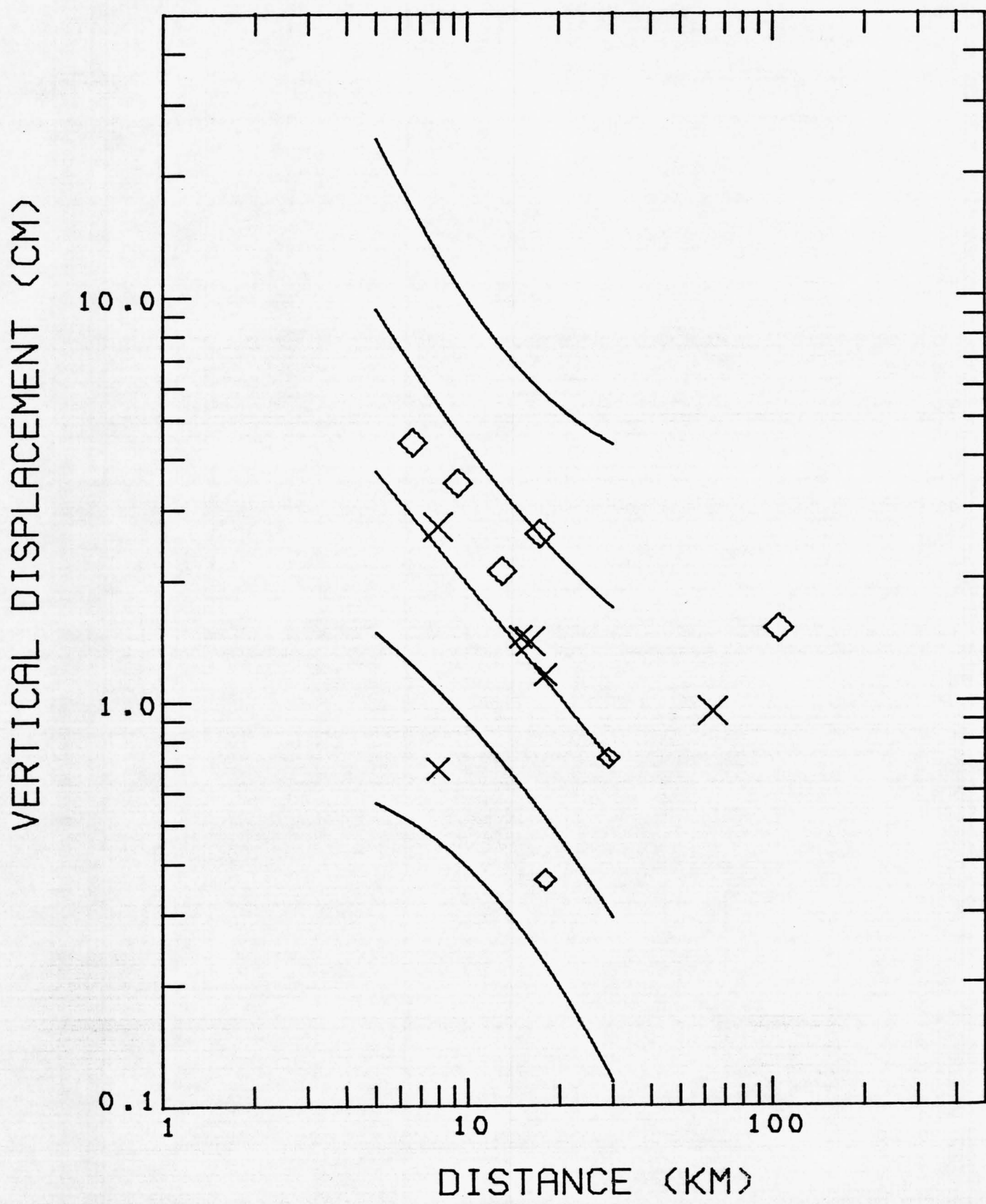


Figure 21. Peak vertical displacement versus distance to the slipped fault
for magnitude 6.4 recorded at the base of small
structures. Symbols and curves same as in Figure 1.

MAGNITUDE 6.4 SMALL STRUCTURES

X = ROCK

◊ = SOIL

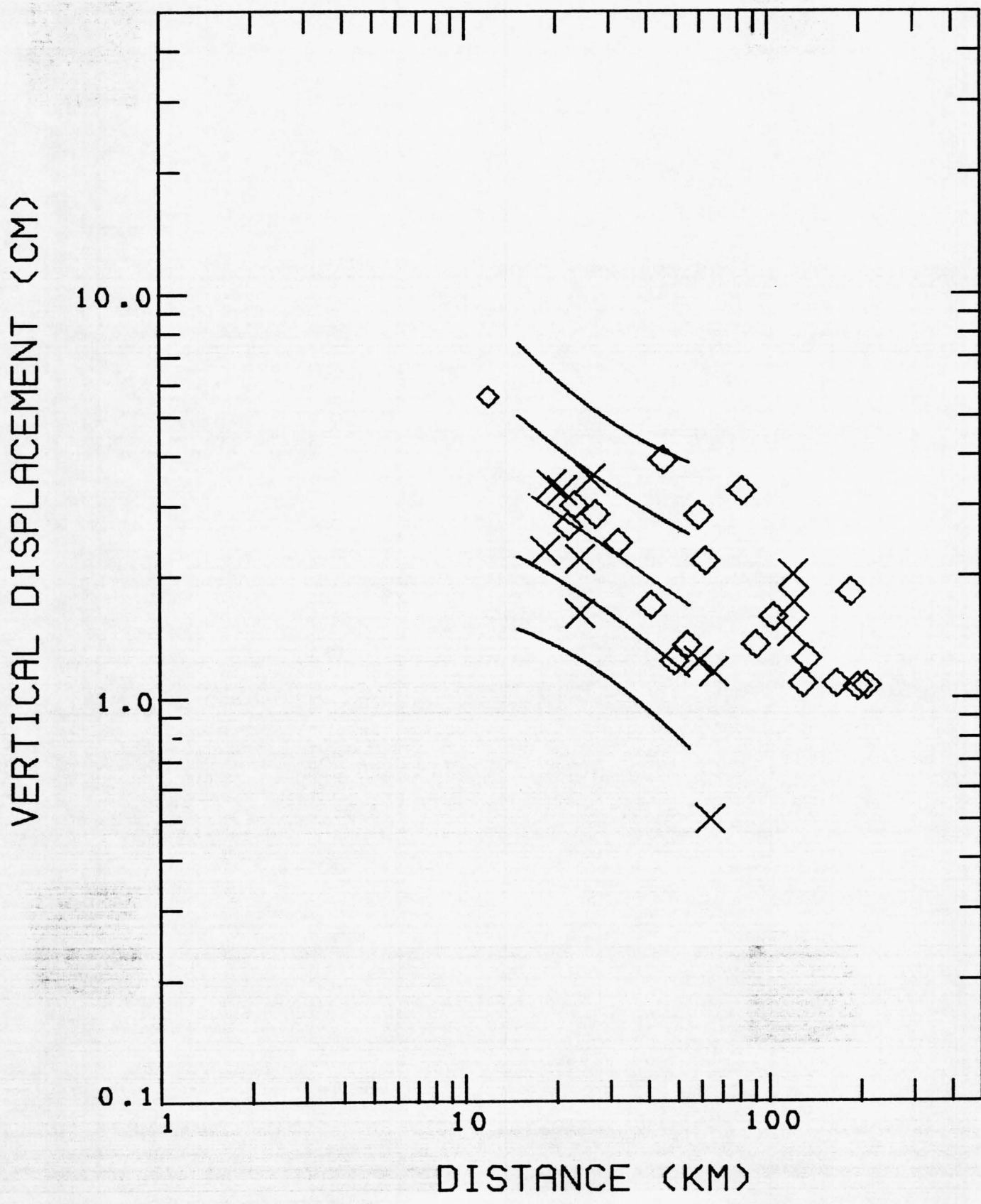


Figure 22. Peak vertical displacement versus distance from the slipped fault for the magnitude range 7.1-7.7 recorded at the base of small structures. Symbols same as in Figure 1.

MAGNITUDE 7.1-7.7 SMALL STRUCTURES

X = ROCK

◇ = SOIL

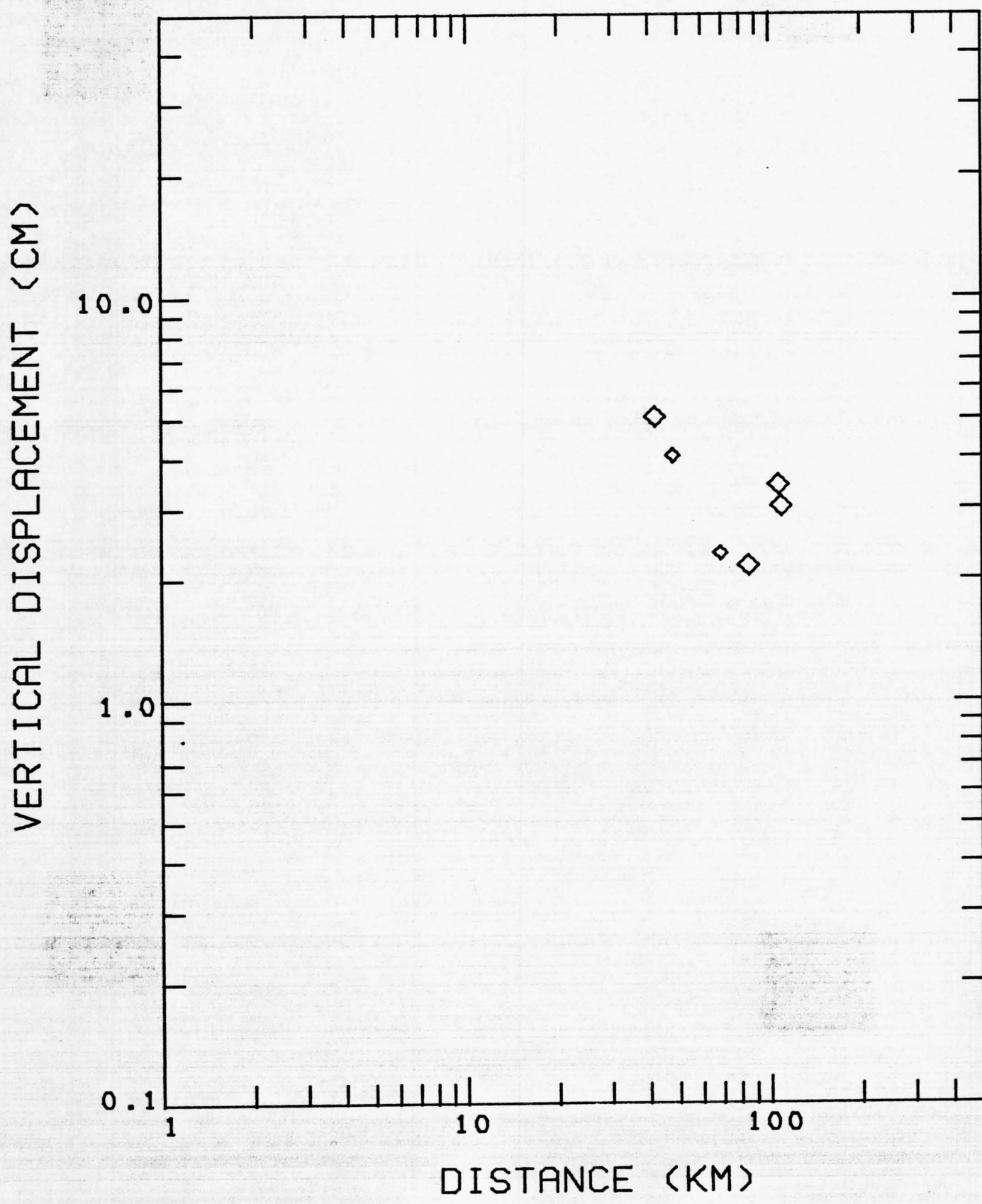


Figure 23. Peak horizontal acceleration versus distance to the slipped fault for the magnitude range 5.0-5.7 including data from both large and small structures. The pluses represent rock sites and the squares soil sites. The center line is the mean regression line. The outer pair of lines represents the 95 percent prediction interval, and the inner pair represents the 70 percent prediction interval. Length of lines represents the distance interval considered in the regression analysis.

MAGNITUDE 5.0-5.7

+ = ROCK

□ = SOIL

HORIZONTAL ACCELERATION (G)

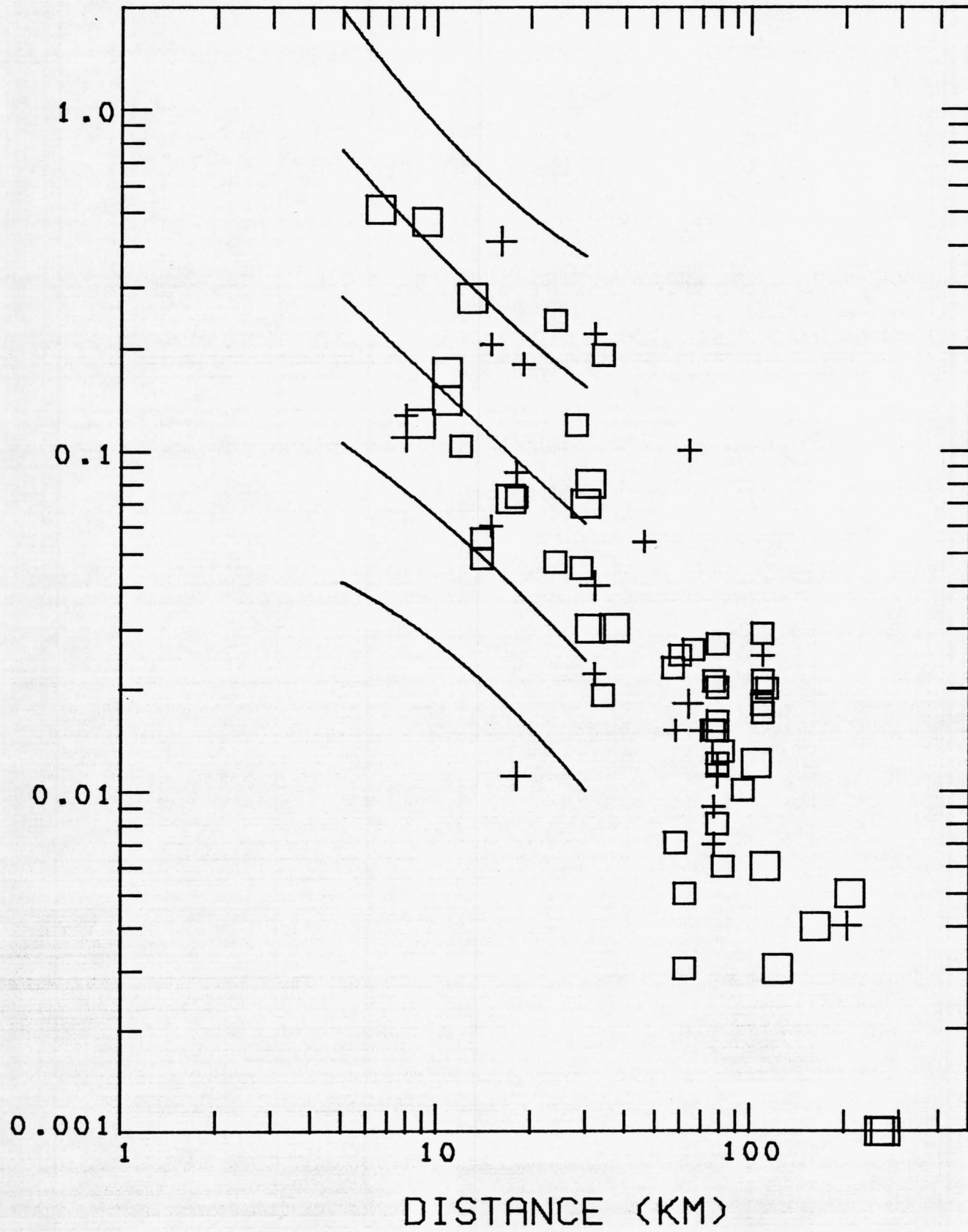


Figure 24. Peak horizontal acceleration versus distance to the slipped fault for the magnitude range 6.0-6.4 including data from both large and small structures. Symbols and curves same as in Figure 23.

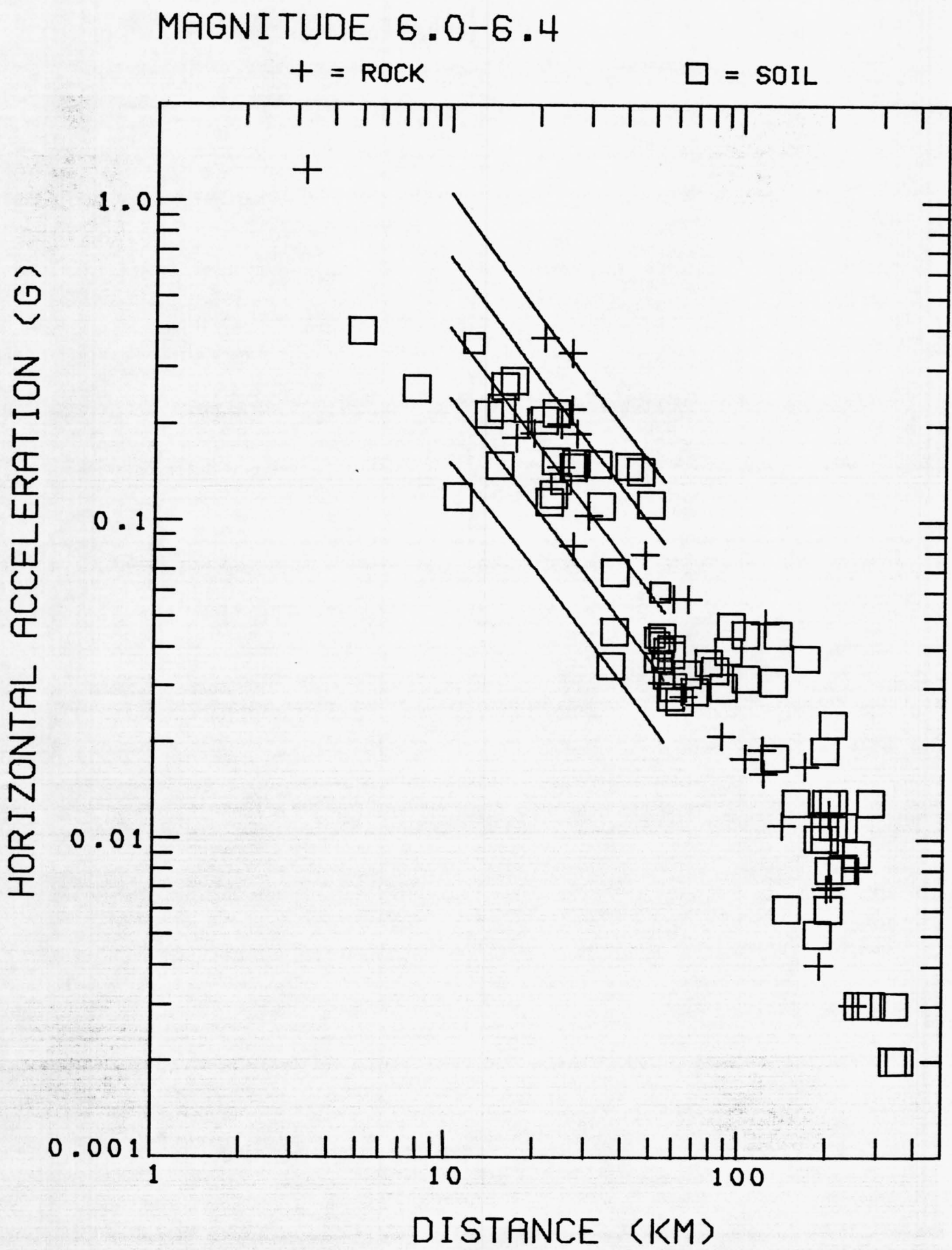


Figure 25. Peak horizontal acceleration versus distance to the slipped fault for the magnitude range 7.1-7.7 including data from both large and small structures. Symbols and curves same as in Figure 23.

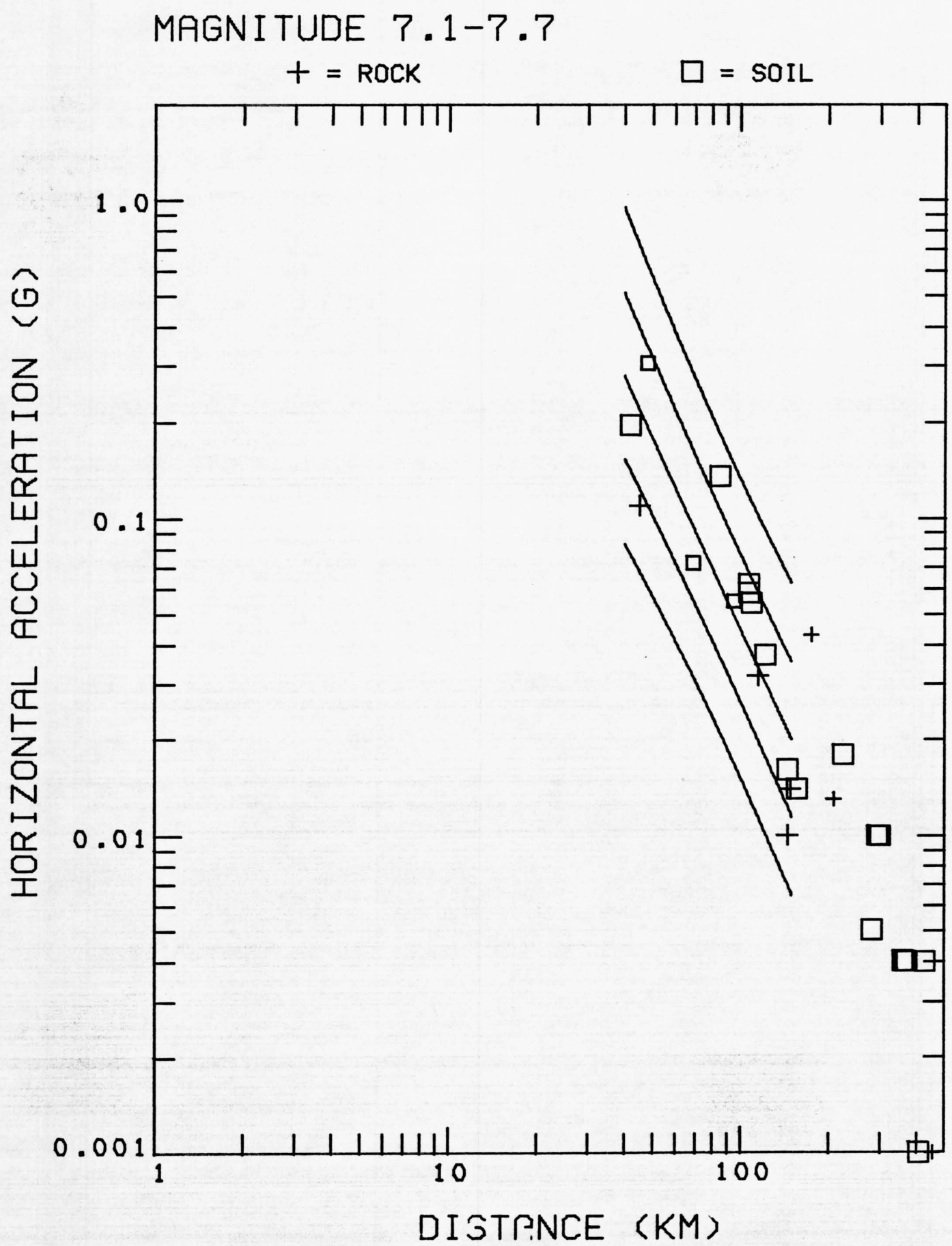


Figure 26. Peak horizontal velocity versus distance to the slipped fault for the magnitude range 5.3-5.7 including data from both large and small structures. Symbols and curves same as in Figure 23.

MAGNITUDE 5.3-5.7

+ = ROCK

□ = SOIL

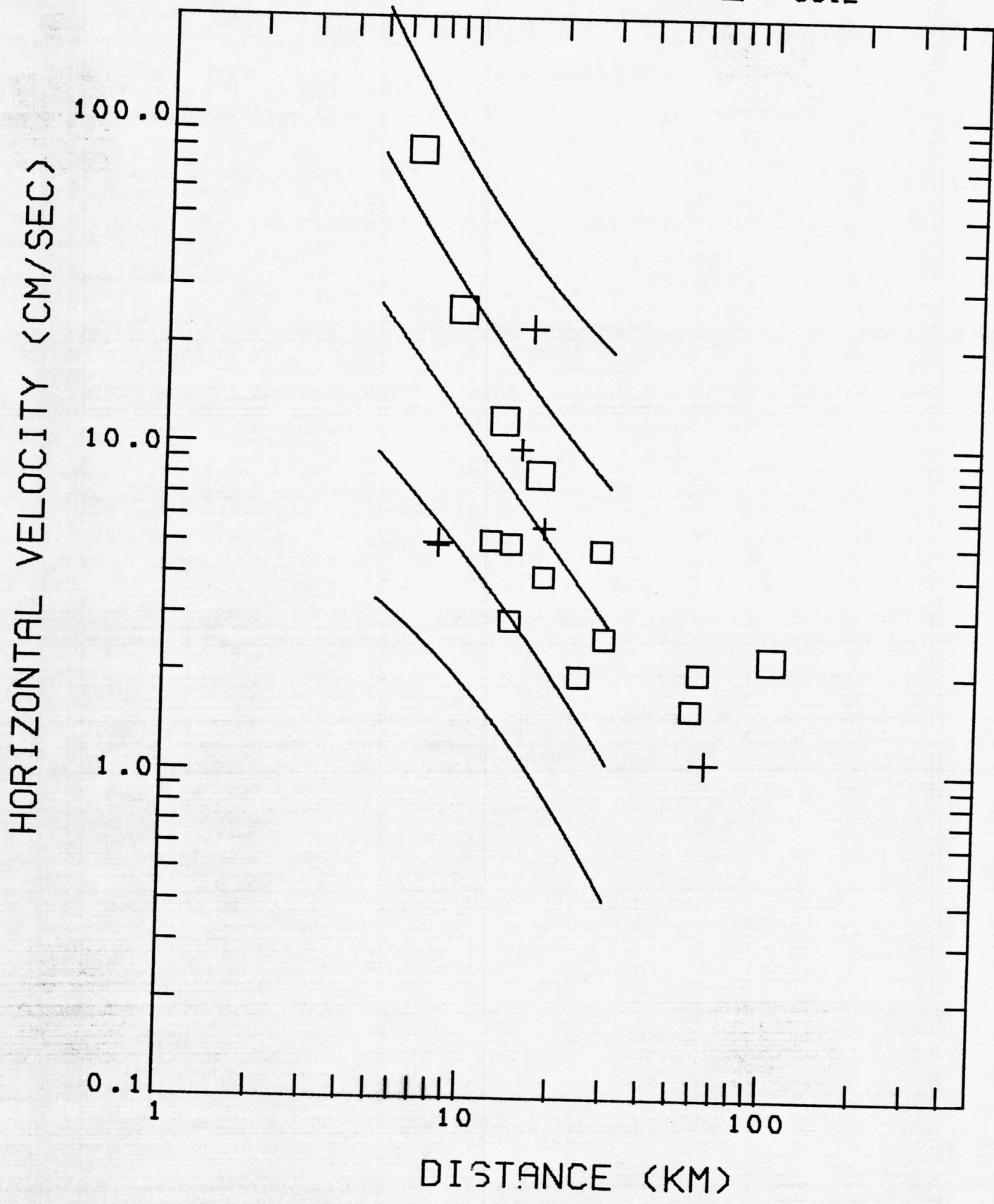


Figure 27. Peak horizontal velocity versus distance to the slipped fault for magnitude 6.4 including data from both large and small structures. Symbols and curves same as in Figure 23.

MAGNITUDE 6.4

+ = ROCK

□ = SOIL

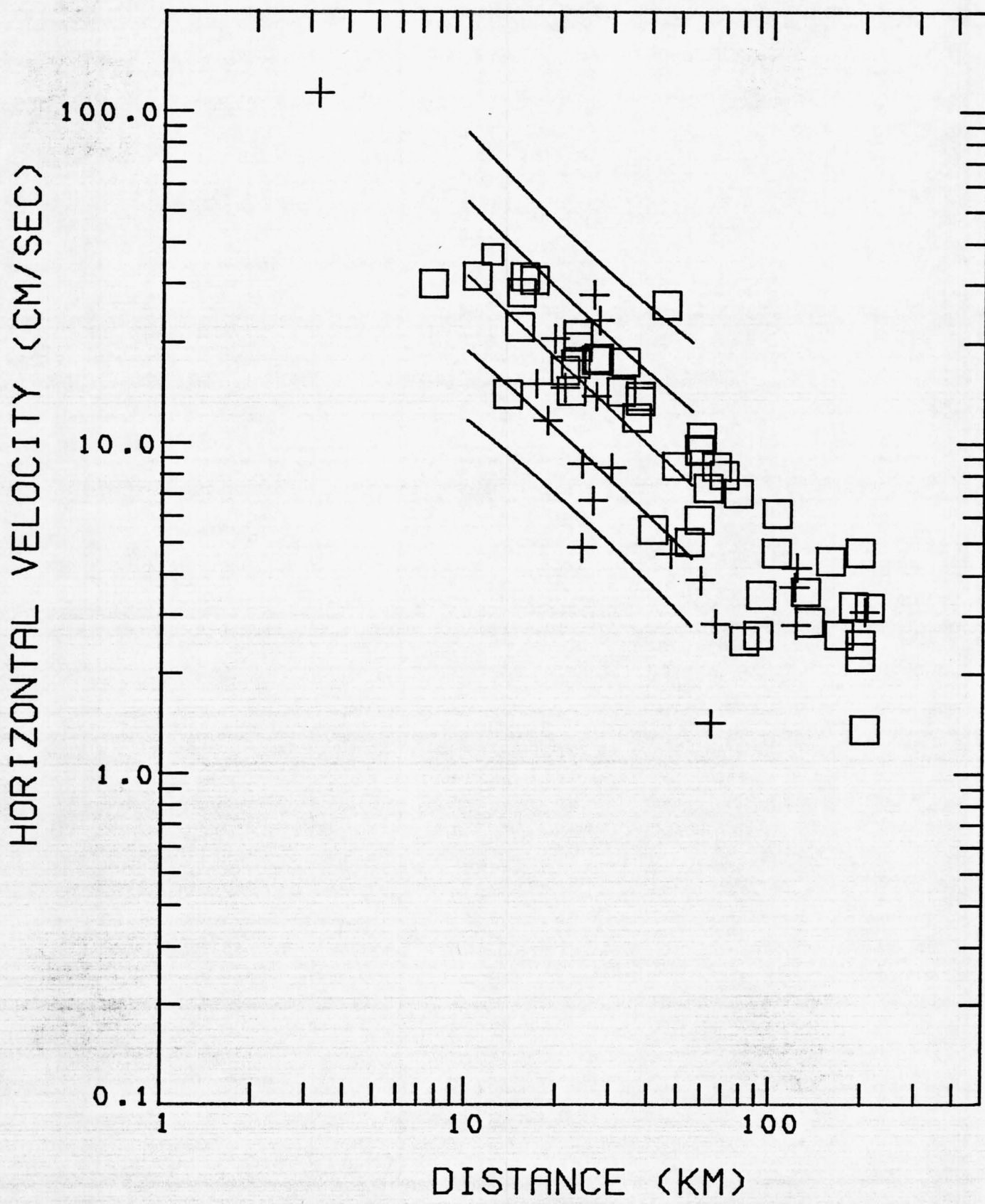


Figure 28. Peak horizontal velocity versus distance to the slipped fault for the magnitude range 7.1-7.7 including data from both large and small structures. Symbols same as in Figure 23.

MAGNITUDE 7.1-7.7

+ = ROCK

□ = SOIL

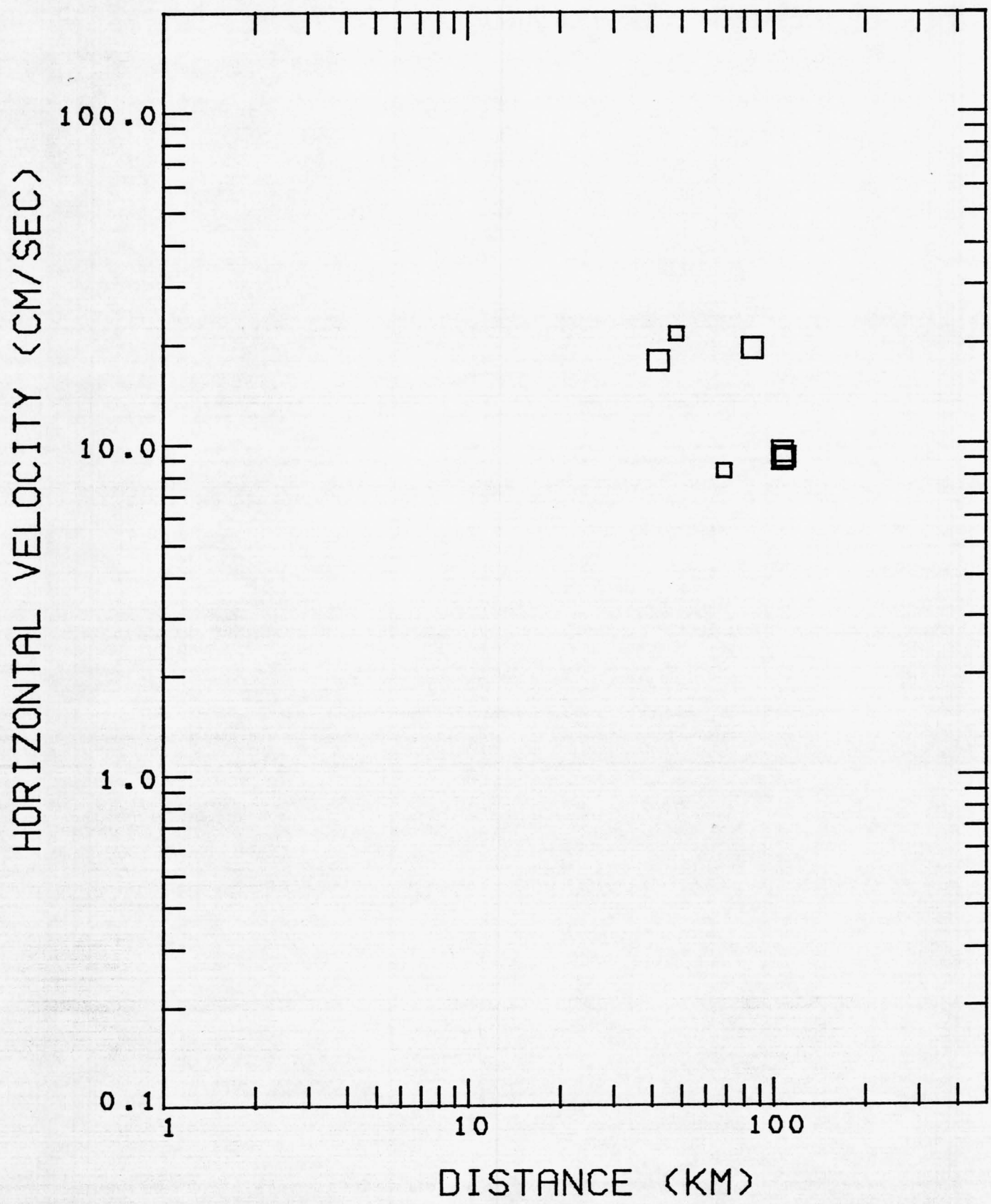


Figure 29. Peak horizontal displacement versus distance to the slipped fault for the magnitude range 5.3-5.7 including data from both large and small structures. Symbols and curves same as in Figure 23.

MAGNITUDE 5.3-5.7

+ = ROCK

□ = SOIL

HORIZONTAL DISPLACEMENT (CM)

10.0

1.0

0.1

DISTANCE (KM)

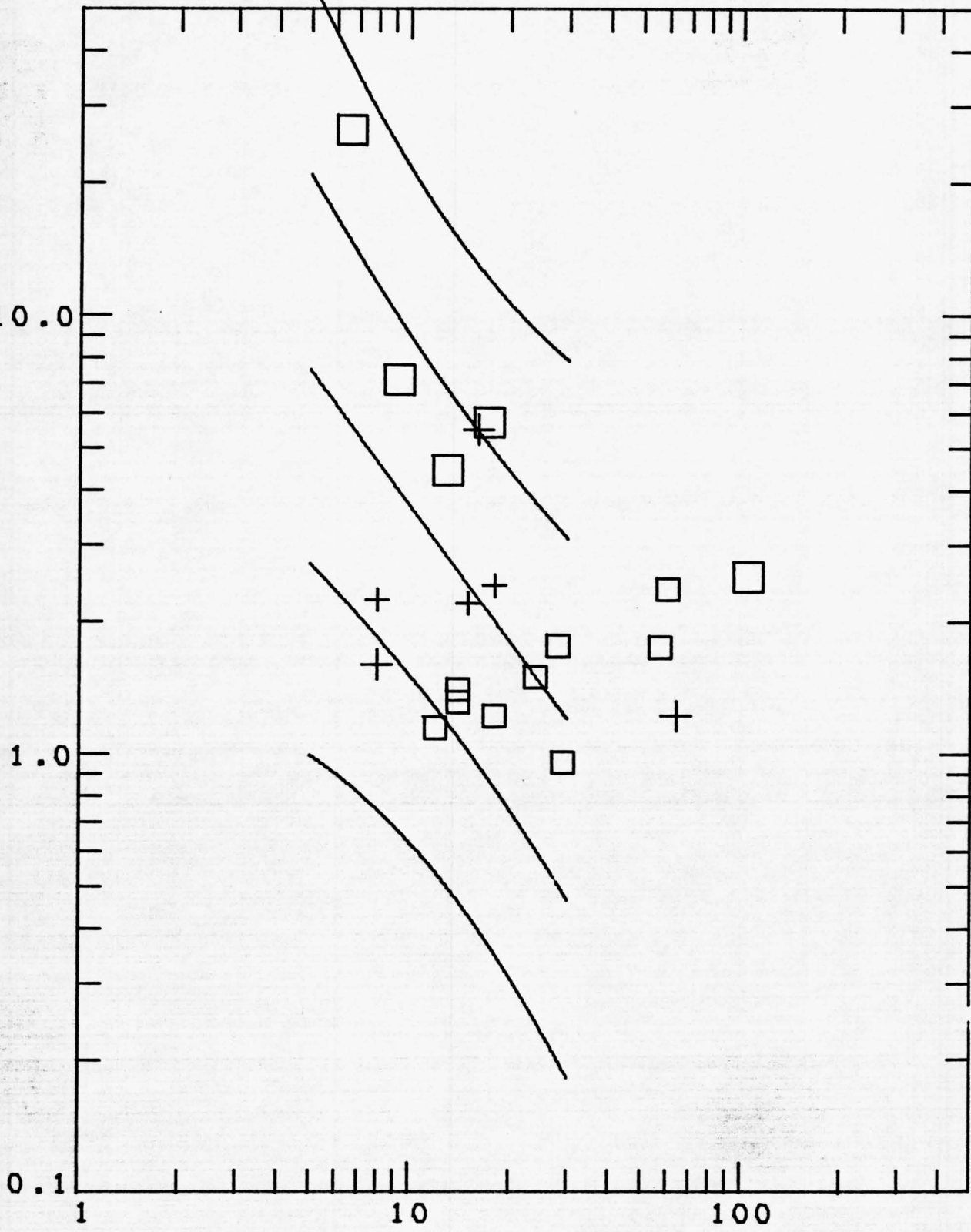


Figure 30. Peak horizontal displacement versus distance to the slipped fault for magnitude 6.4 including data from both large and small structures. Symbols and curves same as in Figure 23.

MAGNITUDE 6.4

+ = ROCK

□ = SOIL

HORIZONTAL DISPLACEMENT (CM)

10.0

1.0

0.1

DISTANCE (KM)

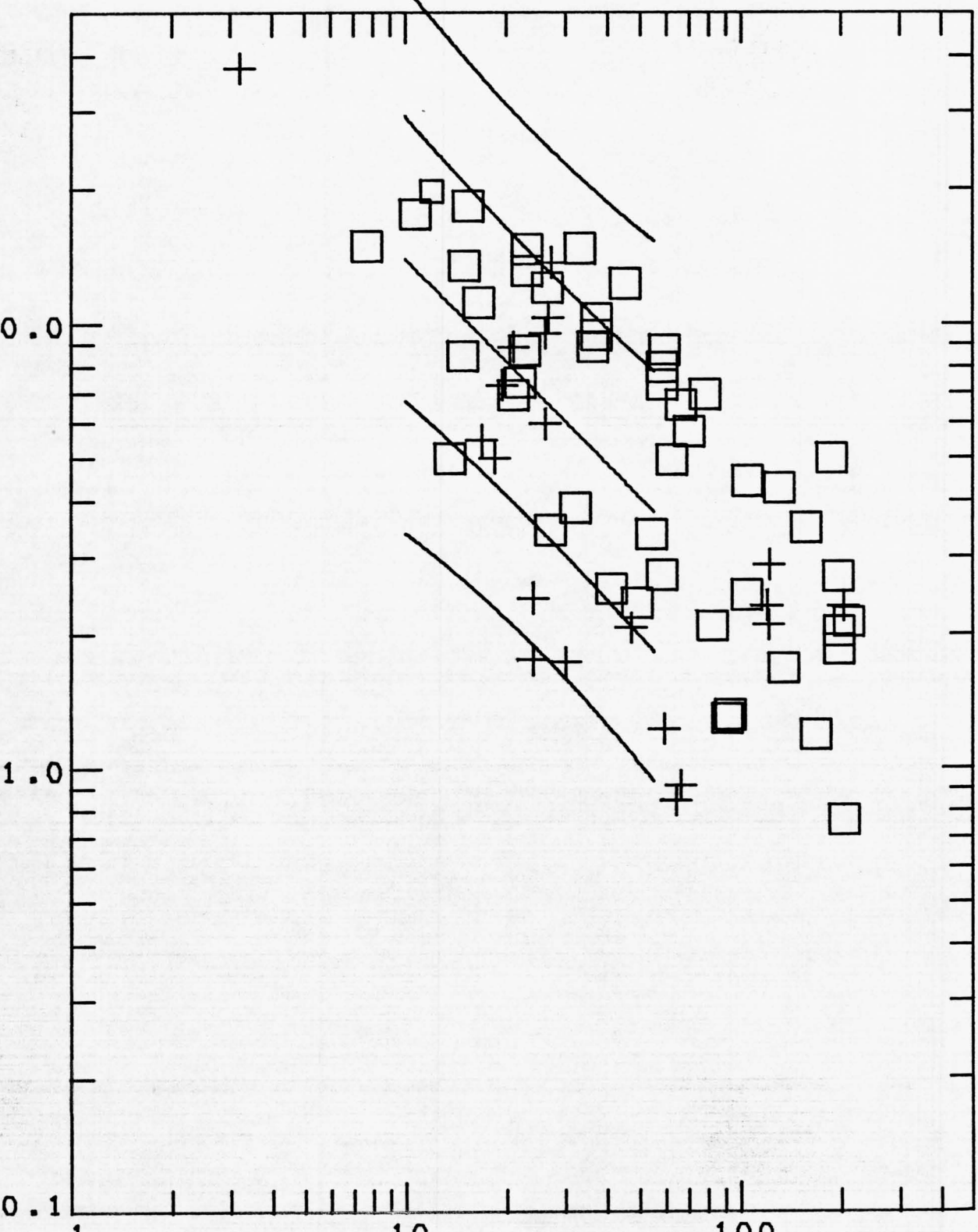


Figure 31. Peak horizontal displacement versus distance to the slipped fault for the magnitude range 7.1-7.7 including data from both large and small structures. Symbols same as in Figure 23.

MAGNITUDE 7.1-7.7

+ = ROCK

□ = SOIL

HORIZONTAL DISPLACEMENT (CM)

10.0

1.0

0.1

1

10

100

DISTANCE (KM)

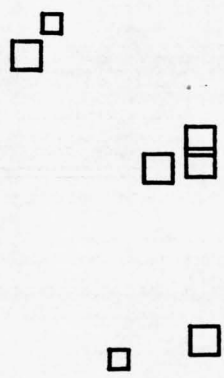


Figure 32. Peak horizontal acceleration versus distance to the slipped fault at soil sites in the San Fernando earthquake. Diamonds represent small structures and asterisks large structures.

SAN FERNANDO SOIL SITES

STRUCTURES: \diamond = SMALL $*$ = LARGE

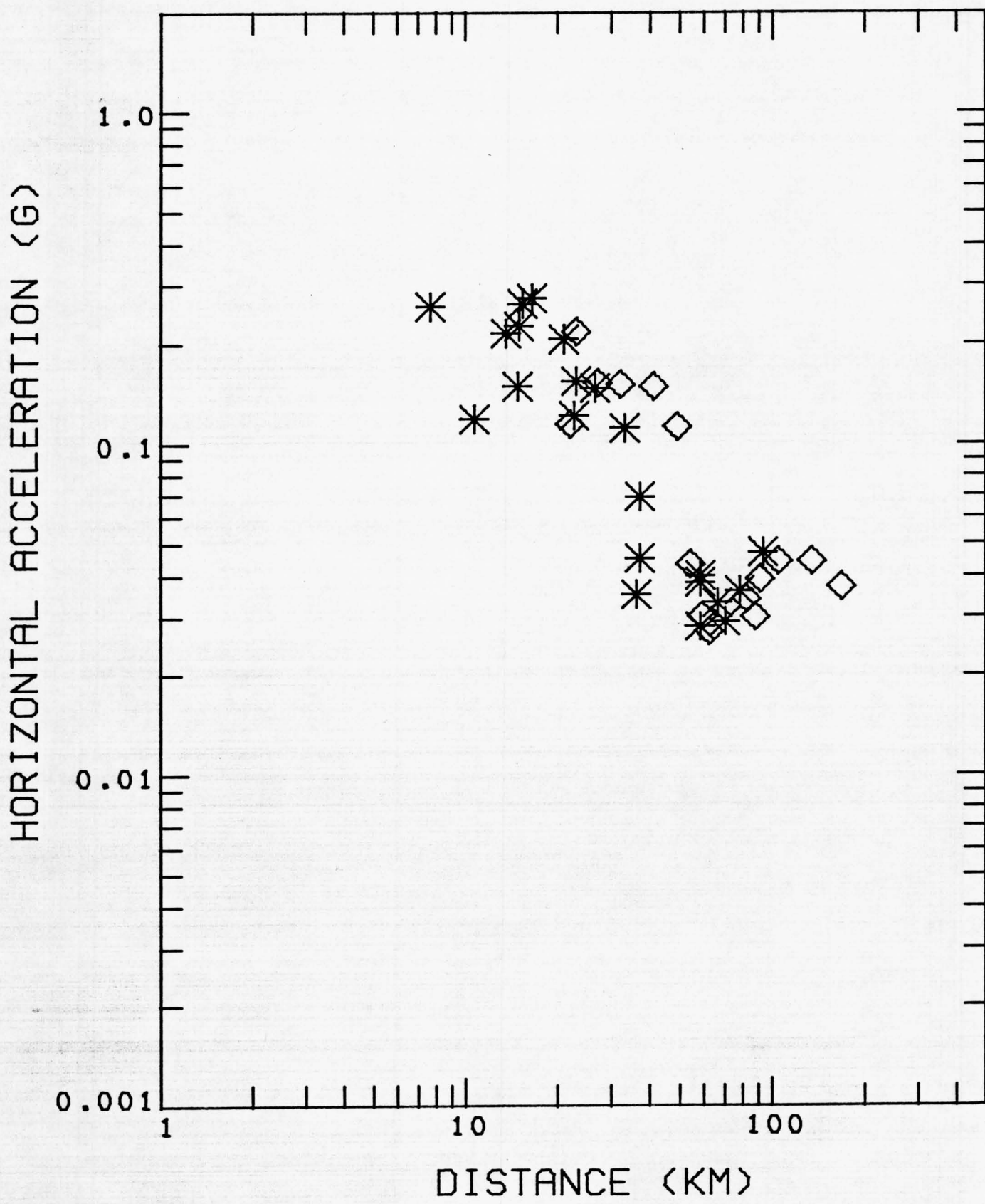


Figure 33. Comparison of mean regression lines and 70 percent prediction intervals for small structures (solid lines) and large structures (dashed lines) for peak horizontal acceleration at soil sites in the San Fernando earthquake.

SAN FERNANDO SOIL SITES

— SMALL STRUCTURES

— — LARGE STRUCTURES

HORIZONTAL ACCELERATION (G)

1.0

0.1

0.01

0.001

1

10

100

DISTANCE (KM)

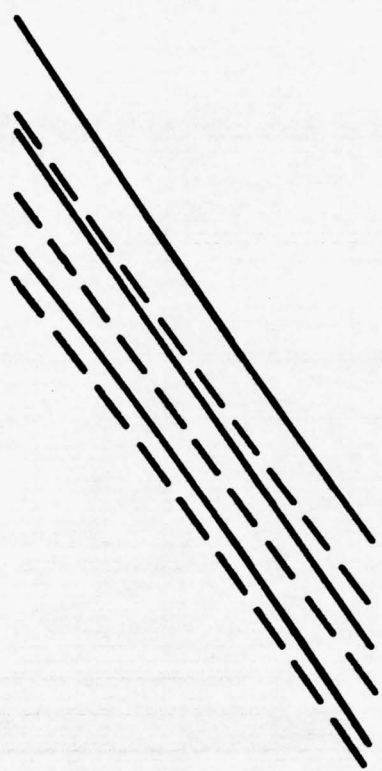


Figure 34. Peak horizontal velocity versus distance to the slipped fault at soil sites in the San Fernando earthquake. Diamonds represent small structures and asterisks large structures.

SAN FERNANDO SOIL SITES

STRUCTURES:

◇ = SMALL

* = LARGE

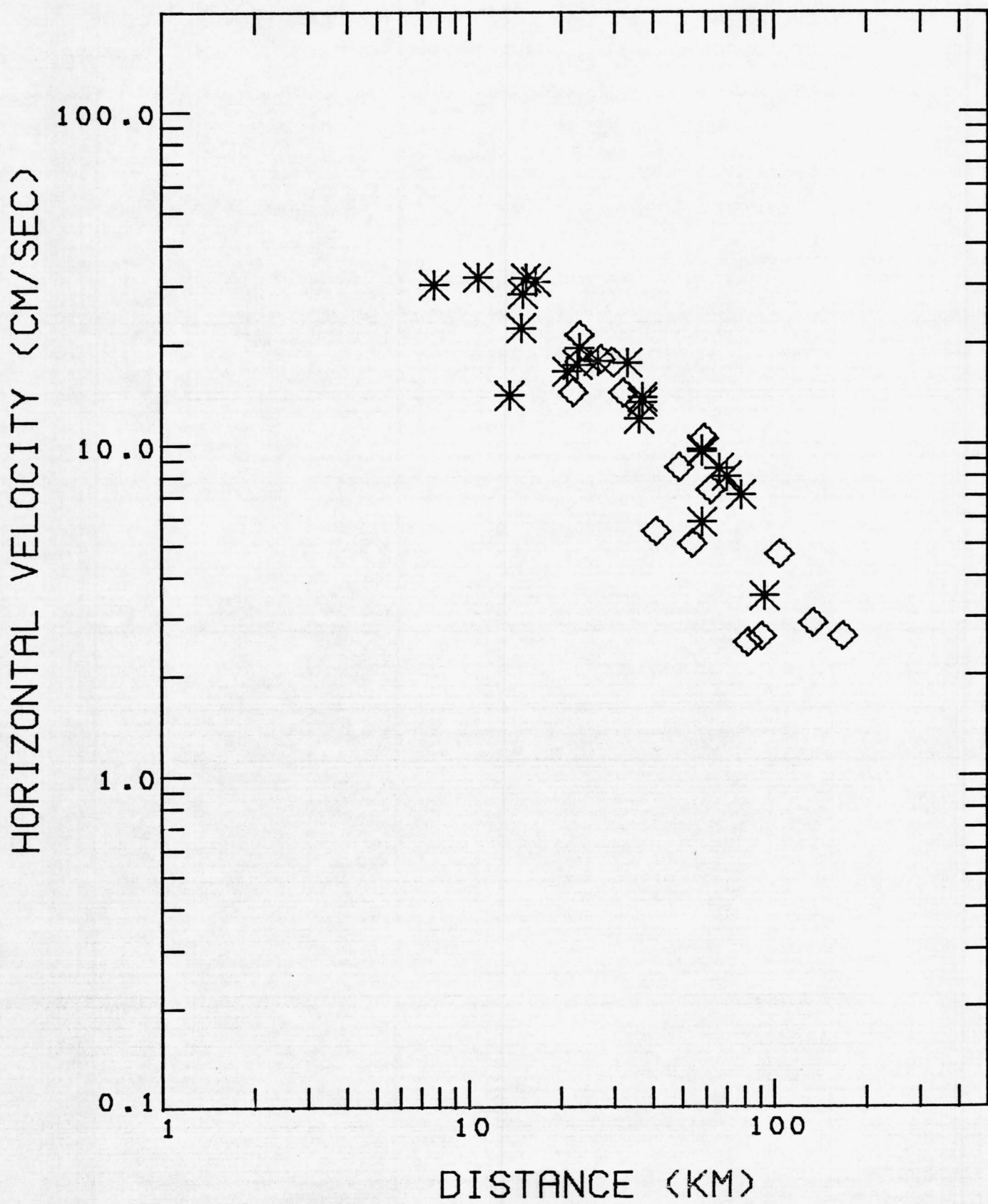


Figure 35. Comparison of mean regression lines and 70 percent prediction intervals for small structures (solid lines) and large structures (dashed lines) for peak horizontal velocity at soil sites in the San Fernando earthquake.

SAN FERNANDO SOIL SITES

— SMALL STRUCTURES

— — LARGE STRUCTURES

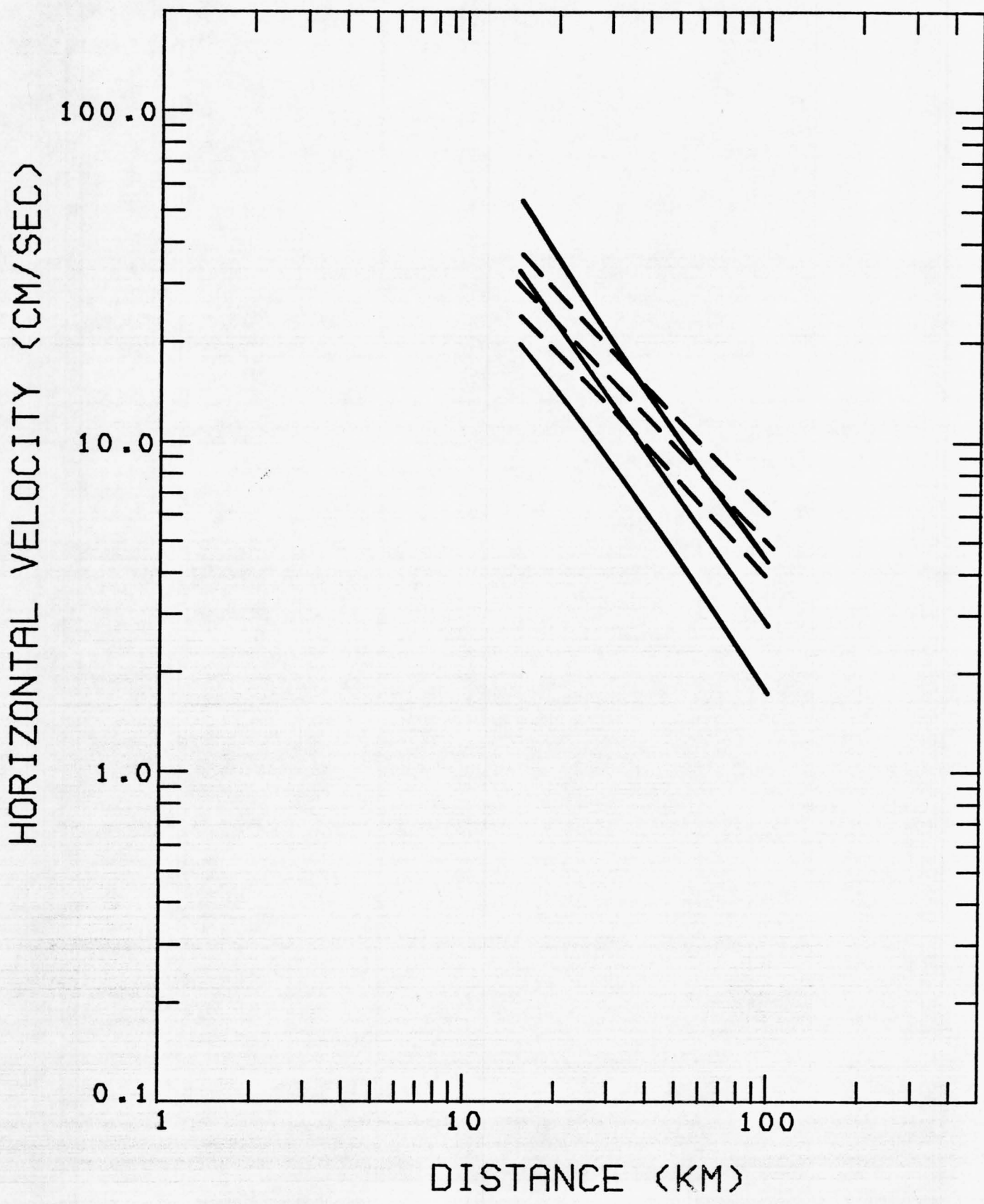


Figure 36. Peak horizontal displacement versus distance to the slipped fault at soil sites in the San Fernando earthquake. Diamonds represent small structures and asterisks large structures.

SAN FERNANDO SOIL SITES

STRUCTURES:

◇ = SMALL

* = LARGE

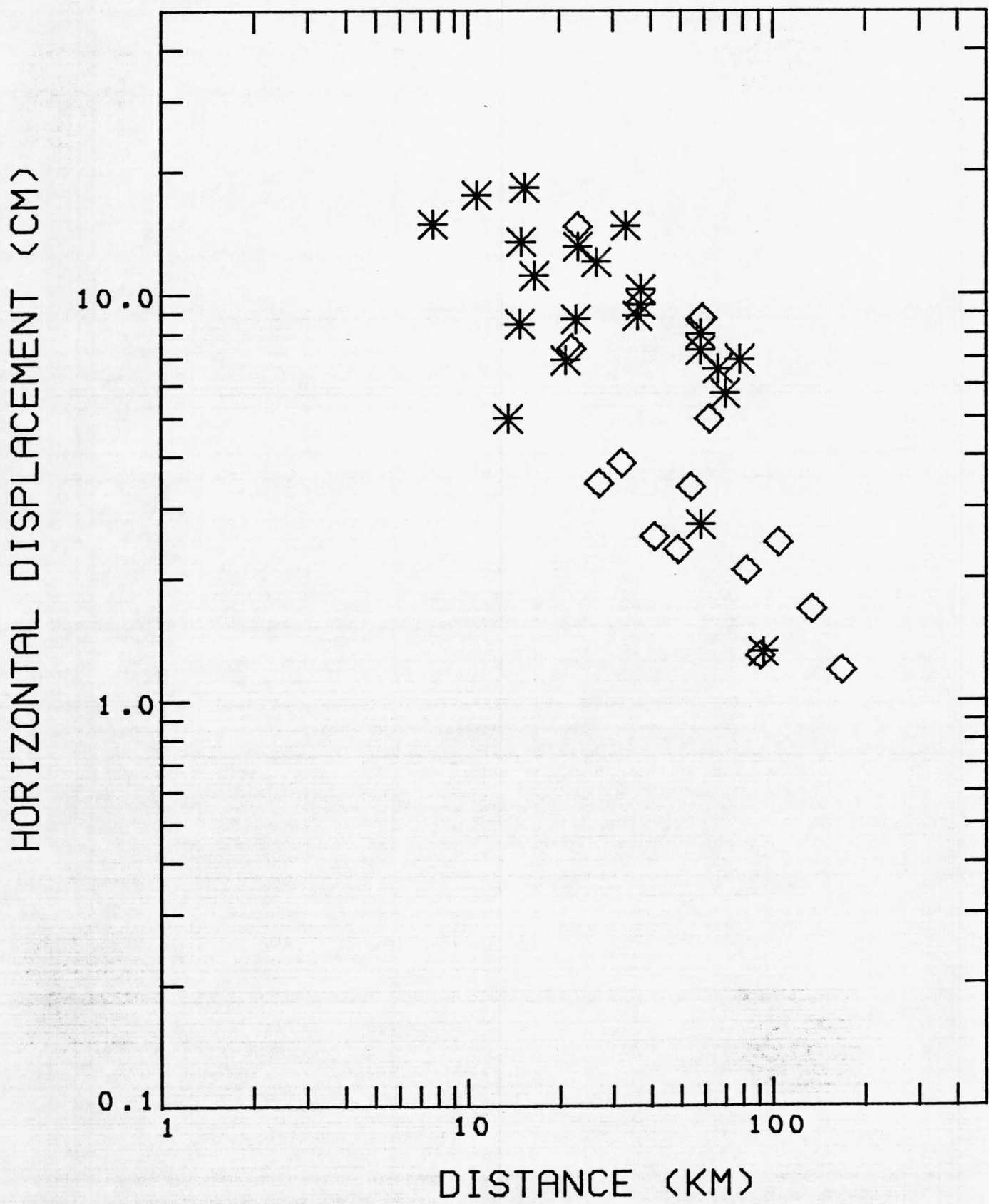


Figure 37. Comparison of mean regression lines and 70 percent prediction intervals for small structures (solid lines) and large structures (dashed lines) for peak horizontal displacement at soil sites in the San Fernando earthquake.

SAN FERNANDO SOIL SITES

— SMALL STRUCTURES - - - LARGE STRUCTURES

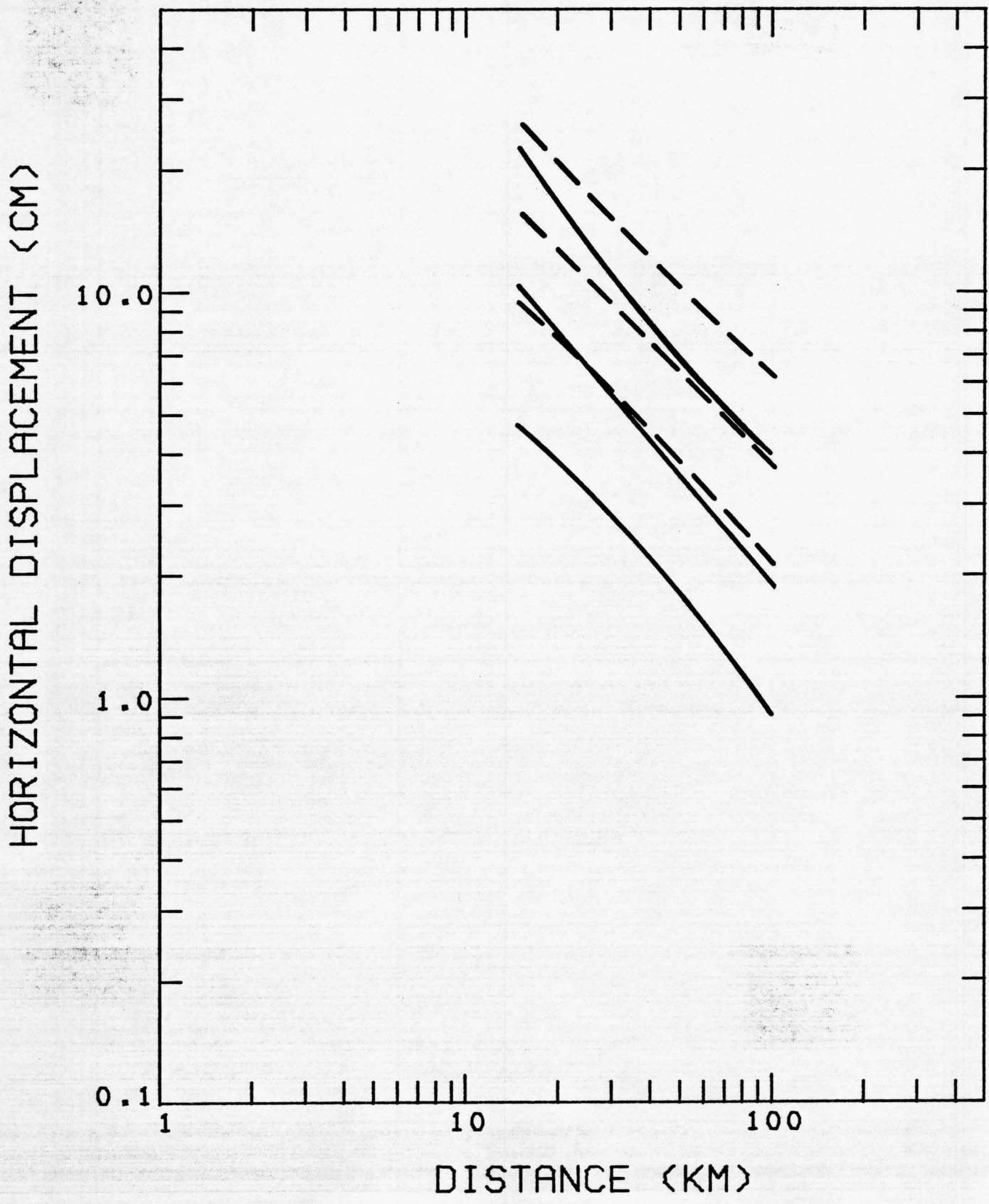


Figure 38. Peak horizontal acceleration recorded at the base of small structures versus distance to the slipped fault in the San Fernando earthquake. Symbols same as in Figure 1.

SAN FERNANDO SMALL STRUCTURES

X = ROCK

◊ = SOIL

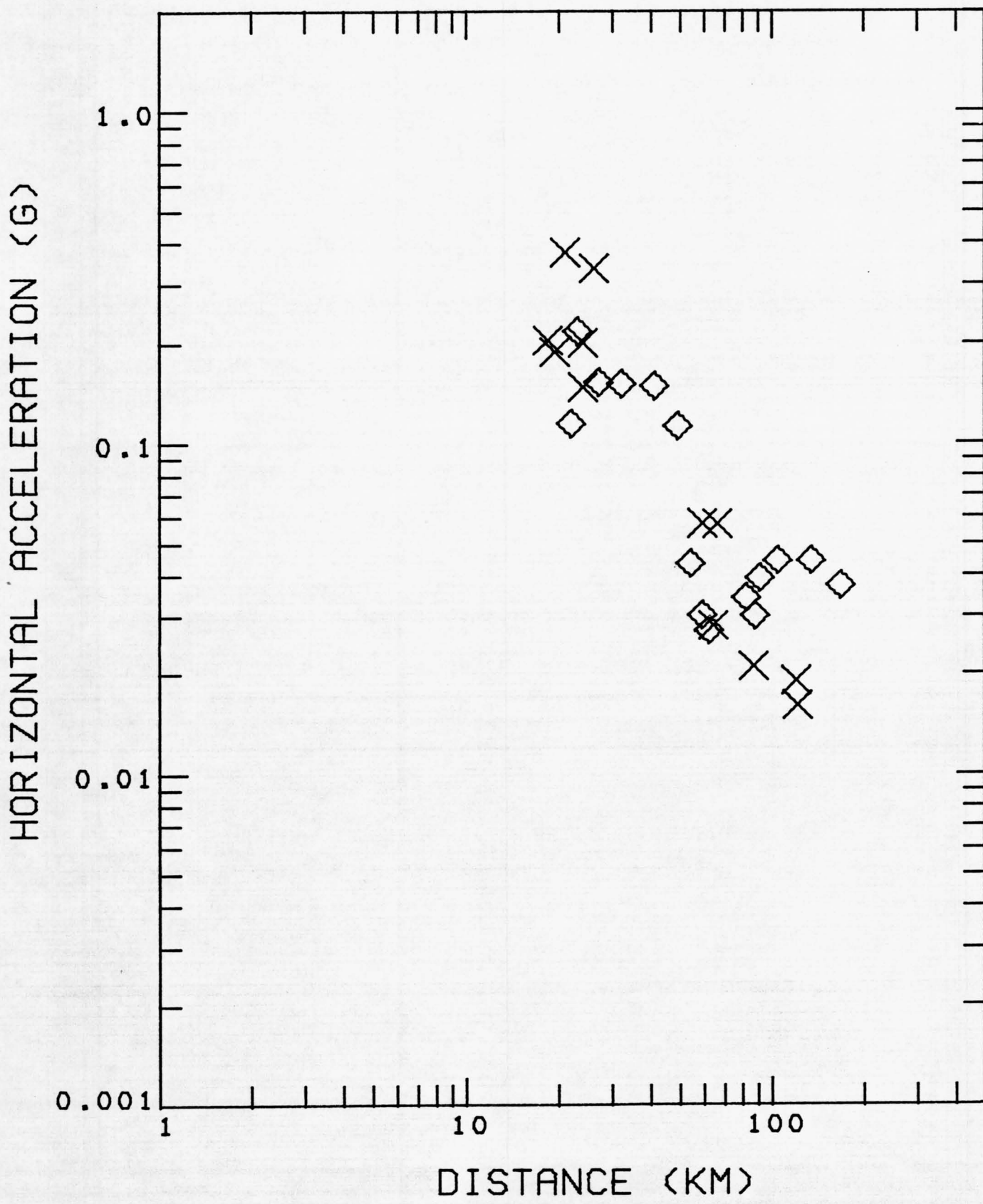


Figure 39. Comparison of mean regression lines and 70 percent prediction intervals for rock sites (solid lines) and soil sites (dashed lines) for peak horizontal acceleration recorded at the base of small structures in the San Fernando earthquake.

SAN FERNANDO

— ROCK — SOIL

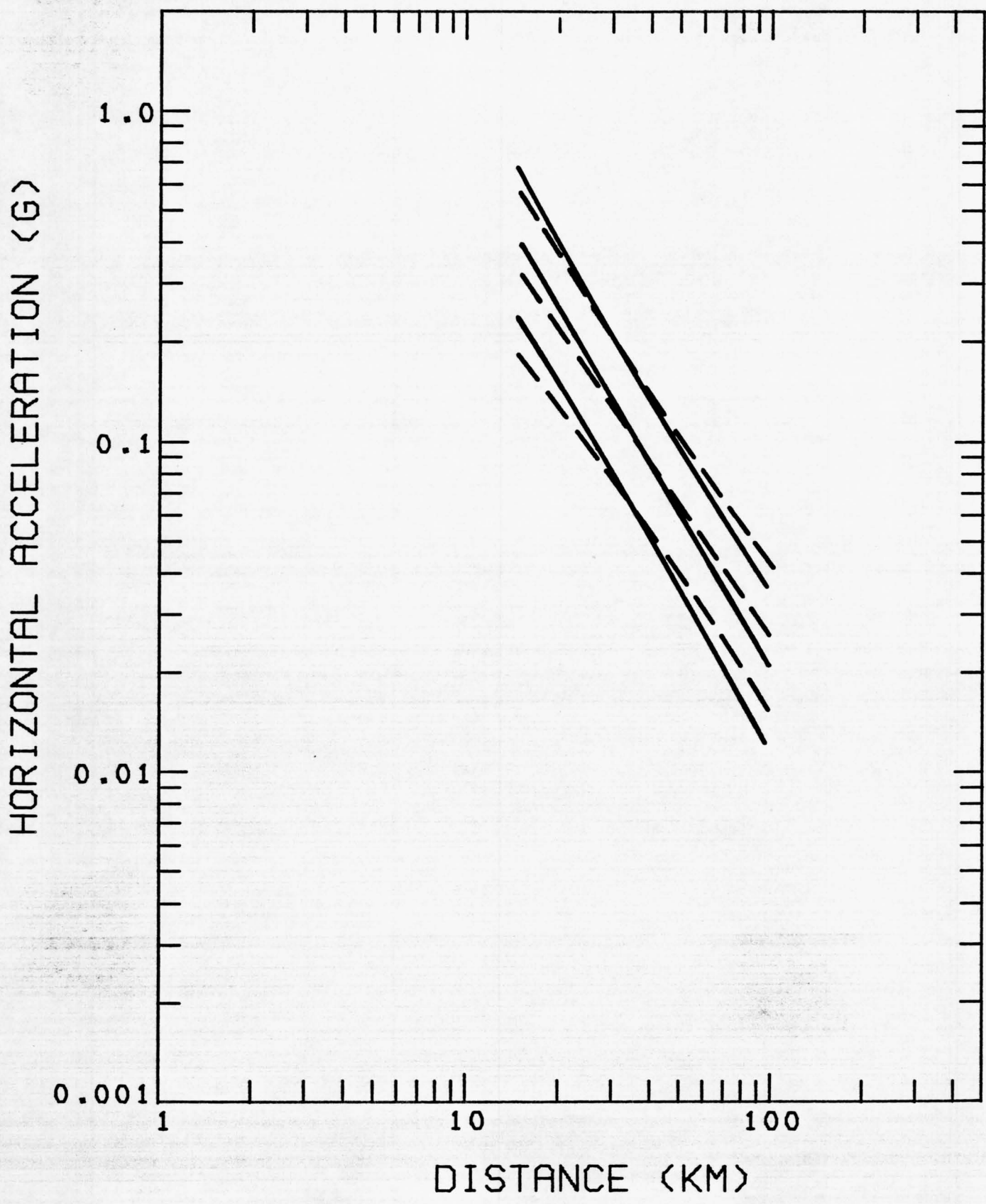


Figure 40. Peak horizontal velocity recorded at the base of small structures versus distance to the slipped fault in the San Fernando earthquake. Symbols same as in Figure 1.

SAN FERNANDO SMALL STRUCTURES

X = ROCK

◊ = SOIL

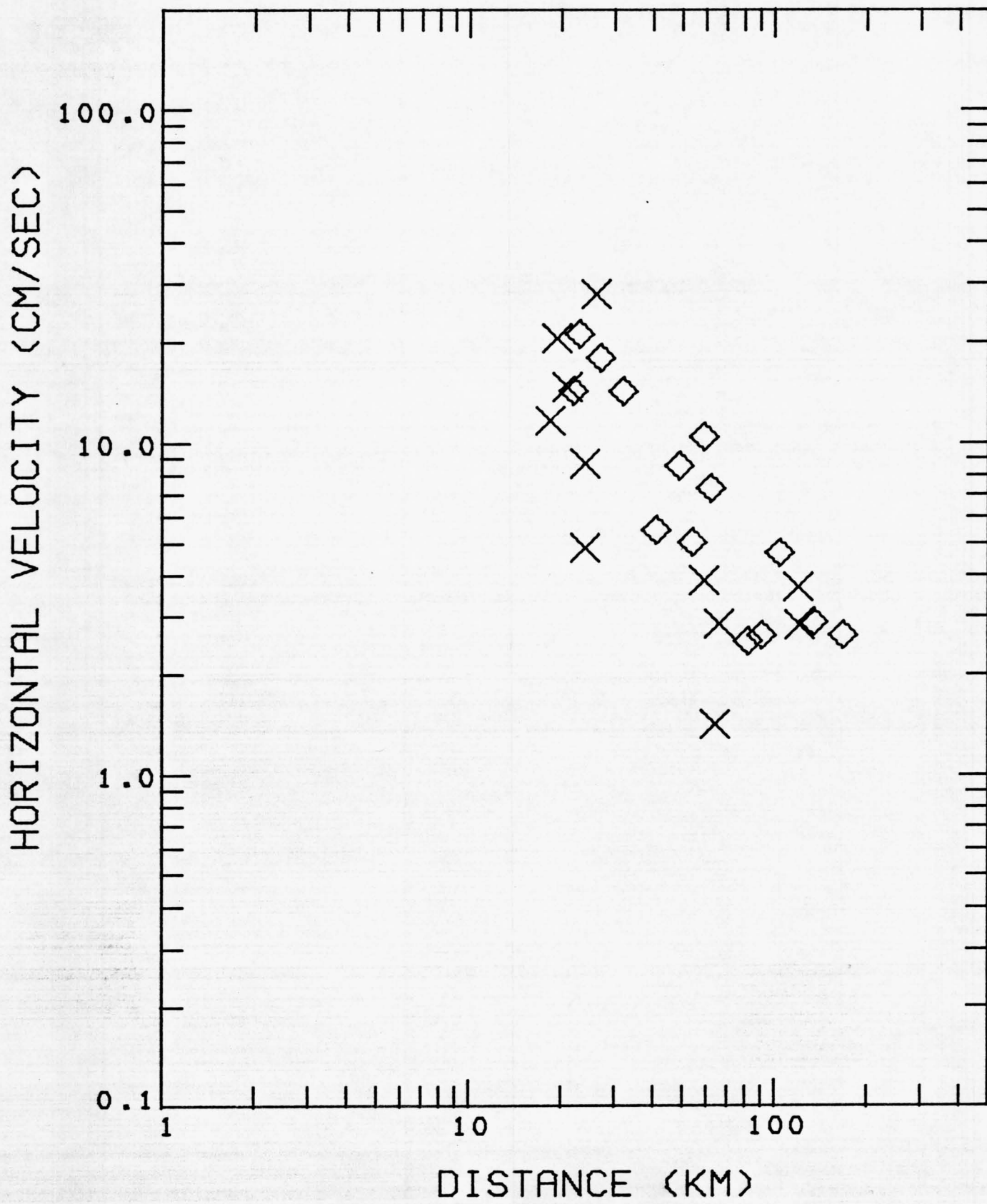


Figure 41. Comparison of mean regression lines and 70 percent prediction intervals for rock sites (solid lines) and soil sites (dashed lines) for peak horizontal velocity recorded at the base of small structures in the San Fernando earthquake.

SAN FERNANDO

— ROCK - - - SOIL

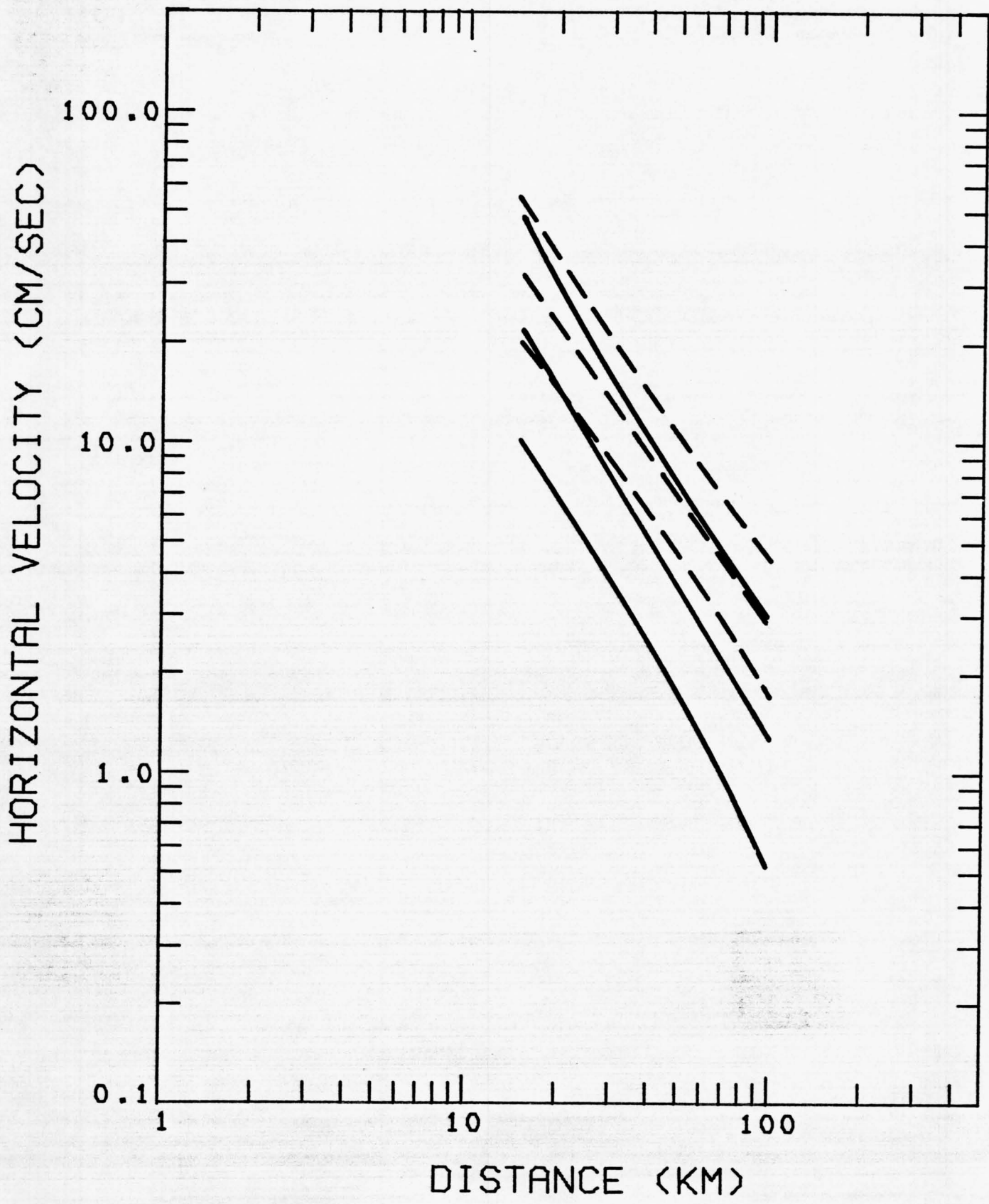


Figure 42. Peak horizontal displacement recorded at the base of small structures versus distance to the slipped fault in the San Fernando earthquake. Symbols same as in Figure 1.

SAN FERNANDO SMALL STRUCTURES

X = ROCK

◇ = SOIL

HORIZONTAL DISPLACEMENT (CM)

10.0

1.0

0.1

1

10

100

DISTANCE (KM)

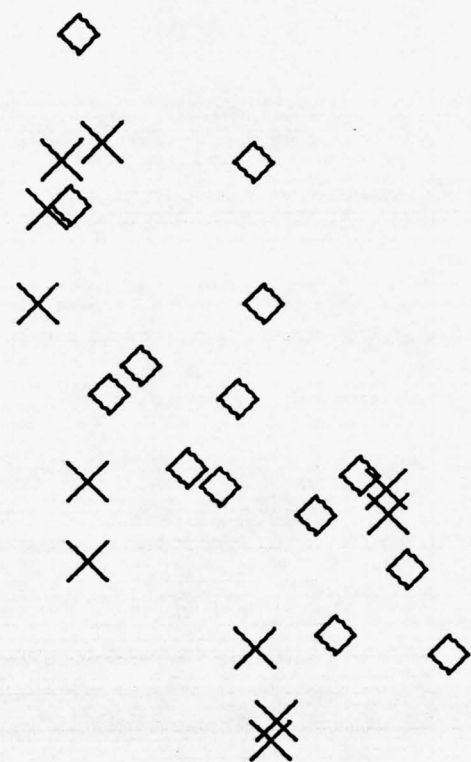


Figure 43. Comparison of mean regression lines and 70 percent prediction intervals for rock sites (solid lines) and soil sites (dashed lines) for peak horizontal displacement recorded at the base of small structures in the San Fernando earthquake.

SAN FERNANDO

— ROCK — SOIL

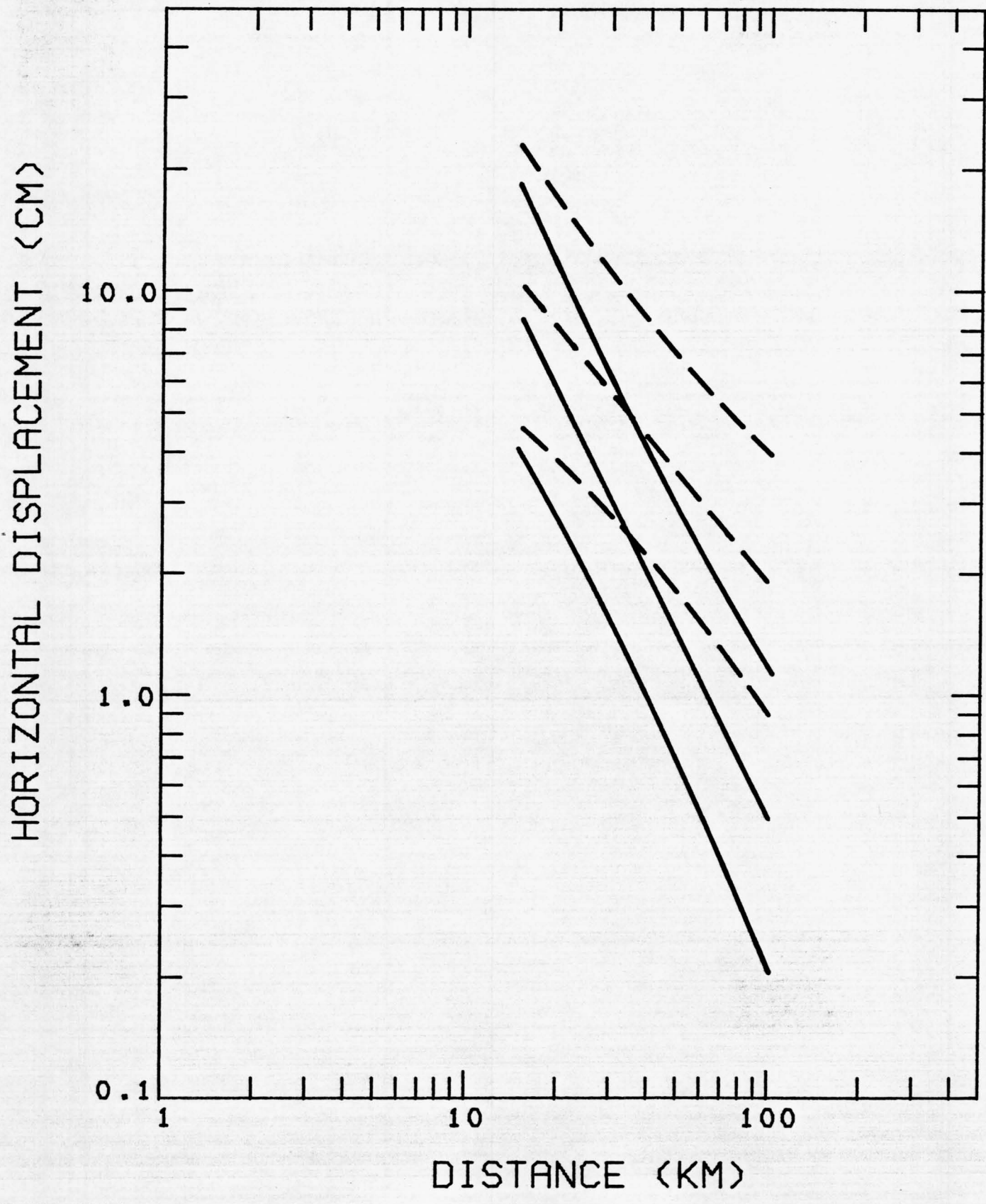
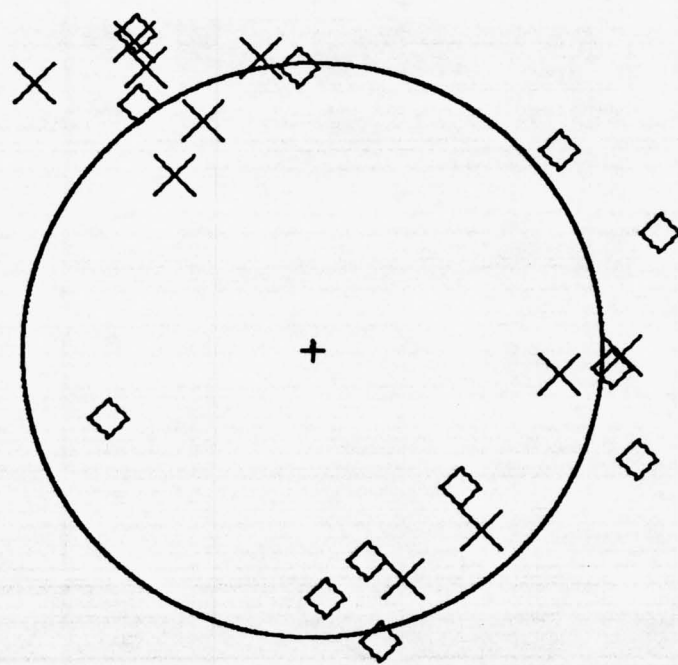


Figure 44. Peak horizontal acceleration in the San Fernando earthquake recorded at the base of small structures. Azimuthal dependence of the residuals from the mean regression line. See text for further explanation. Symbols same as in Figure 1.

SAN FERNANDO

ACCELERATION

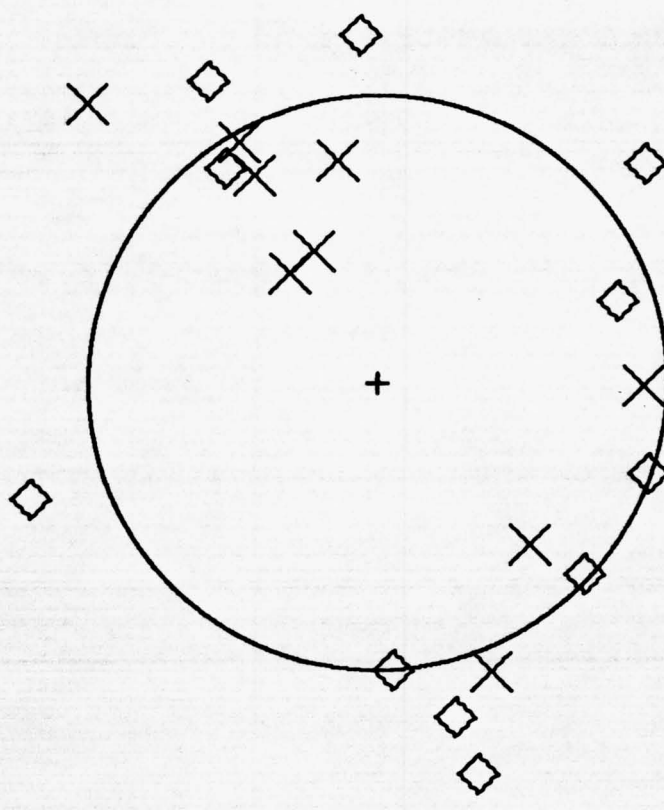


A FACTOR OF TWO

Figure 45. Peak horizontal velocity in the San Fernando earthquake recorded at the base of small structures. Azimuthal dependence of the residuals from the mean regression line. See text for further explanation. Symbols same as in Figure 1.

SAN FERNANDO

VELOCITY



A FACTOR OF TWO

Figure 46. Peak horizontal displacement in the San Fernando earthquake recorded at the base of small structures. Azimuthal dependence of the residuals from the mean regression line. See text for further explanation. Symbols same as in Figure 1.

SAN FERNANDO

DISPLACEMENT

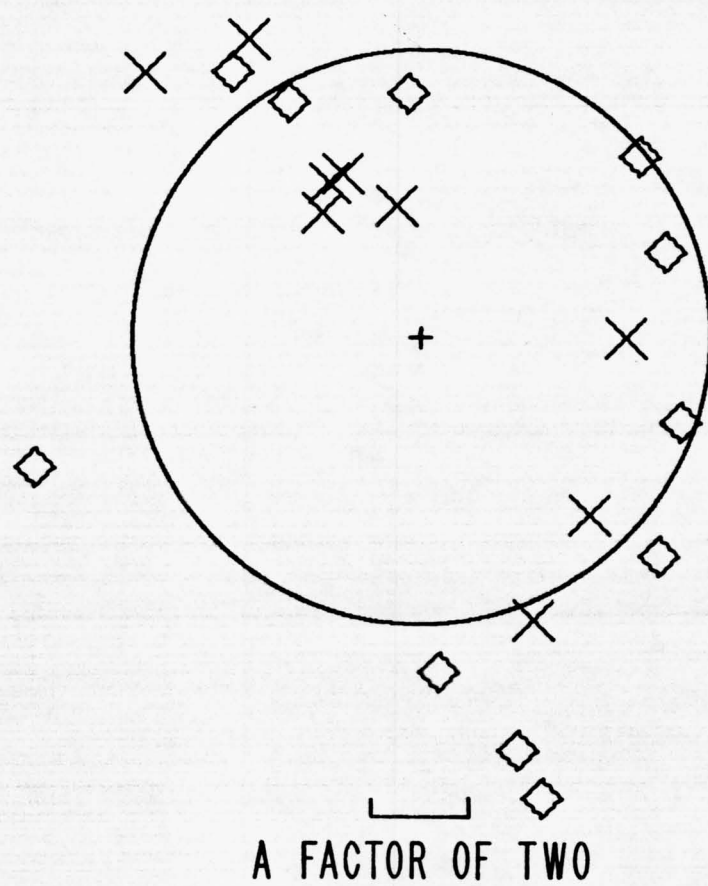


Figure 47. Proposed relationships for peak horizontal acceleration from a magnitude 6.6 earthquake. The curve labeled S is given by Schnabel and Seed (1973) for rock sites, the curve labeled D is given by Donovan (1973) for soil sites, and the curves labeled T0 and T2 are the mean curves given by Trifunac (1976) for soft and hard sites respectively. The solid lines show the 70 percent prediction interval for the small-structure magnitude 6.0-6.4 data set of this report.

HORIZONTAL ACCELERATION (G)

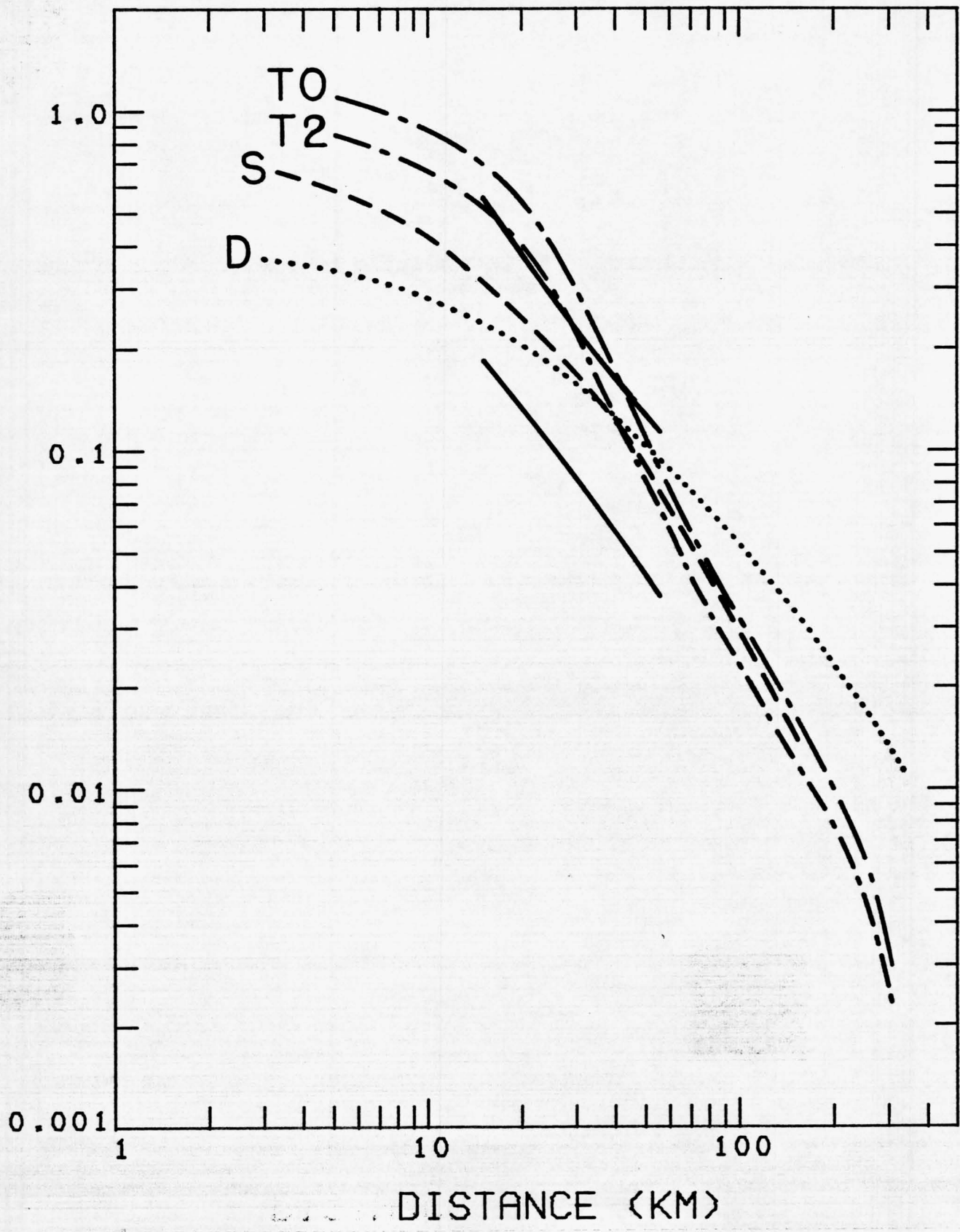


Figure 48. Proposed relationships for peak horizontal acceleration from a magnitude 7.6 earthquake. Curves labeled S, D, T0 and T2 are from the sources given in Figure 41. The solid lines show the 70 percent prediction interval for the small-structure magnitude 7.1-7.7 data set of this report.

HORIZONTAL ACCELERATION (G)

